Efficacy and safety evaluations of topical proretinal nanoparticles

Miss Benchaphorn Limcharoen

จุฬาลงกรณ์มหาวิทยาลัย
CHULALONGKORN UNIVERSITY

A Dissertation Submitted in Partial Fulfillment of the Requirements
for the Degree of Doctor of Philosophy in Veterinary Pathobiology
Department of Veterinary Pathology
Faculty of Veterinary Science
Chulalongkorn University
Academic Year 2018

การประเมินประสิทธิศักย์และความปลอดภัยของอนุภาคนาโนโปรวิตามินเอแบบทาเฉพาะที่

น.ส.เบญจพร ลิ้มเจริญ

Thesis Title	Efficacy and safety evaluations of topical proretinal nanoparticles
By	Miss Benchaphorn Limcharoen
Field of Study	Veterinary Pathobiology
Thesis Advisor	Associate Professor WIJIT BANLUNARA, D.V.M., Ph.D., D.T.B.V.P.
Thesis Co Advisor	Professor Supason Wanichwecharungruang, B.Sc.,Ph.D.

Accepted by the Faculty of Veterinary Science, Chulalongkorn University in Partial Fulfillment of the Requirement for the Doctor of Philosophy

-- Dean of the Faculty of Veterinary Science

(Professor ROONGROJE THANAWONGNUWECH, D.V.M., M.Sc., Ph.D., D.T.B.V.P.)

DISSERTATION COMMITTEE

-- Chairman

(Associate Professor THEERAYUTH KAEWAMATAWONG, D.V.M., Ph.D., D.T.B.V.P.)

-- Thesis Advisor

(Associate Professor WIJIT BANLUNARA, D.V.M., Ph.D., D.T.B.V.P.)

-- Thesis Co-Advisor

(Professor Supason Wanichwecharungruang, B.Sc.,Ph.D.)

-- Examiner

(Assistant Professor PATCHAREE RITPRAJAK, D.D.S., Ph.D.)

-- Examiner

(KASEM RATTANAPINYOPITUK, D.V.M., M.Sc., Ph.D., D.T.B.V.P.)

-- External Examiner

(Associate Professor AMNART POAPOLATHEP, D.V.M., Ph.D.)

เบญจพร ลิ้มเจริญ : การประเมินประสิทธิศักย์และความปลอดภัยของอนุภาคนาโนโปรวิตามินเอแบบทาเฉพาะที่. (Efficacy and safety evaluations of topical proretinal nanoparticles) อ.ที่ปรึกษาหลัก : รศ. น.สพ.ดร.วิจิตร บรรลุนารา, อ.ที่ปรึกษาร่วม : ศ. ดร.ศุภศร วนิชเวชารุ่งเรือง

เรตินัลหรือเรตินัลดีไฮด์ (retinal หรือ retinaldehyde) เป็นหนึ่งในอนุพันธ์ตามธรรมชาติของวิตามินเอ ซึ่งเรตินัลในรูปแบบยาทาผิวหนังเฉพาะที่มีใช้อย่างแพร่หลายในทางการ รักษาโรคผิวหนัง เช่น การรักษาสิวและหลุมสิว ใช้ในผลิตภัณฑ์ลดเลือนริ้วรอยฟื้นฟูอายุผิว โรคผดสะเก็ดเงิน เนื้องอกผิวหนังบางชนิด หรือการทำงานที่ผิดปกติของต่อมไขมัน โดยฤทธิ์ของวิตามินเอจะ ไปกระตุ้นการเจริญของเซลล์เคอราติโนไซต์แล้วทำให้ผิวหนังชั้นหนังกำพร้า (epidermis) หนาตัวขึ้น สามารถยับยั้งการสลายคอลลาเจน และกระตุ้นการสังเคราะห์คอลลาเจนใหม่ในชั้นหนังแท้ (dermis) แต่อย่างไรก็ตามคุณสมบัติทางเคมีกายภาพของเรตินัลและอนุพันธ์ของวิตามินเอนั้นไม่เสถียรสามารถโดนทำลายได้ง่าย ผลข้างเคียงจากการใช้เรตินัลและอนุพันธ์วิตามินเอแบบทาเฉพาะที่ มักทำให้เกิดหนังอักเสบแบบระคายเคือง เนื่องจากปริมาณในการทาเฉพาะแต่ละที่ไม่คงที่ ผลข้างเคียงจึงจำกัดทั้งหมดนี้จำกัดผลของการรักษาด้วยวิตามินเอแบบทาเฉพาะที่ในโรคผิวหนังต่าง ๆ ในระยะยาว เพื่อลดปัญหาเหล่านี้จึงมีการคิดค้นการนำเรตินัลในรูปแบบเฉพาะที่ด้วยอนุภาคนาโนโดยเรียกว่าอนุภาคนาโนโปรวิตามินเอ (proretinal nanoparticles; PRN) ช่วยเพิ่มความเสถียร ให้เรตินัลรวมถึงมีคุณสมบัติในการควบคุมการปลดปล่อยเรตินัลอย่างช้า ๆ และต่อเนื่อง โดยวัตถุประสงค์ของการศึกษานี้คือ ศึกษาความเป็นพิษระดับเซลล์ของอนุภาคนาโนโปรวิตามินเอกับฮาแคท เซลล์ในหลอดทดลอง ศึกษาฤทธิ์ของวิตามินตามธรรมชาติต่อฮาแคทเซลล์ (HaCaT) และต่อชั้นหนังกำพร้าในสัตว์ทดลอง ศึกษาความสามารถและปริมาณอนุภาคนาโนโปรวิตามินเอในการส่งผ่านสาร เข้าสู่ผิวหนังผ่านทางรูขุมขน (follicular penetration pathway) และผ่านทางระหว่างเซลล์คอร์นิโอไซต์ในชั้นสตราตัมคอร์เนียม (intercellular penetration pathway) ซึ่งอยู่บนสุดของหนัง กำพร้า และสุดท้ายศึกษาความเป็นไปได้ของการนำส่งอนุภาคนาโนโปรวิตามินไปถึงชั้นหนังแท้โดยการใช้ไมโครนีดเติ้ลช่วยในการนำส่งด้วยชิ้นส่วนผิวหนังสุกรซึ่งเป็นตัวแทนที่ดีของผิวหนังมนุษย์

การศึกษานี้เริ่มจากการศึกษาความปลอดภัยของอนุภาคนาโนโปรวิตามินเอในหลอดทดลอง โดยใช้ฮาแคทเซลล์ซึ่งเป็นเคอราติโนไซต์เซลล์ไลน์โดยเป็นตัวแทนในการทดสอบของ เซลล์เคอราติโนไซต์ซึ่งคือประชากรหลักของชั้นหนังกำพร้า โดยผลจากการศึกษาพบว่า อนุภาคนาโนโปรวิตามินเอมีความปลอดภัยต่อฮาแคทเซลล์โดยไม่เป็นพิษกับเซลล์และไม่เหนี่ยวนำการตาย ระดับเซลล์เมื่อทดสอบกับเซลล์ 24 ชั่วโมง และพบว่ามีการแสดงออกของโปรตีน CRABP-2 มากขึ้นเมื่อเทียบกับเซลล์กลุ่มควบคุมที่ทดสอบกับเรตินัล โปรตีน CRABP-2 นี้มีความสำคัญในแง่ของการ กำหนดชีวปริมาณออกฤทธิ์ของวิตามินเอกับเซลล์ชั้นหนังกำพร้า หลังจากนั้นได้ทดสอบความปลอดภัยและประสิทธิศักย์ของอนุภาคนาโนโปรวิตามินเอแบบทาเฉพาะที่ในผิวหนังของหนูแรท โดยทำ การทาที่หลังของหนูทั้งหมด 28 วัน ศึกษาระดับความระคายเคืองของการทาอนุภาคนาโนโปรวิตามินเอทุก 7 วันทั้งหมดพยาธิวิทยาและจุลพยาธิวิทยา วัดความหนาของชั้นหนังกำพร้าโดย เปรียบเทียบกับกลุ่มควบคุม จากการทดลองกลุ่มที่ทาอนุภาคนาโนโปรวิตามินเอไม่พบการอักเสบระบบระคายเคืองตลอดการทาที่หลังทั้งหมด 28 วัน และอนุภาคนาโนโปรวิตามินเอสามารถเข้าสู่ไปรูขุม ขนของหนูแรทได้โดยไม่ขึ้นกับระยะเวลาหลังจากที่ทาบนผิวหนัง ในส่วนของการศึกษาการแสดงออกของโปรตีน 6 ชนิด คือ K5, K10, K14, PCNA, CRABP-2 และ IL-6 ด้วยวิธีอิมมูโนฮีสโตเคมีที่ แสดงออกชั้นต่าง ๆ ของหนังกำพร้าหลังการทาอนุภาคนาโนโปรวิตามินเอ เพื่อศึกษากลไกการควบคุมการเจริญของชั้นหนังกำพร้า พบว่าอนุภาคนาโนโปรวิตามินเอให้ฤทธิ์ตามธรรมชาติที่ดีกว่า ในชั้นหนังกำพร้า ในแง่ของการเพิ่มการหนาตัวของชั้นหนังกำพร้า การแสดงออกของโปรตีนที่ศึกษาข้างต้นเพิ่มมากขึ้นยกเว้น IL-6 ซึ่งสอดคล้องกับการที่ไม่พบการระคายเคืองและการอักเสบของ ผิวหนังตลอดการทาอนุภาคนาโนโปรวิตามินเอ ส่วนการศึกษาปริมาณและความสามารถของอนุภาคนาโนโปรวิตามินเอในการส่งเรตินัลเข้าสู่ผิวหนังผ่านทางรูขุมขนด้วยกล้องจุลทรรศน์คอนโฟคอล เลเซอร์และผ่านทางระหว่างเซลล์คอร์นิโอไซต์ในชั้นสตราตัมคอร์เนียมบนผิวหนังสุกรด้วยเทคนิค tape stripping และ spectroscopy พบความสัมพันธ์ระดับความลึกในรูขุมขนของอนุภาคนาโนโป รวิตามินเอและการปลดปล่อยเรตินัลจากอนุภาคนาโนโดยใช้สีฟลูออเรสเซนต์เป็นตัวแทนของเรตินัลนั้นไม่ขึ้นกับเวลา กล่าวคือระดับความลึกของการปลดปล่อยเรตินัลจากอนุภาคนาโนในรูขุมขนคงที่ ตั้งแต่เริ่มทาลงไปถึงผิวหนัง เมื่อวัดปริมาณเรตินัลที่หลงเหลืออยู่ในชั้นสตราตัมคอร์เนียมชั้นบนสุดของหนังกำพร้าและในรูขุมขนพบว่าผิวหนังกลุ่มที่ทาอนุภาคนาโนโปรวิตามินเอมีระดับเรตินัลที่ มากกว่ากลุ่มควบคุมอย่างมีนัยสำคัญ และการศึกษาสุดท้ายเมื่อใช้ไมโครนีดเติ้ลที่บนอนุภาคนาโนโปรวิตามินเอบรรจุอยู่ในทะลุผ่านชั้นสตราตัมคอร์เนียมและหนังกำพร้าที่ผิวหนังสุกรด้วย dermpscopy, optical coherence tompgraphy และ multiphoton microscopy พบว่าสามารถนำส่งอนุภาคนาโนโปรวิตามินเอและวัดปริมาณเรตินัลได้ไปจนถึงชั้นหนังแท้

จากการศึกษานี้สรุปได้ว่า การใช้อนุภาคนาโนโปรวิตามินเอแบบทาเฉพาะที่ มีความปลอดภัยต่อเซลล์ทั้งระดับหลอดทดลองและไม่ก่อให้เกิดความระคายเคืองต่อผิวหนัง สัตว์ทดลอง มีประสิทธิศักย์และฤทธิ์ตามธรรมชาติของวิตามินเอและอนุพันธ์ในการควบคุมการเจริญของหนังกำพร้า มีความสามารถในการปลดปล่อยเรตินัลให้แพร่ผ่านระหว่างเซลล์คอร์นิโอไซต์ และเข้าไปในรูขุมขนเพื่อปลดปล่อยเรตินัลที่เป็นตัวออกฤทธิ์ได้ตามระดับความลึกที่ต้องการในรูขุมขน อนุภาคนาโนโปรวิตามินเอสามารถลดผลข้างเคียงของการใช้วิตามินเอเฉพาะที่แบบเก่า และ พัฒนาเป็นตัวเลือกในการรักษาโรคทางผิวหนังที่ตอบสนองต่อวิตามินเอได้ในอนาคต

สาขาวิชา	พยาธิชีววิทยาทางสัตวแพทย์	ลายมือชื่อนิสิต ....
ปีการศึกษา	2561	ลายมือชื่อ อ.ที่ปรึกษาหลัก ....
		ลายมือชื่อ อ.ที่ปรึกษาร่วม ....

Retinal (retinaldehyde) is one of natural vitamin A metabolites. It is widely used in clinical dermatology such as acne, acne scar, photoaging, wrinkles, psoriasis, skin neoplasia and seborrheic dermatitis. Retinal is a pivotal key to regulate keratinocyte proliferation and differentiation in the epidermis resulting in epidermal thickening and inhibit collagen destruction in the dermis. However, topical application of retinal is still irritative to the skin and chemically and photochemically unstable. Topically applied retinal can induce a retinoid dermatitis. This inflammation is induced by an overload of non-physiological amounts of exogenous retinoic acid in the skin. The adverse effects and physicochemical stability of retinal limit its topical therapeutic effects in long-term treatment. To eliminate this dose-related side effect and the instability of the chemical, the developingment of topical nanoparticulate controlled-release drug delivery system as proretinal nanoparticles (PRN) which releases retinal continuously to prevent an excessive amount of retinal on the skin immediately after application has been proposed. The aims of this study were to investigate the safety, efficacy and biological activities of topical application of proretinal nanoparticles in term of follicular and intercellular penetration as the major pathways of topical nanoparticles in skin and to assess the possibility of the intradermal derlivery og PRN-loaded microneedle by non-invasive imaging techniques.

In this study, proretinal nanoparticles had barely cytotoxic and apoptotic effects comparing with conventional retinal on exposure HaCaT cells, spontaneous immortalized keratinocytes, for 24 h. The biological activity of retinoid in PRN in HaCaT cells was investigated after 24 h exposure to PRN. CRABP-2, transporting protein for members of the vitamin A family to the cellular nucleus, was inducible and higher when compared with conventional at the same concentration of retinoids. To evaluate the safety and efficat aspects of PRN *in vivo*, daily topical application of PRN to rats for 28 consecutive days produced neither irritation nor inflammation but significantly increased of epidermal proliferation, epidermal thickness, CRABP-2 expression, and up-regulation of various differentiation markers of epidermis including keratin (K) 5, K10, K14, CRABP-2 ,and PCNA except IL-6, proinflammatory cytokine compared with topical applicaton of conventional retinal solution. Through the use of confocal laser scanning microscopy, we observed the *in vivo* follicular penetration of PRN with the depth of penetration independent of post-application time. As nanoparticles preferably penetrating the hair follicles, the follicular penetration depths of PRN at different time points were investigated further in *ex vivo* porcine skin. The release capacity of the nanoparticulate system was studied using fluorescein as a model drug. Additionally, the concentration of retinal in the stratum corneum and in the hair follicles was quantified after application in particulate and non-particulate form. The results showed that the nanocarriers reached the infundibular area of the hair follicles, irrespective of the incubation time. The nanoparticles were able to release their model drug within the hair follicle. The retinal concentration delivered to the stratum corneum and the hair follicles was significantly higher when retinal was applied in the particulate form. To assist the intradermal delivery of PRN for the dermal therapeutic aspect, the use of two combinations transdermal drug delivery strategies were developed as PRN and microneedle and then investigated by non-invasive imaging techniques as dermoscopy, optical coherence tomography and multiphoton microscopy. The localization and skin deposition of PRN localization in dermis has been studied and visualized successfully over the time following the application.

The present study showed that topical application proretinal nanoparticles are safe, non-irritative, successfully penetrate into hair follicles and possess retinoid biological activities to skin as the ability to induct and regulate epidermal proliferation and differentiation. Finally, it could be beneficial in some retinoid-responsive skin conditions in the future. Although further investigations are necessary to clarify the required doses and dose intervals in clinical settings, the suggested system may help to overcome the main problems of topical retinoid therapy, which are skin irritation, chemical ,and photochemical instability and low bioavailability.

จุฬาลงกรณ์มหาวิทยาลัย
CHULALONGKORN UNIVERSITY

Field of Study:	Veterinary Pathobiology	Student's Signature ....
Academic Year:	2018	Advisor's Signature ....
		Co-advisor's Signature ....

ACKNOWLEDGEMENTS

TABLE OF CONTENTS

จุฬาลงกรณ์มหาวิทยาลัย
CHULALONGKORN UNIVERSITY

LIST OF TABLES

LIST OF FIGURES

Introduction

1.1 Importance and Rationale

Retinoids are a group of compounds that include both natural and synthetic derivatives of vitamin A. Vitamin A is one of the fat-soluble vitamins. Retinoids are essential factors in physiological growth, visual function, differentiation in the epithelium, and reproduction [1]. Retinoids are pivotal regulators of differentiation and growth of skin [2]. Retinoids can be classified into three different generations according to the presence of aromatic functionality in their structure : i) retinol, retinal, tretinoin (atRA), isotretinoin (13-cis-retinoic acid; 13-cis-RA), and alitretinoin (9-cis-retinoic acid; 9-cis-RA); ii) etretinate and its metabolite acitretin; and iii) tazarotene, bexarotene, and adapalene [3]. In clinical dermatology, bioactive materials that can promote the proliferation and differentiation of epidermal cells are beneficial for treatment, retinoids are wildly used both systemic and topical forms. Especially, the main effect of retinoids on the skin is to enhance epidermal proliferation and keratinocyte differentiation. Skin diseases that are responsive to retinoids include psoriasis and related disorders, congenital disorders of keratinization, acne, skin cancer, and disorder of pigmentation, seborrhea, rosacea, acneiform dermatoses and photoaging [4]. However, systemic administration of retinoids is frequently associated and reported with various organs side effects, thus limiting their uses in long term therapy. The adverse effects of systemic overdose of vitamin A can be minimalized by using topical therapeutic retinoid preparations.

Retinal is one of the natural precursors of retinoids. It is biologically active when topically applied, but is still irritative to human skin [5]. Therefore, in view of toxicities and side effects, treatment with retinoids needs an appropriate and careful selection of patients, consideration of the benefit to risk ratio for each individual patients and route of administration selection and monitoring of clinical response and laboratory tests [6]. Unfortunately, retinal is highly unstable, the compounds can be easily autooxidized and photooxidized [7, 8]. Both ultraviolet B (UVB) and ultraviolet A (UVA) can reduce the content of retinoids in the epidermis [9].

Drug delivery strategies in pharmaceutical researches aim to develop the potential in optimizing the efficacy of the drugs by either modulating their physiocochemical properties or minimizing the undesirable side effects associated with them [10]. However, efficient topical delivery of vitamin A is difficult since it is extremely labile. Nowadays, there are many dosages forms available for topical drug delivery, e.g., conventional systems (powder, cream, lotion, ointment, emulsion, gel, and aerosol/foam), vesicular systems (liposomes, micelles), particulate systems (solid lipid micro/nanoparticles) and special delivery forms such as hydrogel, patch, films, rapid-dissolving tablet and etc. Various polymers including non- and biodegradable, synthetic and natural, are used in the preparations of those delivery systems [11]. Existing delivery systems for most topical drugs are still based on conventional systems. Skin-targeted drug delivery still remains challenging in spite of the fact that skin is an approachable surface area for potential drug absorption [12].

Through the previous co-study between the Faculty of Veterinary Science and the Faculty of Science, a form of retinal delivery system has been developed. The system is based on the reversible linkage between the retinal molecule and chitosan polymer and the assembling of the retinal-grafted chitosan polymer in nanoparticle form. The preliminary study shows promising physicochemical properties and stabilities of the material [13], therefore, this work drives into the safety evaluation and the establishment of transdermal delivery routes, and also biological activities together with intracellular and cellular targets of these proretinal nanoparticles (PRN).

Till now, there are few studies on potential of nanoparticles for the delivery of vitamin A derivatives and performing *in vitro*, *in vivo and ex vivo* levels. Additionally, porcine ear skin and rodent skin used as a (trans)dermal drug model studies are also interesting. In our *in vitro* study, HaCaT cells were used instead of other primary keratinocytes. This is because HaCaT cells can be maintained in a defined retinoid-free cultured system. It has been shown to provide reproducible results and possess the same full epidermal differentiation capacity as normal keratocytes. The advantages of rodents are their small size, uncomplicated handling and relatively low cost [14] and

are well-suited for human skin studies and initial screening for toxicopathological testing. Also, porcine skin is anatomically comparative to human skin which is indicated as an appropriate model for human skin in topical application study [15].

The aim of this study is to assess the potential use of topical proretinal nanoparticles. The *in vivo, in vitro and ex vivo* approaches including gross and histopathology, immunohistochemistry, advanced imaging techniques, and tape stripping in combination with spectroscopic measurements for the quantitative determination of applied substances and corneocytes were used to investigate the cellular and intracellular targets, efficacy and the safety profiles of the prepared PRN.

The main direct achievement of the studies was the establishment of a set of molecular and imaging tools for the *in vitro, in vivo* and *ex vivo* assessments of epidermal proliferation and differentiation or topical application. The work provides in-depth information on the suitability of the PRN for the topical induction of epidermal proliferation and thickening together with information on toxic side effects through the use of an *in vitro* HaCaT keratinocyte, an *in vivo* animal model and *ex vivo* porcine skin. Information obtained from their work is essential for the development of this retinoid delivery system for the use in clinical dermatology. The work could be a model for other extreme labile substances such as easily degraded vitamins or other active drugs.

1.2 Literature reviews

Retinoids and mechanism

"Retinoids'' is the term introduced in 1976 by Sporn M.B. et al. This term includes both the naturally forms of vitamin A and the many synthetic derivatives of retinol, with or without biological activities. They are lipophilic molecules and easily penetrate the epidermis. For genomic actions, retinoids exert their molecular effects through nuclear receptors which are retinoic acid receptor (RAR) and retinoid X receptor (RXR). The expression of the retinoid nuclear receptors is found that it is tissue-specific and RARγ is the predominant type of RAR mainly expressed in human epidermis [4]. The mechanism of action of topical retinoid in skin occurs when retinoid molecules enter the cellular membrane via non-receptor mediated endocytosis [17]. They are transported to nucleus by cellular retinoic acid-binding protein (CRABP) or cellular retinol-binding proteins (CRBP) and bound to RAR and bind to retinoic acid response elements (RARE) in DNA and modulate transcription of specific genes. Nowadays, there are two recognized types, CRABP-1 and CRABP-2. The latter is shown to express principally in epidermis [18] and control the bioavailability of retinoic acid [19]. Their active forms can influence the expression genes involved in cellular differentiation and proliferation. For non-genomic actions of retinoids, these actions include ultraviolet (UV) adsorption, antimicrobial, antimicrobial, anti-oxidant, and pigmentation activities. The genomic effects of topical retinoids are inducing many of the biologic effects involved in skin aging for example the decreasing the activation of matrix metalloproteinase and oxidative stress, epidermal hyperplasia, epidermal differentiation modulation. These benefits and advantages made many of the vitamin A derivatives topical anti-aging cosmeceutics.

Table 1 Classification of retinoid compounds [20]

Generation	Members
First (non-aromatic retinoids)	Retinol (all-*trans*-retinol,Vitamin A)
	Retinaldehyde
	Tretinoin (all-trans retinoic acid)
	Isotretinoin (13-cis retinoic acid)
Second (mono-aromatic retinoids)	Etretinate
	Acitretin
Third (poly0aromatic retinoids)	Adapalene
	Tazarotene
	Bexarotene

Retinal (Retinaldehyde; RAL)

Retinal and retinoic acids (RA) are important metabolites of retinol. They are unsaturated isoprenoids which are vital for growth and development, differentiation of epithelial tissues, and reproduction. Topical retinoids have been used as therapeutic agents in many dermatological conditions for nearly 4 decades. Additionally they are well recognized as the gold standard for both the prevention and treatment of photoaging [21]. Retinoic acid and many of the synthetic retinoids are used as prescribed preparation only for therapeutic and medical purposes, while other retinoids for example retinaldehyde, retinol and retinyl esters are considered as cosmeceuticals. This is because of their controlled conversion to retinoic acid or their metabolism (direct receptor-independent biologic action) [22].

Retinal (Retinaldehyde;RAL) is a natural metabolites of retinol. It has been proposed for topical use in human. RAL does not bind to retinoid nuclear receptors [23]. Its biological activities for topical use result from enzymatic transformation by epidermal keratinocyte into ligands for these receptors, such as *at*-RA and 9-*cis*-RA [24]. Saurat et al. studied biological effects and tolerance of topical RAL on human skin in 1994 and indicated that 0.05-0.1% topical RAL for 1-3 months has a biologic activity

through the induction of CRABP-2 mRNA and protein and morphologic observations as an increasing of epidermal thickness and alteration in expression of differentiation marker such as K5-6, K14, involucrin, filaggrin and Ki67 immunoreactivity in epidermis. They also studies the tolerance of this topical RAL on human skin in various dermatological conditions and found that more than 20% of patients still had the signs of irritation which were burning, erythema, edema and scaling when they applied 0.1-1% topical RAL while 0.05% topical RAL group induced the irritation only 7% of patients. From this study, they suggested to improve the delivery of RAL which may increase the tolerance of high concentrations. There were many studies that confirmed and extended the biologic activity of retinoids on skin in mouse models at the molecular levels. Didierjean et al. in 1996 conclude that RAL does not bind to retinoid nuclear receptor, its retinoid biologic activity should result from its enzymatic transformation in to all-trans retinoic acid (*at*-RA) by epidermal keratinocytes and murine skin *in vivo* also transforms RAL into *at*-RA. This indicates that RAL can be used topically as a precursor for at-RA, the ligand for retinoic acid receptors which is likely to account for the retinoid biologic effects observed which were the induction of orthokeratosis, loricrin, filaggrin, epidermal thickness, cell proliferation and keratin 50-kDa and the suppression of keratin 65-kDa and 70-kDa.

Mechanism of side effect and irritation

Among retinoic acid receptors (RARs) α, β and γ, RARγ is an important regulator of retinoic acid efficacy in skin because of its abundant expression in epidermis. The researchers found the correlation between the efficacy and irritation of retinoid in *in vivo* models and RARγ mediated transcription activation [27]. The irritation mechanism may be explained by an overload of non-physiological amounts of exogenous retinoic acid in the skin. The pharmacological application of retinal may avoid an overload of RA and less the RA-induced irritation because the conversion of the precursors RAL into RA is controlled by rate-limiting enzymatic steps within the cells [28]. All topical retinoid preparations may induce erythema, exfoliation, dryness, desquamation of skin, pruritus, burning, scaling and even alopecia at the site of

application. Light sensitivity and sunburn may be from the epidermal rarefaction. Systemic administration of retinoids is highly associated with teratogenicity especially early in pregnancy. Fetal deformities by retinoid administration side effects include central nervous system malformation, craniofacial dysmorphisms and heart defects [29].

The ranking order of retinoid-like activity following topical application is as follows: retinoic acid, retinaldehyde, retinol and finally retinyl esters. On other sides, it can be explained and correlated with the metabolic pathway as the closer to retinoic acid, the higher retinoid-like activity they have. The enzymes catalyzed conversion and the metabolic pathway are retinyl esters are turned to retinol, then retinal and finally to retinoic acid. But for the tolerance ranking profile is the opposite way. Retinyl esters is better tolerate than retinol and retinaldehyde while retinoic acid cause severe skin irritation and least for tolerance ranking order [22]. Therefore, cutaneous irritation is a major side effect that is found in topical use and called "**retinoid reaction**" or "**retinoid dermatitis**" [22]. Sensory irritation is characterized by developing itching, stinging or burning on contact with certain substance. It has been known that damaged keratinocytes from the irritant and epidermal barrier interaction can secret plethora of immunoregulatory cytokines and chemokines for instances IL-1, IL-6, IL-8, Il-10, IFN γ, TGFβ [30]. The chemicals or surfactants induce the irritation and initiate the release of IL-1a and subsequently lead to the induction of secondary mediators and molecular responses, finally followed by morphological alterations and the onset of typical symptoms of contact dermatitis. There are currently many known biomarkers of skin irritation for example cell viability (measurement of cell viability; MTT conversion and membrane integrity, neutral red uptake or Lactate dehydrogenase (LDH) release), IL-1α, IL-6, IL-8, TNF-α and IL-10 [31].

Skin drug delivery system

Topical delivery of drug to the skin surface is continually and currently being explored and studied for the local treatment for dermatological diseases. Topical drug delivery systems are classified into 1) conventional systems 2) vesicular systems 3) emulsion systems 4) particulate systems 5) controlled drug delivery system 6) polymer systems. Topical drug delivery is created mainly for the local effect. It can avoid the systemic administration and minimize the systemic administration related-adverse effects.

Nanoparticles as a drug delivery system

Nanotechnology and nanoscience are widely known to have a great potential and impact to bring to many areas of researches and applications especially in biomedical researches and drug delivery systems. Nanoparticles (also sometimes referred to as nanocarriers) are now being designed to improve the transport of agents for diagnosis and therapeutic purposes through biologic barriers; to facilitate entering to molecules or to medicate molecular interactions and also to detect a sensitive molecular changes [32].

One of benefits of nanoparticles (NPs) in biomedical fields or nanomedicine is as a drug delivery agent at desirable sites because of their nanoscale sizes that enhance the effects of drugs. There are two concepts of an ideal drug-delivery system which are firstly the capability to target and secondly to control the drug release [33]. There are many types of nanoparticles for example inorganic nanoparticles, polymeric nanoparticles, solid lipid nanoparticles, liposomes, nanocrystals, nanotubes and dendrimers [34]. There are several advantages of nano-sized particle as a drug carrier. Firstly, it can be designed for targeted treatment. Secondly, it provides sustained and controlled released of encapsulated drugs. Thirdly, it increases the stability of the drug by modified the physic-chemical properties. Finally, it delivers higher concentration of drugs to target area due to an Enhanced Permeation and Retention (EPR) effect [35].

Polymer-based nanopartculate drug-delivery systems: chitosan a natural polymeric nanoparticle

Several polymers and non-lipid materials have been considered and evaluated as carriers for drugs in the nanoparticulate forms [33]. These drug delivery systems have shown advantages and the different properties. Chitosan (CS) is the common name of a linear, random copolymer of β-(1–4)-linked D-glucosamine and N-acetyl-D-glucosamine derived from chitin. Chitosan-Based nanoparticulate drug delivery system, one of the polymeric system, has been researched for a carrier in delivery system and varieties of application such as antigen delivery, transmucosal of peptides and proteins, gene therapy, trans ocular/dermal drug delivery and anti-cancer drug delivery [36]. The advantages of this system help prolong the circulation time of chitosan-bound drug, lead to enhance drug bioavailability and control by the degradation of polymer [37, 38].

Development of new delivery systems for vitamin A derivatives

Over decades, there are many attempts to improve the various delivery systems for vitamin a derivatives such as liposome [39, 40], noisome [41], solid lipid nanoparticles (SLN) [42-44] and polymeric nanoparticles (NP) [45]. The new preparations compared with conventional carriers which are based on improving stability, solubility, efficacy, non-irritative and non-toxic for topical use seem to be well appropriated for skin. For example, It has been shown by Jenning and colleagues in 2000 that retinol and retinyl palmitate encapsulated in SLN could be effectively deliver to the upper or outermost skin layers and had a sustained release properties. Within the first 6 hours retinol in solid lipid nanoparticles displayed controlled release. In 2007, SLN was used for topical delivery preparation for skin-targeting outcome and effect of isotretinoin as a new formulation for the treatment of severe acne. It was shown to be a good stability of chemicals during the period of 3 months and the *in vitro* permeation ability into skins of isotretinoin from SLN by using Franz diffusion cells [42]. However the experiments to enhance the drug penetration to skin are successful, the skin target mechanism is unclear and the other relative mechanism need further

investigations in future [46]. In addition, encapsulation using nanoparticulate system especially polymeric nanoparticles (NP) which are biodegradable is an increasingly and expanding implement scheme in drug delivery [47]. Additionally, NPs have also been proposed for topical administration to improve percutaneous transport into the skin through its biological barrier. There were several works have been demonstrated the advantages of vitamin A derivatives in matrix type polymeric nanoparticles [45, 48-50].

In 2011, our laboratory has demonstrated a new delivery system which can deliver retinyl acetate at the hair follicle [51] and in this 2016 we can successfully prepared water dispersible PRN which is still stable although it was kept in the water at neutral pH and at room temperature up to 8 months protected from light. Moreover, it clearly exhibited the sustained release or controlled release property of retinal into human synthetic sebum (pH 5) [13].

All studies demonstrated that the novel forms of vitamin A derivatives delivery system can be an effective way to stabilize and encapsulate them with NPs system for pharmaceutical applications. Use of the newly innovative methods of delivery is also a feasible way to maintain or even improve efficacy and minimize the irritative or undesirable side effects [52]. However, the possibility to encapsulate vitamin A derivatives in polymeric nanoparticles (NPs) and their potential to improve the skin conditions both *in vitro* and *in vivo* have not been yet evaluated.

Skin as a site for particle delivery

The main entrance routes for nanoparticles and topical nanoparticles drug delivery occurs in three main sites in stratum corneum surface as intercellular pathway, follicular pathway as openings of the hair follicle and transepidermal pathway [53]. In principle, for penetration of nanocarrier into the skin, the intercellular and follicular route in healthy skin may be most relevant. Particulate depositing in furrow atop the stratum corneum may continuously release their payload, which may become effective only if these molecules show suitable features for skin penetration such as moderate lipophilicity [54]. Currently, it has been known that nanoparticle with a

diameter of 20-320 nm can be kept in hair follicle up to 10 days and considered as an important reservoir or storage structure and shunt penetration pathway [47, 55]. And the researchers also found that the particle penetration *in vitro* was presented to be increased if the massage was applied [56].

Skin biology and the influence of vitamin A on epithelial proliferation and differentiation

As we known that the skin is the largest organ in the body. Skin functions are protection, sensation, thermoregulation, metabolic functions and sexual attractant [57]. The skin has three main layers: epidermis, dermis, subcutis or hypodermis and the skin appendages which are hair follicles, sweat glands and sebaceous glands.

Histologically, the type of the main population of cell in the epidermis is the keratinocyte. At haired skin, the epidermis has four layers or strata. From the basal layer which is innermost to the outermost which are the differentiated layers, theses layers in the epidermis are the stratum basale, spinosum, granulosum, and corneum. The basement membrane separated the epidermis from the dermis. Keratinocytes are joined to each other by desmosomes. The germinal cells which is the cells in the stratum basale undergo mitosis and produce epidermal cells while cells in the stratum spinosum and granulosum are maturing. They can generate the keratin filaments and also keratohyalin granules. In the cells of stratum corneum, there are composed of a compacted layer of anuclear squamous cells be form of keratin filaments and keratohyaline granules. [58].

The keratins are structural proteins which belong to the family of intermediate filament [59]. They are prominent in epidermal cells and also present in stratified squamous epithelia other than epidermis. The expression pattern is very specific and is frequently used as a paradigm of epidermal differentiation and physiology [60]. The stages of epidermal differentiation are characterized by the expression of specific markers [61].Only keratinocytes in the basal layer proliferate and move toward the surface. They express K5 and K14 [60]. In suprabasal layer, K10 is expressed. In addition, the cornified envelopes (CE) including involucrin (IVL), filaggrin (FLG) and loricrin are synthesized during the terminal stages of keratinocyte differentiation in granular layer

[62]. During this process keratinocytes initiate synthesis of important differentiation-depepndent structural protein.

Vitamin A exerts an important influence on epithelial differentiation and profoundly affect epithelial cell organization and among the genes affected by retinoids in epidermis are keratin. The different keratin profiles are observed when vitamin A and its derivatives added to topically delivered to human skin *in vivo* focused on K1, K5, K10 and K14 [25, 63-73]. The studies reported changes which are both reduction, induction and no effect. Therefore, keratin gene expression may be influenced by retinoids in many complex means [74]. The physiological importance of these direct interaction of keratin expression in epidermal differentiation and retinoid is still needed to be explore focusing on the K5, 14 and 10 which express mainly on basal and suprabasal layers of epidermis.

Skin models for transdermal absorption studies

To evaluate and assess transdermal activities and absorption of a novel chemicals, many of the animal models are well-suited for human skin studies and initial screening for toxicopathological testing. These animals include primate, porcine, rodents which are mouse, rat, rabbit and guinea pig. Due to its accessibility, laboratory rodents' skin (mice, rats and guinea pigs) is the most widely and generally used in *in vitro* and *in vivo* percutaneous permeation studies [75]. The preferences of the use of rodents are due to their small size, easy handling, relative low cost and much more convinience for the study of dermal toxicity than the pig [76]. In regard to human skin structural similarity, rat and pig skin show the thickness of whole skin, epidermis close to human [76, 77] **(Table 2)**. Other than rat skin, other rodent skins always exhibit the higher permeation rates than human skin [78, 79]. The permeation kinetic parameters of the rat skin are regularly comparable with those in human. However, one of the disadvantages of rat skin is a greatly high density of hair follicles. It is required hair removing and clipping before the beginning of the experiment. With all their limitations, transdermal absorption studies in animal models are multi-factorial multistep process with influenced factors mentioned above and will provide a screening purposes and

predictions for topical drug delivery development and some certain biological and clinical effects. To predict and screen the cutaneous irritant possibility of novel chemical products is the important procedure for the complete evaluation program. A main achievement in the optimization and development of dermal or transdermal drug preparation is to understand the factors that may influence a good *in vivo* performance and relationship [75]. From the past, the main approach in the preclinical studies of the novel topical drug development is to use the animal models by topical apply to animal skin [80]. Some animal testing studies are not possible in the first or initial steps in novel drug developments researches. Additionally, it is suggested that the reliable data for skin absorption should be collected from human studies. Therefore, the demanding tasks in the transdermal drug researches is to find relationship between *in vitro* and *in vivo studies* and both in animals and human approaches.

Table 2 Thickness of skin strata and size of hair follicles in mice, rat, pig and human *[76]*

	Stratum corneum (µm)	Epidermis (µm)	Whole skin (mm)	Diameter of follicle (µm)
Mouse	6	13	0.84	26
Hairless Mouse	9	29	0.70	46
Rat	18	32	2.09	25
Pig	26	65	3.43	177
Human	17	47	2.97	97

1.3 Research hypotheses

1. Proretinal nanoparticles have no cytotoxicity and possess retinoid biological activities *in vitro* HaCaT cells.

2. Topical application of proretinal nanoparticles can eliminate the side effect of retinoid dermatitis in *in vivo* model.

3. Topical application of proretinal nanoparticles has higher retinoids biological activities in term of epidermal proliferation and differentiation and the expression of cellular retinoic acid binding protein-2 (CRABP-2) compared with conventional retinal.

4. Intercellular and follicular pathway could be the major penetration pathways of topical proretinal nanoparticles.

5. The use of microneedle loaded with proretinal nanoparticles is possible to deliver and bypass proretinal nanoparticles to dermis directly.

1.4 Research objectives

1. To investigate the safety of proretinal nanoparticles in the toxicopathological views in *in vitro* HaCaT cells and *in vivo* rat skin

2. To investigate efficacy of proretinal nanoparticles in the views of biological effects of the proretinal nanoparticles on epidermal proliferation and differentiation

3. To investigate the intercellular and follicular penetration behavior of proretinal nanoparticles and the released model drug

4. To assess the possibilities of the intradermal delivery of PRN-loaded microneedles by non-invasive imaging techniques

To fulfill these objectives, this dissertation presents our findings into 5 separated chapters including chapter (1) introduction and literature reviews, (2) the studies of topical application of proretinal Nanoparticles in biological Activities, epidermal proliferation and differentiation, follicular penetration, and skin tolerability, (3) percutaneous absorption and follicular penetration of retinal by topical application of proretinal nanoparticles, (4) microneedle-facilitated intradermal proretinal nanoparticles delivery and (5) general conclusion, discussion, and future recommendations.

1.5 Experimental designs
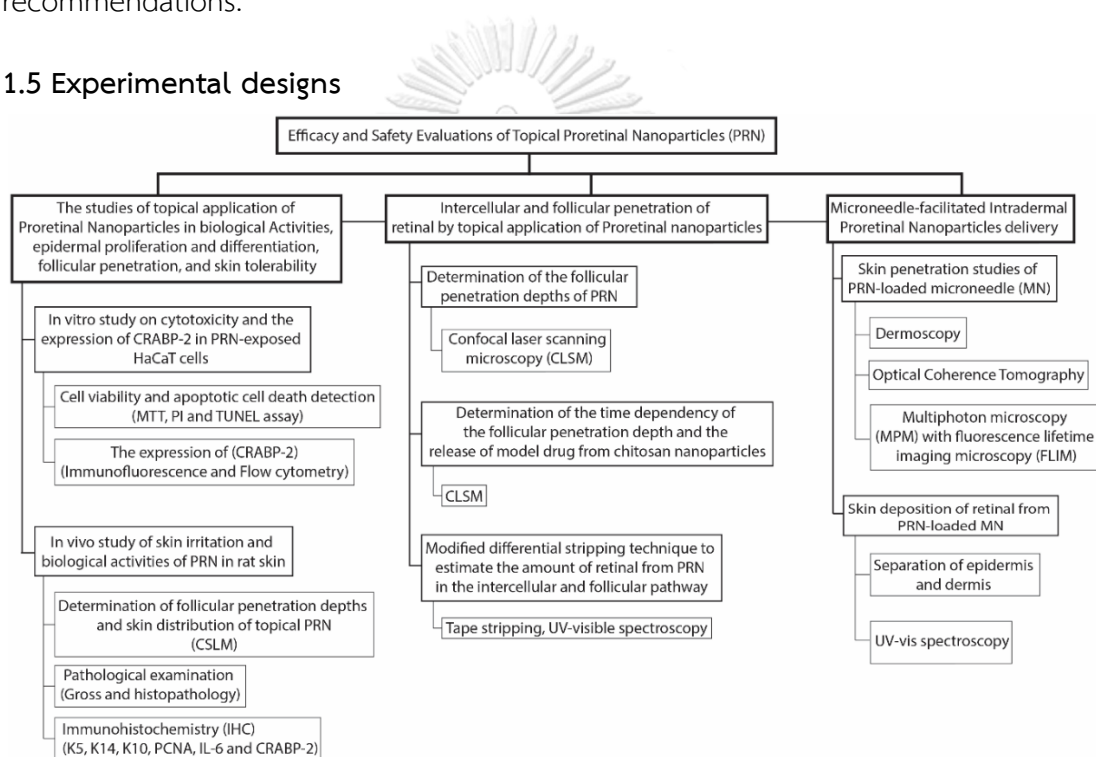
1.6 Advantage of study

This study formed the basis for the establishment of a novel transdermal drug delivery system that would be of particular use in clinical dermatology for the topical application of extreme labile substances such as easily degraded vitamins or other active drugs. Based on the outcomes and results of this research, topical application of proretinal nanoparticles showed that topical application proretinal nanoparticles are safe, non-irritative, successfully penetrate into hair follicles and possess retinoid biological activities to skin as the ability to induct and regulate epidermal proliferation

and differentiation. Additional approaches can be taken to further clinical studies, it could be beneficial in some retinoid-responsive skin conditions in the future. Although further investigations are necessary to clarify the required doses and dose intervals in clinical settings, the suggested system may help to overcome the main problems of topical retinoid therapy, which are skin irritation, chemical, and photochemical instability and low bioavailability.

Keywords: Retinal; Nanoparticles; Epidermis; Hair follicles; Skin; Vitamin A

คำสำคัญ เรตินัล อนุภาคนาโน หนังกำพร้า รูขุมขน ผิวหนัง วิตามินเอ

CHAPTER II

The studies of topical application of proretinal nanoparticles in biological activities, epidermal proliferation and differentiation, follicular penetration, and skin tolerability

Manuscript in submission process in the topic of

Topical application of proretinal nanoparticles in biological activities, epidermal proliferation and differentiation, follicular penetration, and skin tolerability

Benchaphorn Limcharoen, Pimolphan Pisetphakdeekul, Pattrawadee Toprangkobsin, Supason Wanichwecharungruang and Wijit Banlunara

Highlight

- Proretinal nanoparticles (PRN) has been developed to overcome the side effect of the use of topical application of retinoids as retinoid dermatitis.

- *In vitro* increased expression of cellular retinoic binding protein-2 (CRABP-2) by Proretinal nanoparticles (PRN) with no short-term cytotoxicity was clarified in HaCaT cells.

- Proretinal nanoparticles (PRN) served as an excellent retinal reservoir with effective follicular penetration in time-independent behavior.

- Topical application of PRN for 28 days clearly increased cell proliferation and differentiation in rat epidermis resulting in the thickening of the epidermis and increased levels of various retinoid associated biochemical markers such as K5, K14, K10, PCNA, and cellular retinoic binding protein-2 (CRABP-2) except IL-6 without side effect of retinoid dermatitis.

2.1 Abstract

Proretinal nanoparticles (PRN), the retinilidene-chitosan nanoparticles, has been developed to overcome the physicochemical instability of retinal and to lessen the dose-dependent cutaneous irritation, through sustaining the release of retinoid. Comparing to conventional retinal at the same concentration, PRN had no cytotoxicity and could induce HaCaT cells to express more CRABP-2 protein. Comparing to rats topically applied with conventional retinal which showed clear skin irritation and inflammation, daily topical application of PRN to rats for 28 consecutive days produced neither irritation nor inflammation, but significantly increased of epidermal proliferation, epidermal thickness, CRABP-2 expression, and up-regulation of various differentiation markers including keratin (K) 5, K10, K14, CRABP-2 and PCNA. Through the use of confocal laser scanning microscopy, we observed the *in vivo* follicular penetration of PRN with the depth of penetration independent of post-application time.

Key words*: Retinaldehyde; Nanoparticles; Epidermis; Skin; Vitamin A

2.2 Introduction

Retinoids are pivotal regulators for differentiation and growth of skin [2] and have been used in clinical dermatology for their activating effects on epidermal proliferation and differentiation [26] in some skin diseases including psoriasis, acne, disorder of pigmentation, seborrhea and photo aging [4]. Topical retinoids are used mainly for the local effect with the benefit of minimized systemic adverse effects. Retinal, a natural precursor of retinoic acid, is bioloically active when topically applied, but is still irritative to human skin [5] and highly unstable. The compounds can be easily autooxidized and photooxidized [7, 8]. Like other topical retinoids, topical retinal formulations may induce cutaneous irritation as erythema, exfoliation, dryness, burning and scaling at the site of application [81]. These major side effects for all topical retinoids have been called "retinoid dermatitis" [22]. Since retinoid irritation is dose dependent [82], a drug delivery system that can improve the transport of retinoids to the site of action and sustainably release the drugs at the level below the irritating level could improve retinoid action and also solve the irritation side effects.

For genomic action, the mechanism of topical retinoids starts when retinoid molecules cross the cell membrane via non-receptor mediated endocytosis [17]. They are then transported to nucleus by cellular retinoic acid-binding protein (CRABP). There in the nucleus, they modulate transcription of specific genes by binding to retinoic acid receptor (RAR) and retinoic acid response elements (RARE) in DNA. One of the important genes involves by this mechanism is the cellular retinoic acid binding protein-2 (CRABP-2), the protein that mainly is expressed in epidermis [18]. This CRABP-2 is thus being controlled by the bioavailability of retinoic acid [19]. Furthermore, among other genes regulated by retinoids is keratin [74]. Keratins, intermediate filament proteins, are vital to epidermal integrity and are usually expressed selectively in dividing cells and terminally differentiating cells [83]. Therefore, they are useful biochemical markers for the study of the molecular mechanisms during the process of epidermal proliferation and differentiation [83].

We have developed proretinal nanoparticle (PRN) that can target retinal to the needed skin sites and sustained release the retinal at the sites so that optimal efficacy can be achieved without the undesirable side effects associated with an overloading of non-physiological amounts of exogenous retinoid in the skin [84]. This PRN is based on the reversible linkage between retinal molecule and chitosan polymer and the assembling of the retinal-grafted chitosan polymer into nanoparticle. Previous study of the material has shown promising physicochemical properties and stability with promising *in vivo* clinical results.

To understand how PRN exerts those physiological effects on skin, it is essential to know the distribution of this material on skin. Thus, here we show and discuss the results from our studies on the follicular penetration depths and skin distribution of topical PRN. Then we perform various experiments to understand the molecular mechanisms of how this material wield its effect on skin proliferation and differentiation. We studied the effects of topical PRN on key molecular specific markers for epidermal proliferation and differentiation and skin irritation of the damaged keratinocytes including keratin 5 (K5), K14, K10, interleukin-6 (IL-6), proliferating cell nuclear antigen (PCNA), and cellular retinoic acid binding protein-2 (CRABP-2). Cell

viability and the *in vitro* expression of CRABP-2 in keratinocyte, the main population of cells in the epidermis, were also studied in HaCaT cells.

2.3 Materials and methods

2.3.1 Materials

2.3.1.1 Proretinal nanoparticles (PRN) preparation

The synthesis of PRN with approximately 35% w/w of retinal loading was carried out as described in our previous report [84]. Briefly, retinal (Sigma Aldrich) was incubated with chitosan (Taming Enterprise, Samut Sakhon, Thailand) solution which was prepared by dissolving in acidic solution and then adjusting the pH back to around 6, at the retinal to chitosan weight ratio of 1:3 (corresponded to the mole ratio of glucosamine unit to retinal of 4.5:1) and the obtained retinal-grafted chitosan was allowed to self-assemble into nanoparticles. *All-trans*-retinal (conventional retinal solution; RAL, Sigma Aldrich) was dissolved in ethanol at the same retinoid concentration of PRN to serve as the control.

2.3.2 Methods

Experiment A: In vitro **study on cytotoxicity and the expression of cellular retinoic acid binding protein-2 (CRABP-2) in PRN-exposed HaCaT cells**

2.3.2.1 Cell culture and retinoid exposure

The immortalized non-tumorigenic human keratinocyte cells (HaCaT) were maintained in Dulbecco's modified Eagle's medium (DMEM) supplemented with 10% fetal bovine serum (FBS), glutamine and amphotericin B, penicillin and streptomycin at 37°C, 5% CO_2 condition. They were subcultured with 0.25% trypsin-EDTA. All reagents were purchased from Gibco; Thermo Fisher Scientific, Inc., MA, USA.

HaCaT cells were seeded in 24-well plates at a density of 40,000 cells per well. The three control groups were cells incubated with 1) 20% ethanol in DMEM per well as a positive control, 2) DMEM per well as a negative control and 3) chitosan nanoparticles (CS) as the unloaded nanocarrier. The two experimental groups were cells treated with 4) conventional RAL solution and 5) PRN at a concentration of RAL 1 µg/mL (3.33 µM of retinoid). All treatments were incubated for 24 h. Cells and

retinoids were handled and performed in the dark concerning the light sensitivity of retinoid.

2.3.2.2 Cell viability and apoptotic cell death detection

2.3.2.2.1 Cell viability

Cytotoxicity test was studied using MTT (3-(4,5-dimethylthiazol-2-yl)-2,5-diphenyltetrazolium bromide) (Molecular Probe, Life Technologies, OR, USA). The retinoid exposures following above designated experimental groups for 24 h were terminated by washing with PBS, then MTT solution (1 mg/mL) and cells were incubated for 10 min. Dimethyl sulfoxide (DMSO) was added to dissolve the formazan salt and its optical density (OD) was measured using spectrophotometer at 570 nm (Epoch Microplate Spectrophotometer; BioTek Instrument, VT, USA). Each concentration was independent by triplicated. Calculation for cell viability percentage followed this formula OD of the experimental group/OD negative control*100 = % cell viability

2.3.2.2.2 Apoptotic cell death detection

Terminal deoxynucleotidyl transferase-mediated dUTP nick end labeling (TUNEL) assay was done to detect the fluorescein-labeled double-stranded cleavage of DNA using *in situ* cell death detection kit, fluorescein (Roche Applied Science, Germany) following the manufacturer's instruction. Five thousand cells were grown in 8-well chamber (Thermo Fisher Scientific) and incubated following above designated experimental groups for 24 h. Afterward, cells were fixed with 4% paraformaldehyde (PFA) and incubated in 0.1% Triton X-100 in 0.1% sodium citrate solution. The cells were then incubated with the TUNEL reaction. Subsequently, the cells were counterstained with DAPI (Fluoroshield®, Abcam, Cambridge, UK). Cell were examined by EVOS FLoid Cell Imaging Station (Thermo Fisher Scientific) and 5 non-overlapping fields were examined at an objective lens of 200x magnification for analysis.

2.3.2.3 The expression of cellular retinoic acid binding protein-2 (CRABP-2)

2.3.2.3.1 Immunofluorescence of CRABP-2 of PRN-exposed HaCaT cells

HaCaT cells were seed in an 8-well-chamber at 20,000 cells/well. After the incubation with designated groups of treatment, cells were fixed with 4% PFA, then permeated with 0.1% v/v Triton X100, blocking with 1% BSA, incubated with polyclonal rabbit anti-CRABP-2 antibody (Sigma Aldrich) at 4°C overnight, further incubated with secondary antibody (Alexa Fluor® 647-conjugated goat anti-rabbit IgG H&L antibody, ab150079, Abcam) at dilution of 1:200 in BSA, finally counterstained with DAPI and analyzed under confocal laser scanning microscopy (FV10i-DOC, Olympus, Tokyo, Japan).

2.3.2.3.2 Flow cytometric analyses of propiodium iodine (PI) and CRABP-2 expression in PRN-exposed HaCaT cells

After *in vitro* incubation, HaCaT cells were harvested and washed twice with Ca^{2+}, Mg^{2+} free PBS supplemented with 1% FBS and sodium azide (FAC buffer) at 4°C, 1000 RPM for 4 min. The cells were then fixed in 4% PFA. For staining of PI, the cells were stained with 50 mg/mL PI (Sigma Aldrich) diluted in 0.1% Triton X-100 at 4°C for 15 min. For staining of CRABP-2, the dilution of 1:50 of CRABP-2 antibody diluted in 0.25% Triton X-100 were added and incubated in the dark, at 4°C for 45 min. Then, the dilution of 1:200 of Alexa Fluor® 647-conjugated goat anti-rabbit IgG, the secondary antibody, was added and incubated in the dark at 4°C for another 45 min. Isotype control antibodies were included for background cut-off the fluorescent minus one (FMO). The cells were analyzed using FC 500 MPL flow cytometry (Beckman Coulter, CA, USA).

Experiment B: *In vivo* study of skin irritation and biological activities of PRN in rat skin

2.3.2.4 Animals

Twenty-nine-week-old male Wistar rats were obtained from National laboratory animal centre (Mahidol University, Bangkok, Thailand). The animal care and use protocols were approved by the guidelines for the use of animal for the scientific purpose of Chulalongkorn University animal care and use committee (protocol

no.13310063 and 1731034). The 200 µL of liquid samples was topically applied on skin of dorsal back area and massaged in circular motion for 1 min.

2.3.2.5 Determination of follicular penetration depths and skin distribution of topical PRN

PRN was labelled with 5(6)-carboxytetramethylrhodamine (Sigma Aldrich). A detailed description of the synthesis of the rhodamine-labelled PRN is provided in the appendix A of supplementary materials (SA). Nine animals were used in this study. The animals were anesthetised, and their hair at dorsal back was shaved off. The skins were biopsied at 3, 6 and 12 h after a single topical application by 8 mm-diameter biopsy punches. The biopsied samples were snapped frozen in liquid nitrogen, embedded in OCT compound (Leica biosystem, Wetzlar, Germany) and sectioned into 10 µm thickness. To identify epidermis by immunostaining technique, the sections were treated with monoclonal mouse anti-pan-cytokeratin antibody (Sigma Aldrich), dilution of 1:300, incubated with dilution of 1:200 FITC conjugated goat anti-mouse IgG 1 antibody 1 h (BioRad, CA, USA) and stained nuclei with DAPI examined with confocal laser scanning microscope (CLSM, FV3000, Olympus, $\lambda_{ex/em}$ of 555/580 nm). The fluorescent signals at 100x magnification were observed. The skin distribution and averages of follicular penetration depth of 5(6)-carboxytetrarhodamine-labelled PRN at various post-application time points were determined using 10 hair follicles/animal at each time point (9 animals, total of 90 samples for each time point), using FV30S-SW software (Olympus). Hair follicles of the untreated skin area were observed as negative control.

2.3.2.6 Pathological examination

Twenty rats were divided into 4 groups: two control groups including 1) distilled water (DW) as negative control and 2) chitosan nanoparticles (CS) as unloaded nanocarriers, and two sample-treated groups including 3) topical application of conventional retinal solution (RAL; 0.1 % w/v or at 3.33 mM of retinoid) and 4) PRN (at 3.33 mM of retinoid). Rats in each group were topically applied with the reagent assigned by the groups once daily for 28 days. On day 7, 14, 21 and 28, the test protocol followed the OECD 410 guideline for testing of chemicals "Repeated Dose

Dermal Toxicity: 21/28-day Study".[85] Scoring system was evaluated through the signs of skin reaction (animal irritation test) followed ISO 10993-10: biological evaluation of medical devices- Part10: Tests for irritation and skin sensitization (Draize test),[86] and the modified of Machtinger et al., 2004 [87]. The full thickness of skin biopsies was punched at day 7, 14, 21 and 28 and fixed in 10% buffered formalin. The paraffin embedded skin samples were sectioned at 4 μm and stained with hematoxylin and eosin (H&E) for histological evaluation. Thickness of the epidermis was microscopically measured in five random repetitions per section at 400X magnification (I-solution software, IMT, Canada).

2.3.2.7 Immunohistochemical evaluations

Immunohistochemistry (IHC) of these proteins (K5, K14, K10, PCNA, IL-6 and CRABP-2) were analyzed from samples on day 7, 14, 21 and 28 of treatment. The details of primary antibodies were provided in supplementary materials **(Table 3)**. Quantification of immunochemical staining were microscopically performed hereinafter; the percentage of K5, K10, K14, and CRABP-2 positive area in epidermis and IL-6 in dermis over the area on five consecutive serial sections from each animal at 100X magnification. Images were then quantified by computerized image analysis (ImageJ software, NIH) for the determination of the positive stained area. The percentage of the stained area was calculated as the ratio of binary threshold image and the total field area. For PCNA staining, the average numbers of positive PCNA in nucleus of cells were counted in the 1000 μm length of epidermis. The PCNA index was determined as the percentage of positive cells in 1000 μm of epidermis.

2.3.2.8 Statistical analyses

Statistical analyses of data were conducted using the GraphPad Prism software (GraphPad Software, CA, USA) using one-way ANOVA, two-way ANOVA) followed by Turkey's multiple comparison tests, pair t-test for comparison of two pairs of samples by the unpaired t-test. Significant differences were considered significant at p value < 0.05.

2.4 Results

Experiment A: In vitro study on cytotoxicity and the expression of cellular retinoic acid binding protein-2 (CRABP-2) in PRN-exposed human HaCaT keratinocytes

2.4.1 Cell viability and apoptotic cell death detection

Through the use of MTT assay, at $p>0.05$, we observed the following order of cell viability: negative control (DMEM) $\approx$ unloaded nanocarriers (CS) $\approx$ PRN-treated cells $\approx$ RAL-treated cells >> positive control (20% ethanol in DMEM) **(Fig. 1)**. However, the difference between RAL and PRN-treated cells was observed by TUNEL assay which detected DNA strand breaks in the cells **(Fig. 2A-E)**. The quantification of the numbers of apoptotic cells at 24 h are shown in **Fig. 2F**. Comparing to RAL-treated cells, PRN-treated HaCaT cells showed a lower level of DNA fragmentation ($p<0.05$).
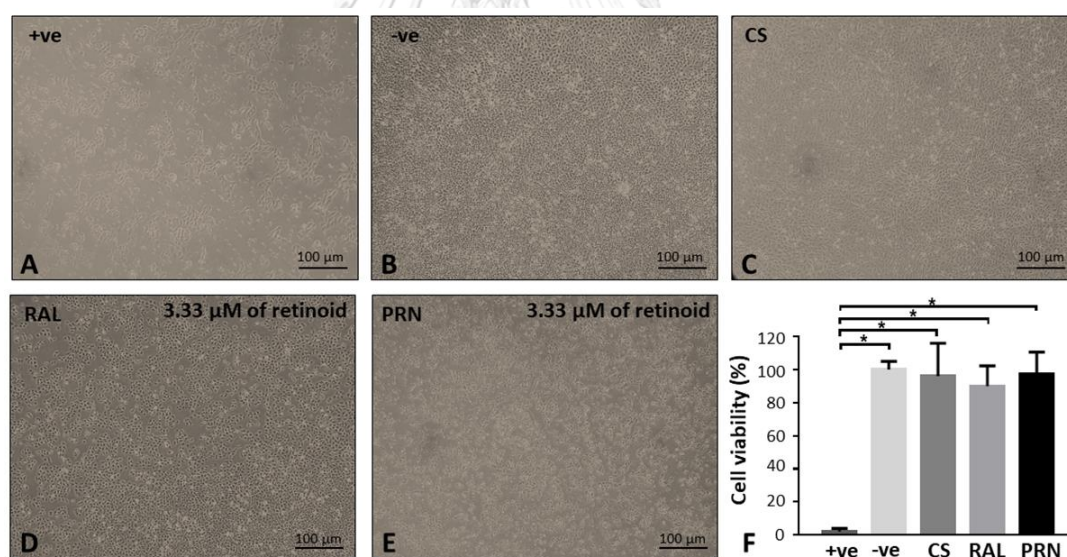
Figure 1 Cell morphology and viability of HaCaT cells after 24 h exposure to treatments. (A-E; +ve; 20% ethanol in DMEM, -ve; DMEM, CS; unloaded nanocarriers, RAL; conventional RAL solution and PRN -treated cells). (F) MTT assay expresses as a percentage of cell viability (mean ± SD). * indicates significant difference ($p<0.05$) between the indicated groups.
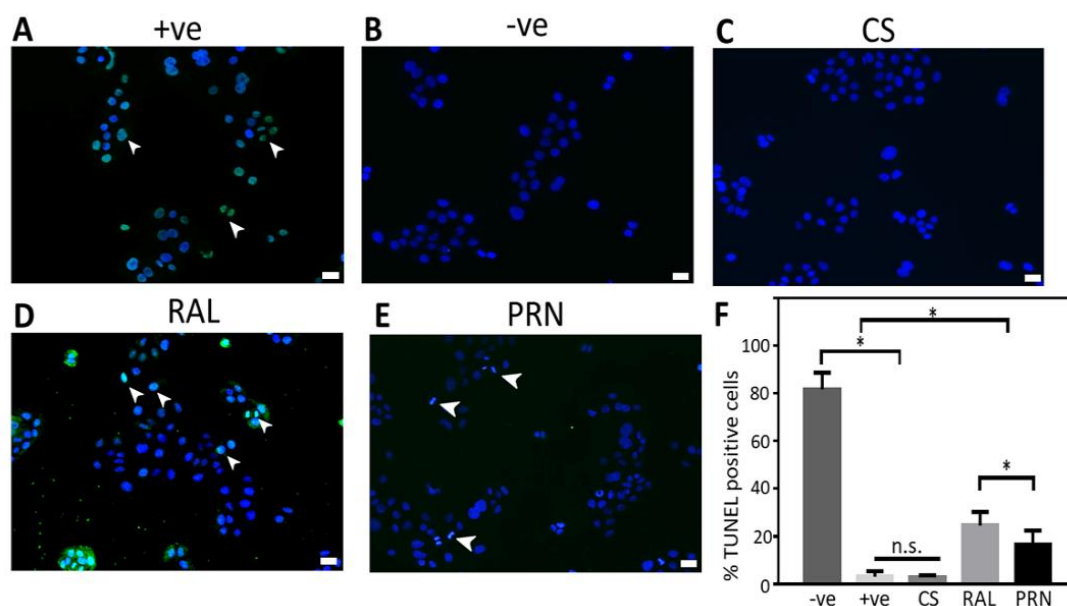
Figure 2 Apoptotic cell death by TUNEL assay

(A-E) with arrows indicating the TUNEL-positive nuclei of HaCaT cells, and quantitative analysis of apoptotic cells (F) with * indicating significant difference (p<0.05) between the indicated groups and n.s. indicates no statistical difference (p>0.05) for cells treated with 20% ethanol in DMEM (+ve), DMEM (-ve), CS (unloaded nanocarriers), RAL (conventional retinal solution) and PRN suspension (PRN). Bars at the lower right corner of Figure A-E denote 10 µm.

2.4.2 The expression of cellular retinoic acid binding protein-2 (CRABP-2) in HaCaT cells

Higher expression of CRABP-2 in cytoplasm was clearly observed in cells exposed to RAL and PRN **(Fig. 3B and 3C)** for 24 h, as compared to that observed in the negative control (DMEM) **(Fig. 3A)**. The mean fluorescence intensity (MFI) of CRABP-2 expression was quantified and HaCaT cells were gated **(Fig. 3D)**. Notably, the mean fluorescent intensity of CRABP-2 expression in PRN-treated cells (MFI 27±1.8) was remarkably greater than that of the RAL treatment (MFI 16±4.6) ($p<0.05$) **(Fig. 3E-F)**. Cells treated with RAL and PRN showed similar insignificant cell death to that of the negative control ($p>0.05$) as measured with the propidium iodide (PI) **(Fig. 3G)**.
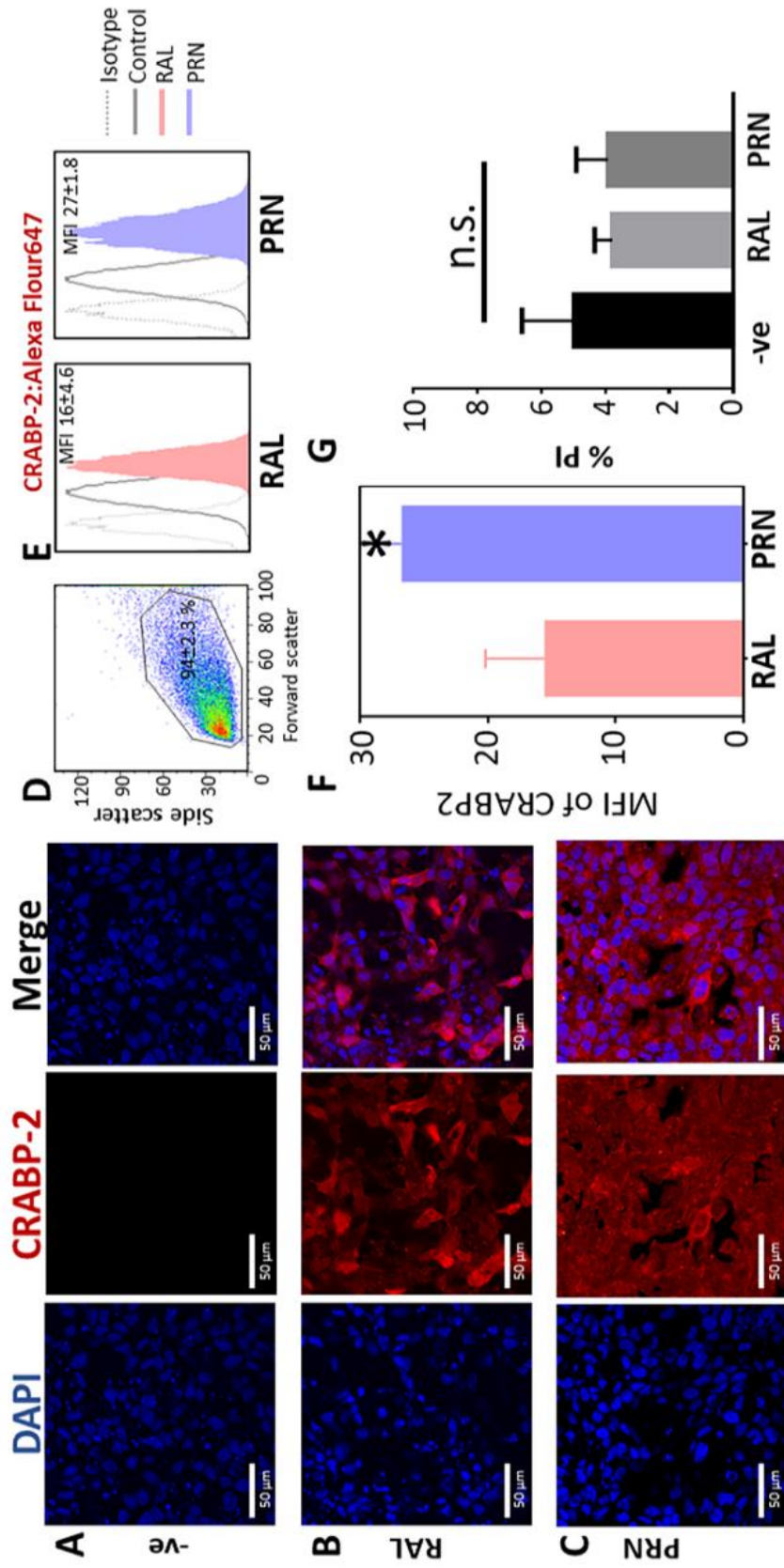
Figure 3 Immunofluorescence and flow cytometry of CRABP-2 in treated HaCaT cell.

The representative confocal images of the intracytoplasmic localization CRABP-2 (red fluorescence) in the monolayer of HaCaT cells after 24 h exposure to DMEM (-ve; negative control), RAL and PRN are shown in **(A)**, **(B)** and **(C)**, respectively. Flow cytometric analyses and histograms of MFI of CRABP-2 expression of the treated cells are shown in **(D)** and **(E)**, respectively. The comparison of MFI of CRABP-2 expression between RAL-treated cells (fill pink) and PRN-treated cells (fill purple) is shown in **(F)**, whereas percentages of PI positive cells are shown in **(G)**, with significantly difference ($p<0.05$) marked with * and insignificant difference ($p>0.05$) marked with n.s.

Experiment B: In vivo **study of skin irritation and biological activities of PRN in rat skin**

2.4.3 Determination of follicular penetration depths and skin distribution of topical PRN application

The CLSM images of the topically PRN-treated skin clearly showed some accumulation of rhodamine-labelled PRN (red fluorescent signals) along the epidermis (green fluorescent signals) and in the hair follicles of the skins collected at 3, 6 and 12 h after single application **(Fig. 4)**. The average PRN follicular penetration depths obtained from samples taken at 3, 6 and 12 h post application were 234±85, 173±64 and 224±82 μm, respectively (**Fig. 4E**) and statistical analysis indicated no significant (p>0.05) difference among the three averages.
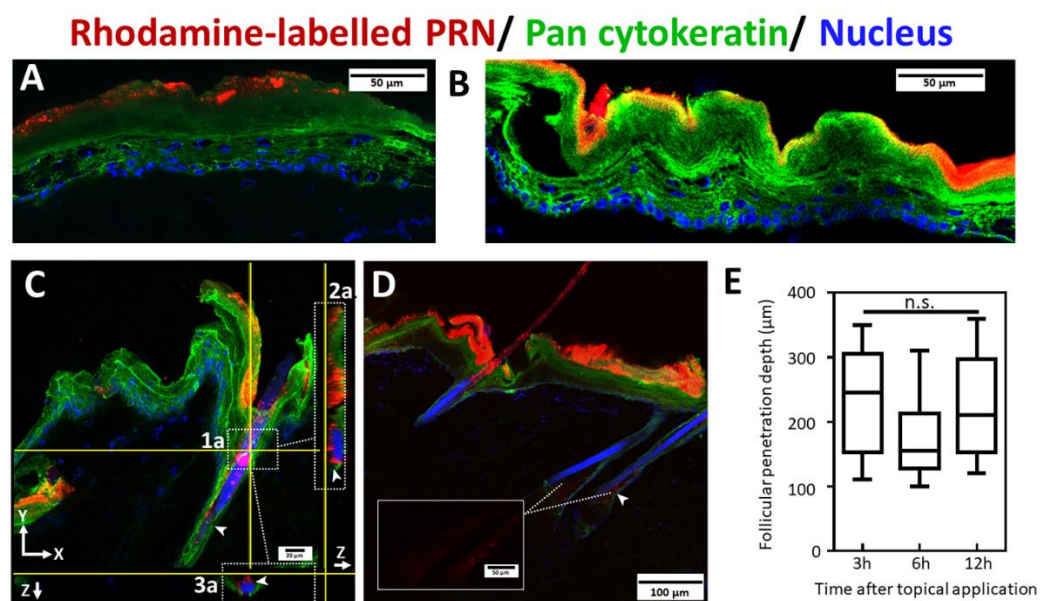
Figure 4 Follicular penetration of rhodamine-labelled PRN in rat skin observed by CLSM. Distributions of the rhodamine-labelled PRN in the skin taken at 3 h and 12 h post PRN application are shown in **(A)** and **(B)**, respectively, with nuclei counterstained with DAPI (blue) and epidermis stained with a pan cytokeratin antibody (green). Follicular penetration of PRN (~220 μm) at 6 h post application is shown in **(C)**. Using optical sectioning, the fluorescence signals in x-y plane is shown in the inset 1a, and the fluorescence signal in x-z axis is shown in insets 2a and 3a, with arrowheads indicating

PRN locations. Distributions of PRN on the epidermis and in hair follicle at 12 h post application are shown in **(D)** and **(E)**, respectively. The bar graph summarizes the follicular penetration depths of rhodamine-labelled PRN over times (*p*>0.05). Images are representatives of observations in 3 rats.

2.4.4 Pathological studies

According to the scoring system for skin irritation (ISO 10993-10: 2010), the results were recorded regarding the formation of erythema, eschar and edema at day 7,14, 21 and 28 post first application. Both the two control groups (DW and CS) and the skin of rats treated once daily with PRN showed no sign of inflammation at any time points **(Fig 5)**. The statistical analyses indicated no significance difference in mean macroscopic skin lesion among PRN-treated group and the two control groups at all time points **(Table 4)**. In contrast, from day 7 skin lesions are noticed in RAL-treated group and started to exhibit the formation of erythema, eschar and edema on day 7 and the signs with irregularly raising and roughened scaling heterogeneously persisted until day 28 **(Fig. 5A).** The grading indicates slight to moderate irritation **(Fig. 5B).**
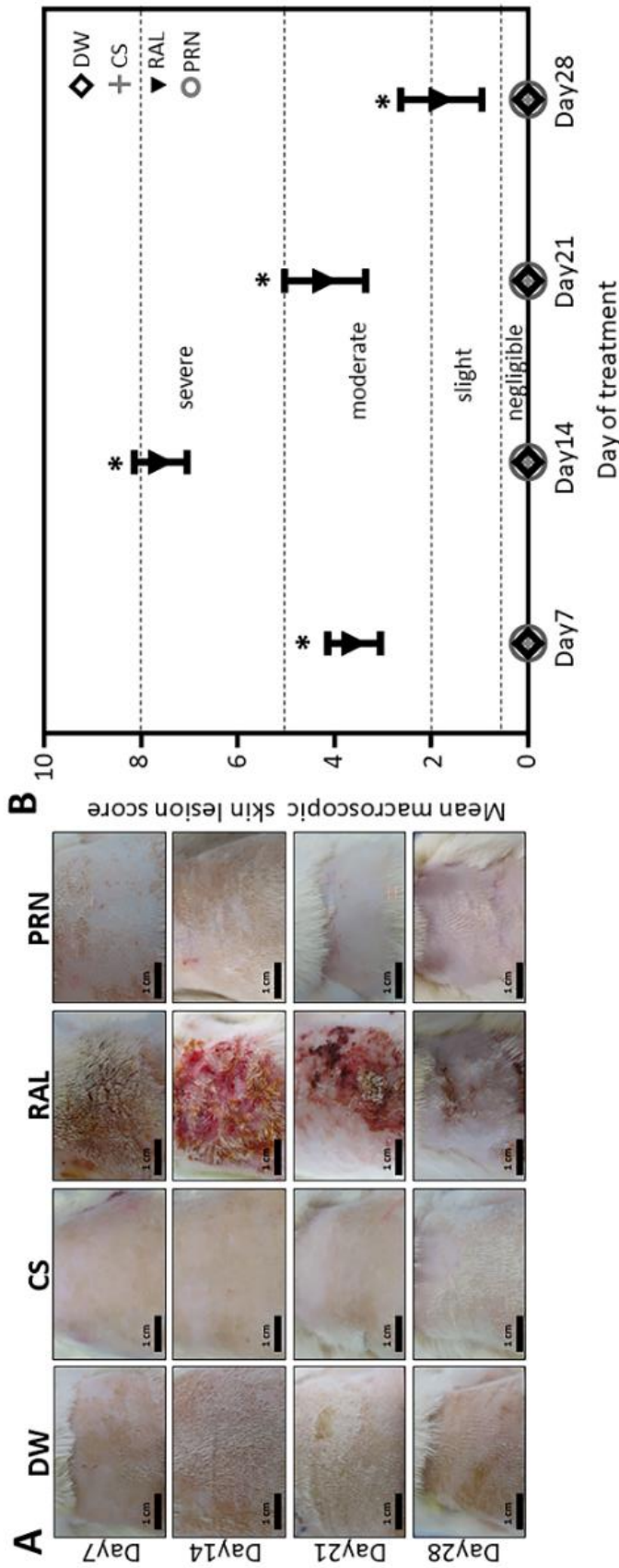
Figure 5 *In vivo* skin irritation of PRN in rats: Pictures of the treated skins

(A) and the mean macroscopic skin lesion scores **(B)** at days 7, 14, 21 and 28 post topical application with significantly difference (*p*<0.05) marked with *. Rat skins were treated with distilled water (DW), CS (unloaded nanocarriers), RAL (conventional retinal solution) and PRN suspension (PRN), and bars in A denote 1 cm.

We observed no significant difference in mean microscopic skin lesion scores among PRN and the two control groups (DW and CS) at all time points. From day 7 until the end of the study period, we observed more than 2 granular cell layers of epidermis, normal stratum corneum and no dermal inflammation in the skin of the PRN-treated group (**Fig. 6A**). Only the RAL-treated group showed signs of irritation and inflammation which resulted in a distinguished irritation index ranging from mild to moderate irritation. The mean microscopic skin lesion score of the RAL-treated groups was significantly different from other groups at all time points (**Table 5**) ($p<0.05$). The epidermal thicknesses measured from the base of the stratum corneum to the basement membrane are shown in **Fig. 6**. For both control groups (DW and CS), the epidermis only consisted of one or two layers of viable cells and the dermis had no organized subepidermal band of connective tissues. There was no difference of epidermal thickness between these two control groups **(Table 6)**. The PRN-treated group produced significantly higher epidermal thickness than the RAL-treated group ($p<0.05$) at all time points except at day 21 **(Table 6)**.
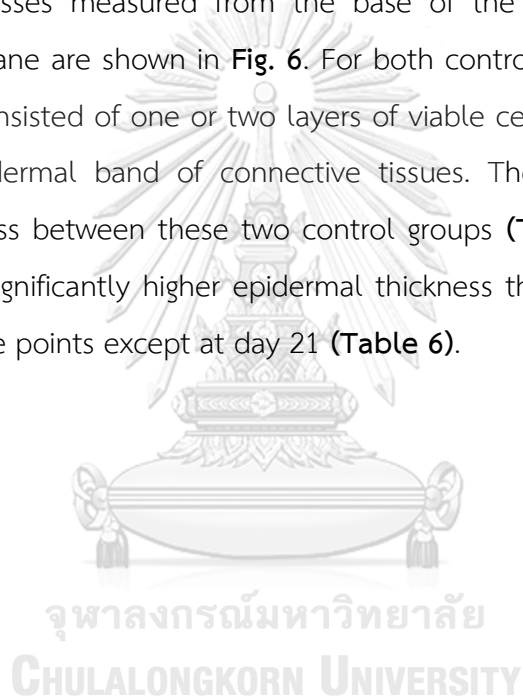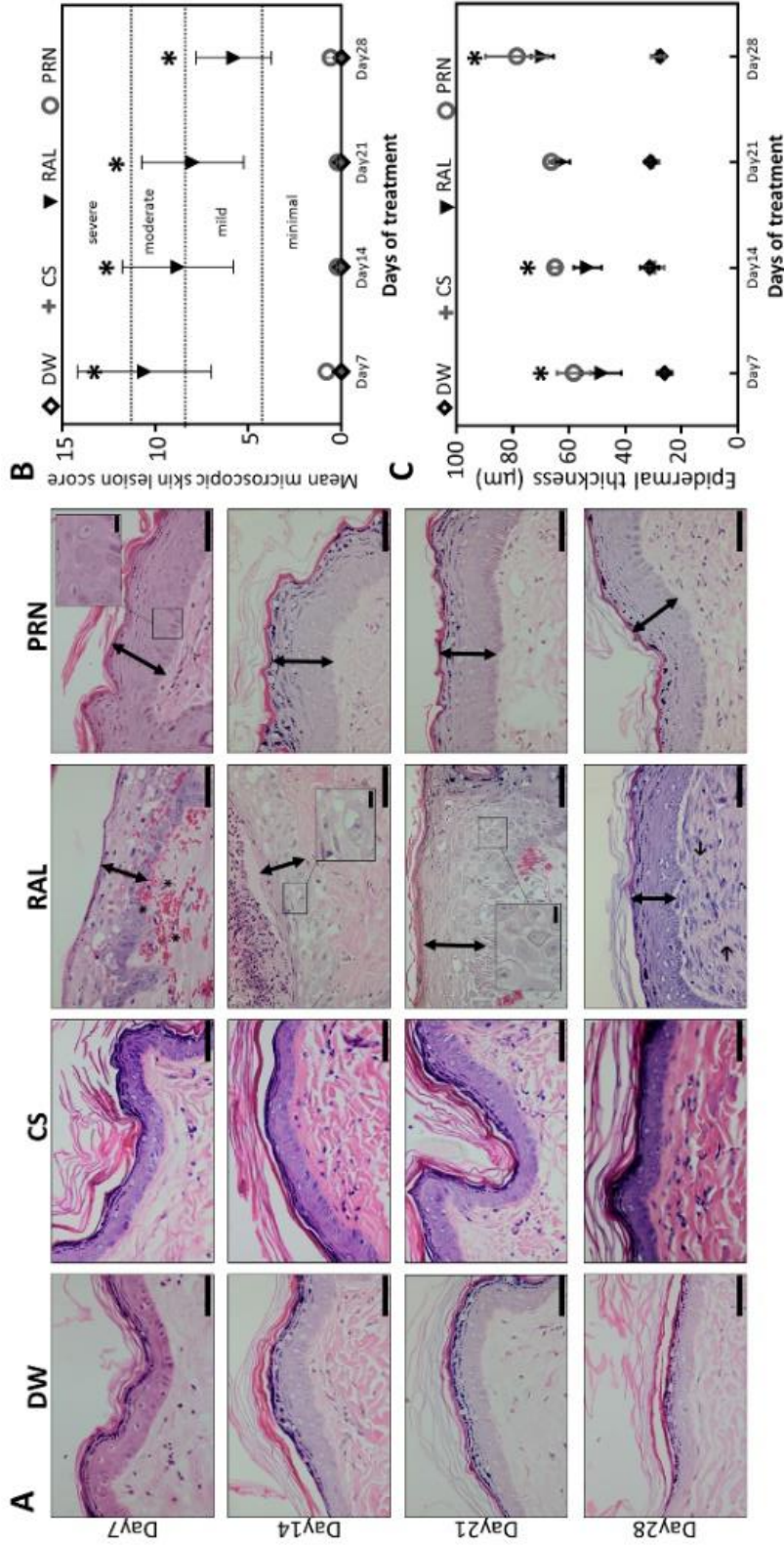
Figure 6 Topical PRN effects on histopathology of rat skin.

(A) Cross-sectional views of the epidermis and dermis of skins from all groups of treatments and black arrows indicate epidermal thickening. Moderate diffuse hyperplastic basal and supra-basal (inset of day 7) and more than 2-3 layers of granular layers of epidermis of topical PRN (inset of day 14, 21 and 28). Only the treatment of RAL responses with various inflammatory features including the locally extensive subepidermal hemorrhage (asterisk of day 7), epidermal hydropic degeneration (inset of day 14), crust formed by dry exudate, severe spongiosis resulting in accentuation of intercellular bridges (inset of day 21) and dermal fibrosis (arrows of day 28), (H&E, bar = 50 µm). **(B)** The mean microscopic lesion score of all treatment groups with significantly difference (*p*<0.05) marked with * **(C)** Quantification epidermal thickness (µm) of all groups (mean ± SD).

2.4.5 Immunohistochemical evaluations for K5, K14, K10, PCNA, IL-6 and CRABP-2 proteins

IHC were applied to the histological specimens. Characteristics and quantifications of IHC from all treatment groups are summarized in **Fig.7-8**. For basal proliferation of epidermis of PRN group, K5 and K14 expressions were strongly positive in the basal layer as well as the suprabasal layer of the hyperplastic epidermis in all time points **(Fig. 7D, L)** while control groups (DW and CS) had weak immunoreactivity **(Fig. 7A-B, I-J)** and RAL group had only strong K14 immunoreactivity **(Fig. 7K)** The marked positive nuclear labeling as more than 1-layer PCNA positive cells in nuclei of basal layer of PCNA of PRN group **(Fig. 7X)** was observed while other groups **(Fig. U-W)** were occasionally detected and scatted in nuclei of basal layer through the same length of epidermis.

The expressions of both K10 **(Fig. 7H)** and CRABP-2 **(Fig. 7T)** of PRN group distributed clearly in cytoplasm of keratinocyte of the suprabasal layer of epidermis and significantly while RAL-treated group appeared only focal expression **(Fig. 7G&S)**. The expression of IL-6 in fibrocytes underneath epidermis and infrequently in keratinocytes was found only in RAL group in all time points **(Fig. 7O)**.

The immunohistochemistry of day 7, 14 and 21 of topical application was provided in supplementary materials **(Fig.10-12)**.
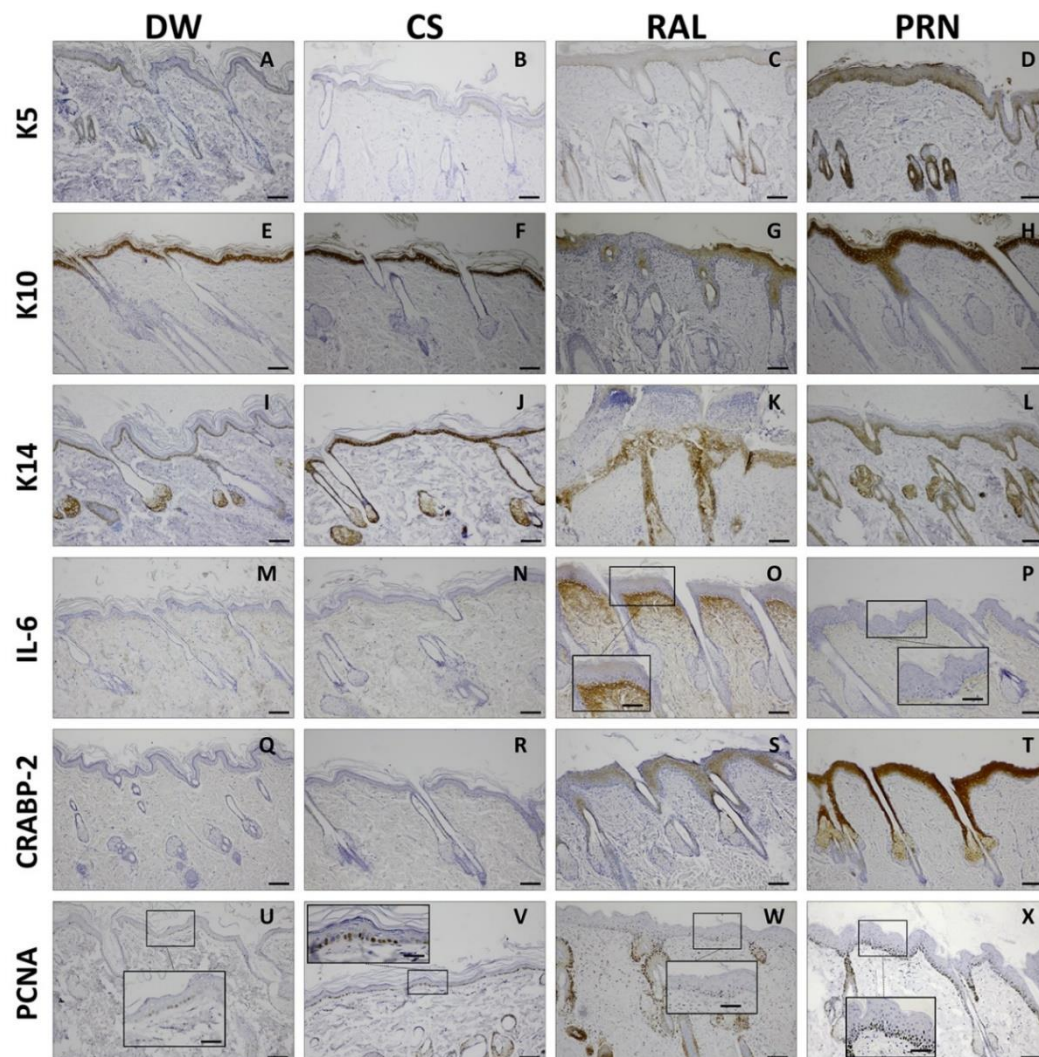
Figure 7 Immunohistochemistry of treated skins at 28 days of topical application. Immunohistochemical features of **(A-D)** K5, **(E-H)** K10, **(I-L)** K14, **(Q-T)** CRABP-2 in epidermis, **(M-P)** IL-6 in dermis, and **(U-X)** nuclear labeling of PCNA in the length of basal epidermal layers express in diffuse intracytoplasmic pattern from all treatment groups (bar = 100 μm). Insets show in higher magnification (bar = 50 μm). Topical application of PRN induced expression of K5, K10, K14, CRABP-2 and PCNA meanwhile faintly expression of IL-6 immunoreactivity. (DW; distilled water, CS; unloaded nanocarriers, RAL; conv.RAL solution and PRN; proretinal nanoparticles).
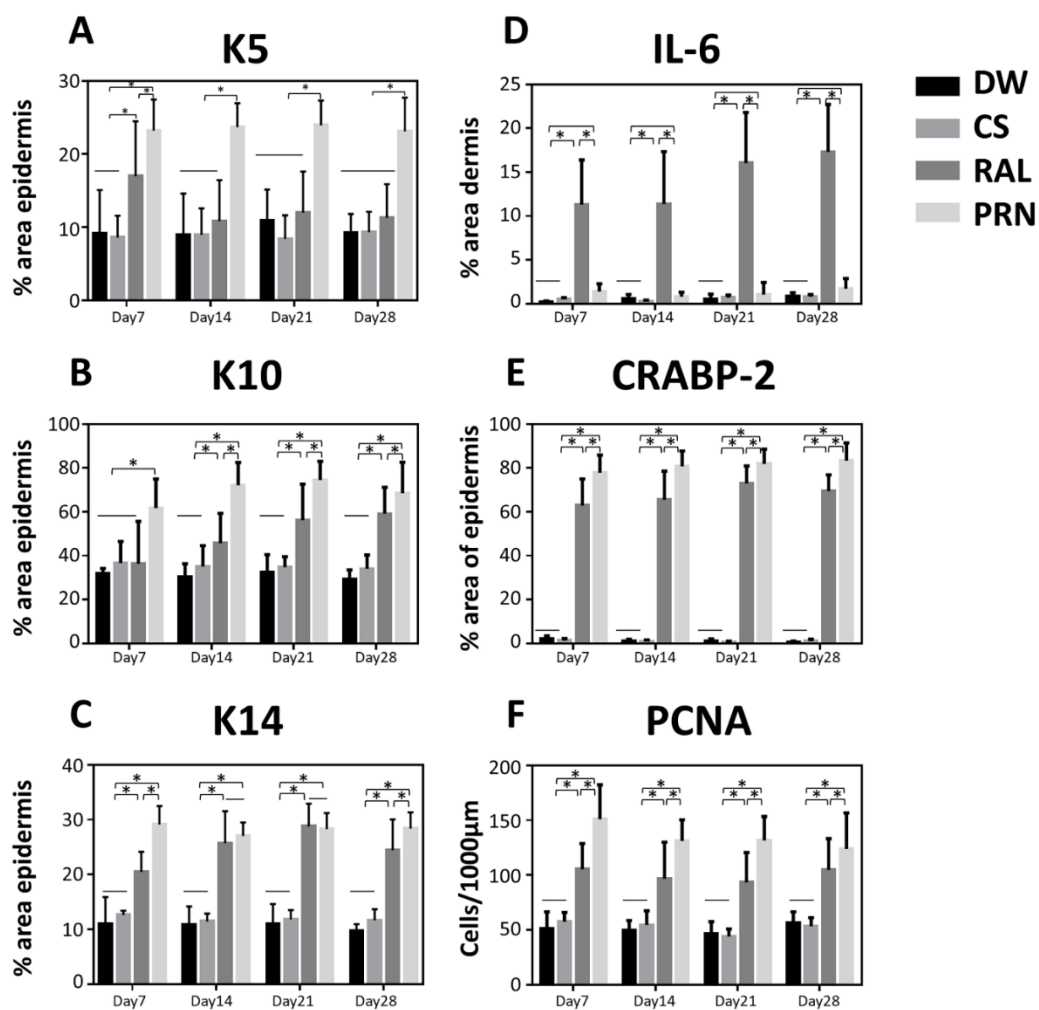
Figure 8 Quantitative analyses of immunohistochemical expressions of (A) K5, (B) K10, (C) K14, (D) IL-6, (E) CRABP-2 and (F) PCNA of treated skins from all time points (mean ± SD) with significantly difference ($p<0.05$) marked with *. (DW; distilled water, CS; unloaded nanocarriers, RAL; conv.RAL solution and PRN; proretinal nanoparticles)

2.5 Discussion

HaCaT cells have been used in several in vitro pharmacological studies of retinoids [88-91] because they can be maintained in a defined retinoid-free cultured system and possess the same epidermal differentiation capacity as normal keratinocytes [92]. Cytotoxicity evaluation is addressed as a key of safety assessment for numbers of living cells. In present study, through MTT and PI assay, we observed that both PRN and RAL at the concentration of 3.33 µM were not cytotoxic to HaCaT cells since the materials showed similar level of cell viability to that of the negative control. This information agrees with previous report which indicated that retinoids at 1-10 µM concentration are minimal cytotoxic to keratinocytes [93]. Nevertheless, TUNEL assay results which alludes key cellular events in apoptosis by detecting DNA fragmentation in the late stage of apoptosis, indicates that the RAL induced significant higher cellular apoptosis effect than the PRN. Previous research has revealed that retinoic acid (RA) can promote apoptosis by regulating apoptosis-associated genes in keratinocyte as early as 4 h post RA exposure and the effect can last to 24 h post exposure [72]. The less cytotoxicity and apoptotic induction of PRN as compared to RAL can be explained through the sustained release of the RAL from the PRN [84]. Intracellular concentration of retinoic acid can be observed through the expression level of the CRABP-2 [94]. It is logical to see that both PRN-treated and RAL-treated HaCaT cells showed higher CRABP-2 expression than the control cells. Interestingly, the PRN-treated cells showed stronger CRABP-2 expression than the RAL-treated cells. We speculate that the less apoptotic induction of PRN may link to the more intense CRABP-2 expression observed in this experiment. It was likely that cellular function was more optimal when the cells were in a less cytotoxic environment.

Observation of the fluorescence signal of the PRN after 12 h of in vivo topical application, the PRN distributed well in the hair follicles and on the stratum corneum. It was expected to see aggregation of PRN along epidermis as the water evaporated. These deposited PRN could supply retinal to skin while maintaining the integrity of the easily degrade retinal structure. The size of the PRNs of 240.1±29 nm [84] fits well with their distribution into the hair follicles since it has been reported earlier that particles

of the size around 256 nm could penetrate rat's hair follicles well through the gear pump mechanism [95]. Another important point we observed here is that the depth of PRN was independent on the post application period [96]. In other words, depth of PRN at 3 h post application and that at 6 or 12 h post application were similar. This indicated that the hair movement together with the massage actions during the application set the depth of the particles in the hair follicles, and the penetrated particles did not move down or up from their positions afterwards, regardless of the animal movement. The hair follicle penetration ability of PRN gives the material prospected applications since hair follicles are the residence of stem cells [97] and immune cells [98]. In addition, the PRN residency in the hair follicles can also serve as a reservoir of retinoid for the skin.

Previous study indicated that 25% of volunteers were irritative to the 0.1% topical retinal uses [99]. The irritation mechanism has been explained by an overload of non-physiological amounts of exogenous retinoic acid, the cellular conversion form of the RAL[28]. Here using rats, we also observed epidermal hyperplasia in RAL-treated group. However, neither macroscopic and microscopic signs of irritation nor inflammation through the 28 day-test was observed in the PRN-treated group. More interestingly, although PRN-treated group showed no skin irritation, epidermal thickening effect was the most potent when compared to the RAL-treated group and the control group. We explained these results through the ability of PRN to sustain the release of RAL so that RAL concentration was stabilized at the effective but un-irritating level.

As shown and discussed above that both PRN and RAL stimulated the thickness of epidermis of the rats that had been topically applied with the materials, here we further confirm that such effect was the biological action of the delivered retinoid by monitoring the biological markers that involve epidermal differentiation and organization, keratins (K) 5, 14 and 10, (CRABP-2), IL-6 and PCNA.

Normally, keratinocytes proliferation is associated with increasing in DNA synthesis and increasing cell mitotic activity [100]. Here, we employed PCNA as a marker to probe over the DNA replication activity. Although PCNA expression was clearly

observed in basal epidermis of both the PRN-treated and the RAL-treated skins, the expression was higher in number of basal cells of epidermis in the PRN-treated group. The result implies that the PRN-treated skin possessed higher keratinocyte proliferation, comparing to the RAL-treated skin. This is in accorded with the better increase in epidermis thickness reported and discussed above. Retinal released from PRN probably involves in epidermal keratinocyte proliferation by either stimulating or modulating the actions of mitogenic growth factors [101]. This observation agrees with the CRABP-2 expression. Although CRABP-2 expressions were observed in suprabasal layers of the epidermis of both the PRN-treated and the RAL-treated rats, the expression in the PRN-treated group was more intense and well distributed. This discrepancy implies the better cellular function of the epidermal cells of the PRN-treated group and it was likely due to the more optimal and more steady retinal concentration available to those cells. CRABP-2 itself plays important roles in retinoic acid metabolism and maintenance of vitamin A homeostasis and is key molecule to control bioavailability of retinoid by transporting retinoic acid to cellular nucleus [19, 102, 103].

More interestingly, only the PRN-treated group showed PCNA and CRABP-2 expression in the sebaceous glands. This implies that only the PRN, not the conventional RAL, could deliver retinoid to the sebaceous glands. This is very likely because PRN was observed in the hair follicles at the depth around the location of the sebaceous gland. This finding would be very beneficial in clinical application focused on sebum production as retinoids are fat-soluble vitamin.

Epidermal proliferation and differentiation usually occur continuously through the upward move of keratinocytes from the basal to the suprabasal layers [103]. As shown above in the increased CRABP-2 and PCNA expressions and the thickening effect of epidermis layer that both RAL and PRN produced, it is likely that these effects were the results of stimulation at the protein level. Therefore, here we monitored the expression of keratin proteins, K5 and K14 in the basal layer and the K10 in the suprabasal layers. All these expressions could be observed in both the RAL-treated and the PRN-treated skins. These three proteins are known to be affected by retinoids

[69, 72, 104]. These results thus confirm that PRN could produce the retinoid biological activities in regulating epidermis by stimulating high expressions of K5, K14 in basal cells and K10 in suprabasal layers. As expected, in PRN-treated skin, intense expressions of K5,14 and 10 were observed through the 28 days of the treatment, agreeing well with previous studies on the topical application of retinoid [67, 99, 104]. These alterations in keratin expressions of RAL-treated skin could be contributed from the chronic irritation and inflammation. The re-epithelialization in the wound healing process were found in all time points of RAL-treated skins. The expression of K5 in RAL-treated skin was observed in the basal cells, or occasionally in the suprabasal layers focally in the wound bed at all time points. Our finding is in agreement with previous study that described the subtype of keratinocytes which involved in the re-epithelialization of the wound healing [105]. Normally, the expression of K10 appears only in suprabasal layers of intact epidermis [106]. That's why K10 in RAL-treated skin expressed irregularly and lowly when comparing to PRN-treated skin. The explanation of high expression of K14 in RAL-treated skin could be the K14 expression found in suprabasal cells during re-epithelialization process of injured epidermis [107] while the K14 expression of PRN-treated skin clearly confined in hyperplastic basal cells. Additionally, In RAL-treat skins through 28 day-test, the marked expression of IL-6 was observed. This phenomenon agrees with the disruption of epidermal barriers and their chronic pathological conditions as the increased level of IL-6 reflects the skin pathology of retinoid dermatitis [108].

In Summary, PRN could serve as an excellent retinal reservoir with effective follicular penetration and induction of skin proliferation. Follicular penetration of PRNs and their time-independent localization was observed. In vitro increased expression of CRABP-2 by PRN with no short-term cytotoxicity was clarified in HaCaT cells. Topical application of PRN for 28 days clearly increased cell proliferation and differentiation in rat epidermis resulting in the thickening of the epidermis and increased levels of various retinoid associated biochemical markers such as K5, K14, K10, PCNA and CRABP-2 except Il-6 without side effect of retinoid dermatitis.

Funding information

B. Limcharoen was supported by 100th anniversary Chulalongkorn University Fund for doctoral scholarship of Graduate school of Chulalongkorn University. This research was supported by the 90th Anniversary of Chulalongkorn University, Rachadapisek Sompote Endowment Fund.

Conflict of interest statement

The author(s) declare that there are no conflicts of interest.

Acknowledgment

We would like to thank Asst. Prof. Dr. Patcharee Ritprajak, Oral Biology Research Center, Faculty of Dentistry, Chulalongkorn University for providing HaCaT cells, Olympus Bioimaging Center (OBC) at the Faculty of Science, Mahidol University for their technical assistance and especially Prof. Dr. Pasutha Thunyakitpisal, Department of Anatomy, Faculty of Dentistry, Chulalongkorn University for the technical supports.
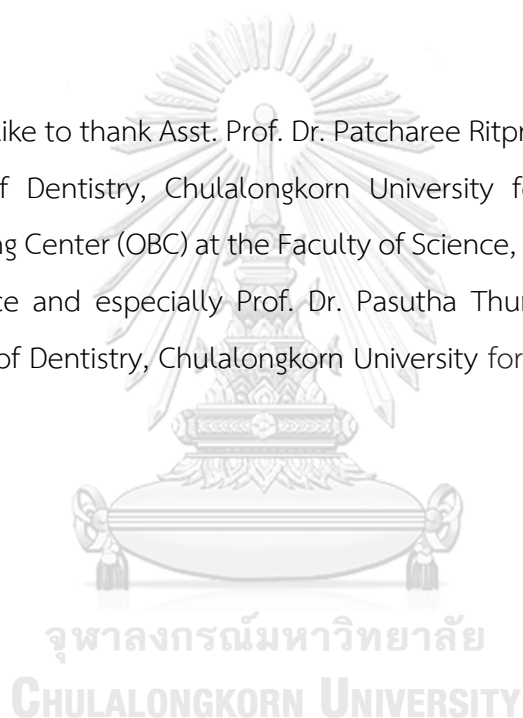
2.6 Supplementary materials

Table 3 Primary antibodies and immunohistochemical techniques

Primary antibodies	Types	Antigen Retrieval	Dilution	Source
K5	Rabbit mAb anti-Human (EP1601Y)	HIER; Citrate buffer, pH6, Microwave, 5 min	1:300	Cell Marque (Sigma Aldrich, MI, USA)
K14	Rabbit mAb anti-Human K14 (SP53)	HIER; Citrate buffer, pH6, Microwave, 5 min	1:300	Cell Marque (Sigma Aldrich, MI, USA)
K10	Mouse mAb anti-Human K10 (DE-k10) (ab9026)	HIER; Citrate buffer, pH6, Microwave, 5 min	1:200	Abcam (Cambridge, UK)
PCNA	Mouse mAb PCNA antibody; PC10	HIER; PBS, Microwave, 10 min	1:200	DAKO (Glostrup, Denmark)
IL-6	Rabbit polyclonal aniti-Human IL-6 antibody (ab6672)	-	1:300	Abcam (Cambridge, UK)
CRABP-2	Rabbit polyclonal anti-Human CRABP-2 antibody (HPA004135)	HIER; PBS, Microwave, 10 min	1:400	Sigma Aldrich, MI, USA

*K; cytokeratin, PCNA; proliferating nuclear antigen, CRABP-2; cellular retinoic acid binding protein-2   HIER; Heat-induced epitope retrieval, PBS; phosphate buffer solution, mAb; monoclonal antibody, pAb; polyclonal antibody

Appendix A.

The fluorescent polymer synthesis of 5(6)-Carboxytetramethylrhodamine-labelled PRN (rhodamine-labelled PRN)

The synthesis of rhodamine-labelled PRN was based on carbodiimide chemistry.Firstly, 5(6)-Carboxytetramethylrhodamine ($\lambda_{ex/em}$ of 555/580 nm) (6.34 mg) was dissolved in dimethylformamide (DMF,0.5 mL) at 0°C under N_2 atmosphere. Then, 1-Ethyl-3-(3 dimethylaminopropyl) carbodiimide (EDCI, 8.45 mg, Sigma Aldrich) was added to the solution and stirred for 30 min at 0 °C. Next N-hydroxy succinimide (NHS, 3.5 mg, Sigma Aldrich) was added, followed with PRN suspension (120 mg in 20 mL water) and the mixture was stirred for another 4 h. The suspension was then dialyzed against water under N_2 and lightproof condition. Suspension in the dialysis bag was then freeze-dried.

Table 4 Summary of mean macroscopic skin lesion score (mean ± SD)

Treatment	Day7	Day14	Day21	Day28
DW	0	0	0	0
	negligible	negligible	negligible	negligible
CS	0	0	0	0
	negligible	negligible	negligible	negligible
RAL	3.6±0.55 [ɫɫ, *, ϒ, ħ]	7.6±0.55 [¶, J, ρ]	4.2±0.84 [ɫ]	1.8 ±0.84 [ɫ, σ]
	Moderate	Severe	Moderate	Slight
PRN	0	0	0	0
	negligible	negligible	negligible	negligible

Mean microscopic lesion score was evaluated based on ISO 10993-10:2010. Statistical analyses were performed using two-way ANOVA followed by Tukey's multiple comparison test. Two control groups including 1) distilled water (DW) as negative control and 2) chitosan nanoparticles (CS) as unloaded nanocarriers, and two sample-treated groups including 3) topical application of conventional retinal (RAL; 0.1 % w/v or at 3.33 mM of retinoid) and 4) PRN (at 3.33 mM of retinoid). Mean microscopic lesion score;

[ɫɫ, ¶, ɫ, ɫ] indicates difference ($p<0.05$) within same day of treatment among all treatment groups.

*indicates difference ($p<0.05$) between day7 and day14 of RAL treatment.

ϒ indicates difference ($p<0.05$) between day7 and day21 of RAL treatment.

ħ indicates difference ($p<0.05$) between day7 and day28 of RAL treatment.

J indicates difference ($p<0.05$) between day14 and day21 of RAL treatment.

ρ indicates difference ($p<0.05$) between day14 and day21 of RAL treatment.

σ indicates difference ($p<0.05$) between day21 and day28 of RAL treatment.

Table 5 Summary of mean microscopic skin lesion score (mean ± SD).

Treatment	Day7	Day14	Day21	Day28
DW	0	0	0	0
	None	None	None	none
CS	0	0	0	0
	None	None	None	none
RAL	10.6±3.59 [†‡, *, ꞕ]	8.8±3.0 [¶, ϒ]	8±2.75 [Ϯ]	5.8±2.03 [†]
	Moderate	Moderate	Mild	mild
PRN	0.8±0.36	0.2±0.11	0.2±0.11	0.6±0.26
	None	None	None	none

Mean microscopic lesion score was evaluated based on ISO 10993-10:2010. Statistical analyses were performed using two-way ANOVA followed by Tukey's multiple comparison test. Two control groups including 1) distilled water (DW) as negative control and 2) chitosan nanoparticles (CS) as unloaded nanocarriers, and two sample-treated groups including 3) topical application of conventional retinal (RAL; 0.1 % w/v or at 3.33 mM of retinoid) and 4) PRN (at 3.33 mM of retinoid). Mean microscopic lesion score;

[†‡, ¶, Ϯ, †] indicates difference ($p<0.05$) within same same day of treatment among all treatment groups.

* indicates difference ($p<0.05$) between day7 and day21 of RAL treatment.

ϒ indicates difference ($p<0.05$) between day14 and day28 of RAL treatment.

ꞕ indicates difference ($p<0.05$) between day7 and day28 of RAL treatment

Table 6 Summary of epidermal thickness

Treatment	DW	CS	RAL	PRN
Day7	26.05±2.63	25.79±2.47	48.39±6.99[a]	58.34±5.96[e, i]
Day14	31.38±3.32	29.55±3.35	53.42±4.95[b]	65±1.53[f, j]
Day21	31.01±2.13	30.35±2.48	62.91±3.22[c,l,n]	66.39±0.93[g,p]
Day28	27.51±1.80	28.44±2.35	69.56±4.10[d,m,o]	78.62±11.07[h, k,q,r,s]

Two control groups including 1) distilled water (DW) as negative control and 2) chitosan nanoparticles (CS) as unloaded nanocarriers, and two sample-treated groups including 3) topical application of conventional retinal (RAL; 0.1 % w/v or at 3.33 mM of retinoid) and 4) PRN (at 3.33 mM of retinoid).

[a,b,c,d,e,f,g,h] indicates difference ($p<0.05$) within same day of treatment among all treatment groups.

[i,j,k] indicates difference ($p<0.05$) within same date between PRN and RAL-treated group.

[l,m] indicates difference ($p<0.05$) when compared with 7days of RAL treatment

[n,o] indicates difference ($p<0.05$) when compared with 14days of RAL treatment

[p,q] indicates difference ($p<0.05$) when compared with 7days of PRN treatment

[r] indicates difference ($p<0.05$) when compared with 14days of PRN treatment

[s] indicates difference ($p<0.05$) when compared with 21days of PRN treatment
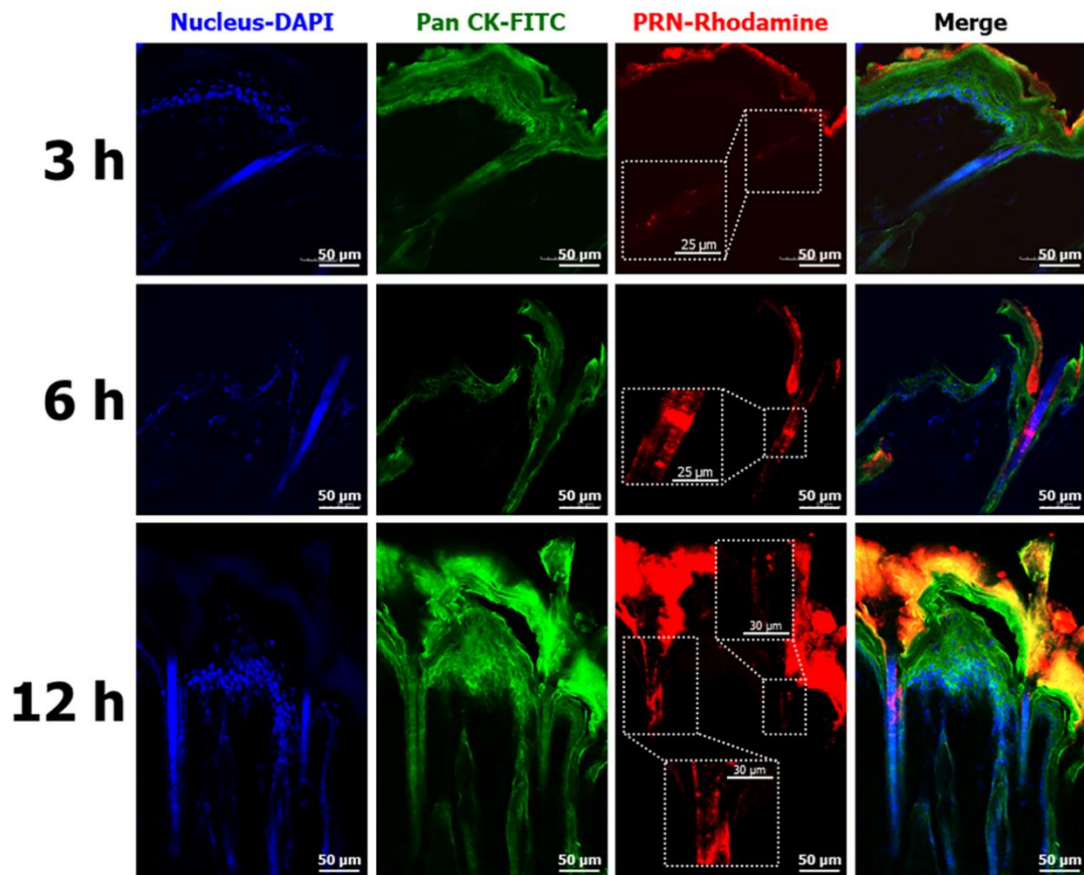
Figure 9 Follicular penetration of rhodamine-labelled PRN in rat skin observed by CLSM at 3 h 6 h and 12 h post topical PRN application.
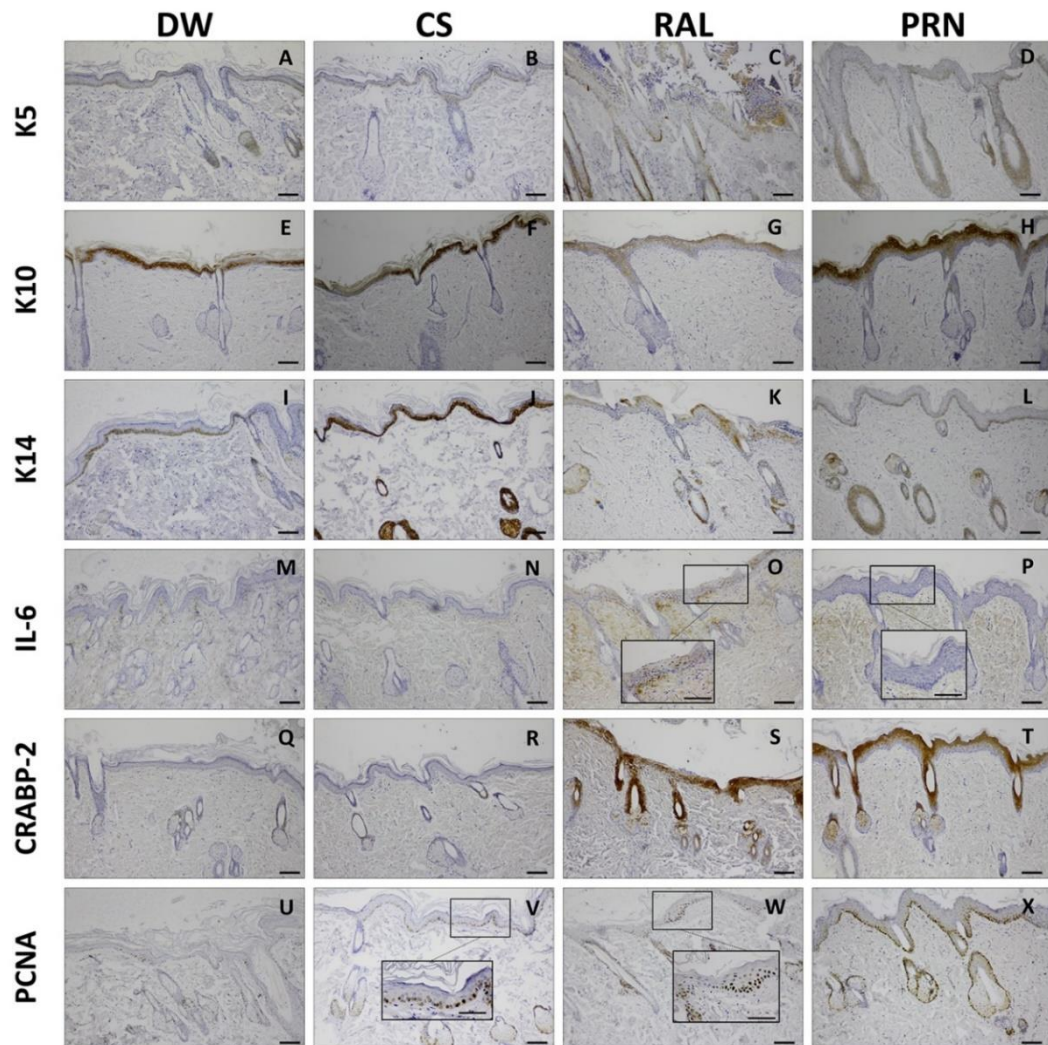
Figure 10 Immunohistochemistry of treated skin at 7 days of topical application. (DW; distilled water, CS; unloaded nanocarriers, RAL; conv.RAL and PRN; proretinal nanoparticles). Immunohistochemical features of diffuse intracytoplamic **(A-D);** K5, **(E-H);** K10, **(I-L);** K14, **(Q-T);** CRABP-2 in epidermis, **(M-P);** IL-6 in dermis, and **(U-X);** nuclear labeling of PCNA in basal epidermal layers in all groups at 7 days of daily topical application (bar = 100 μm). Insets show in higher magnification (bar = 50 μm). Topical application of PRN induces expression of K5, K10, K14, CRABP-2 and PCNA meanwhile slightly expression of IL-6 immunoreactivity compares to DW, CS and RAL-treated groups.
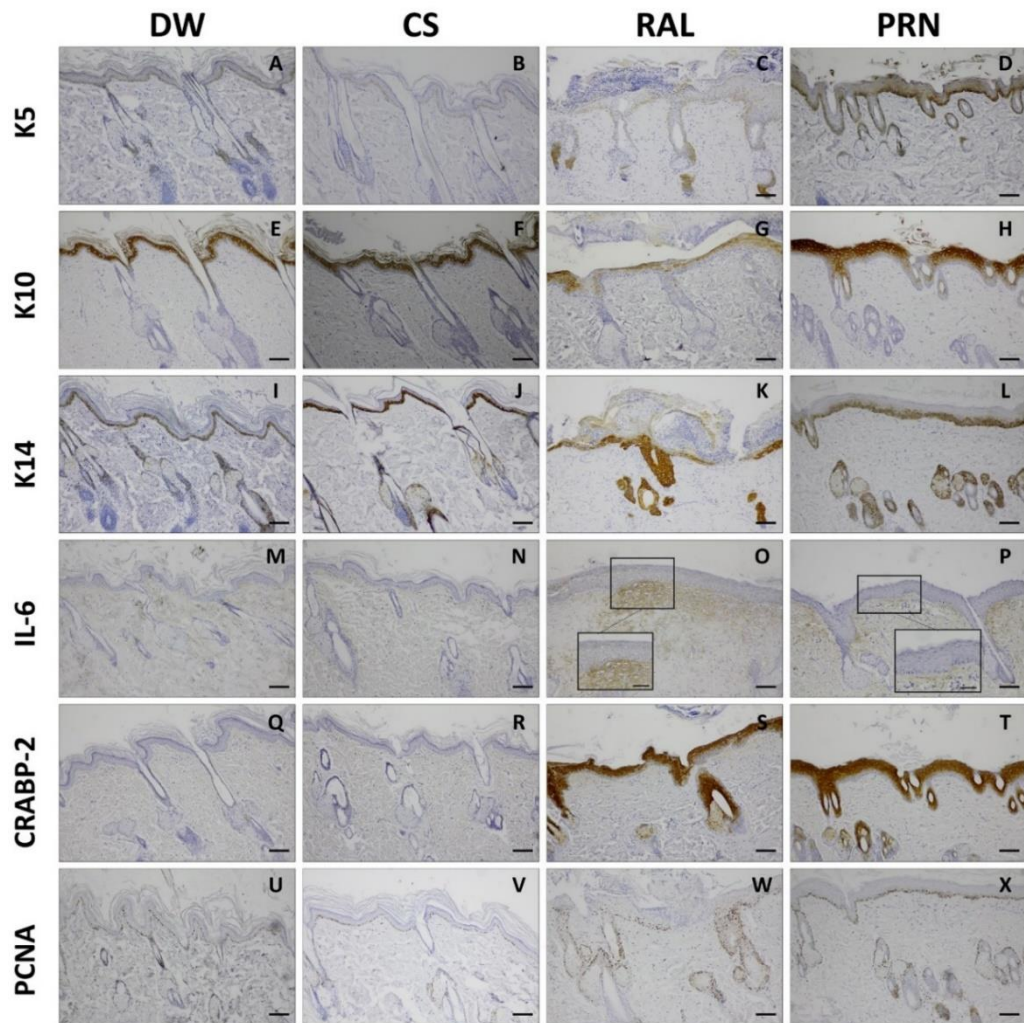
Figure 11 Immunohistochemistry of treated skin at 14 days of topical application. (DW; distilled water, CS; unloaded nanocarriers, RAL; conv.RAL and PRN; proretinal nanoparticles). Immunohistochemical features of diffuse intracytoplamic **(A-D);** K5, **(E-H);** K10, **(I-L);** K14, **(Q-T);** CRABP-2 in epidermis, **(M-P);** IL-6 in dermis, and **(U-X);** nuclear labeling of PCNA in basal epidermal layers in all groups at 14 days of daily topical application (bar = 100 μm). Insets show in higher magnification (bar = 50 μm). Topical application of PRN induces expression of K5, K10, K14, CRABP-2 and PCNA meanwhile slightly expression of IL-6 immunoreactivity compares to DW, CS and RAL-treated groups.
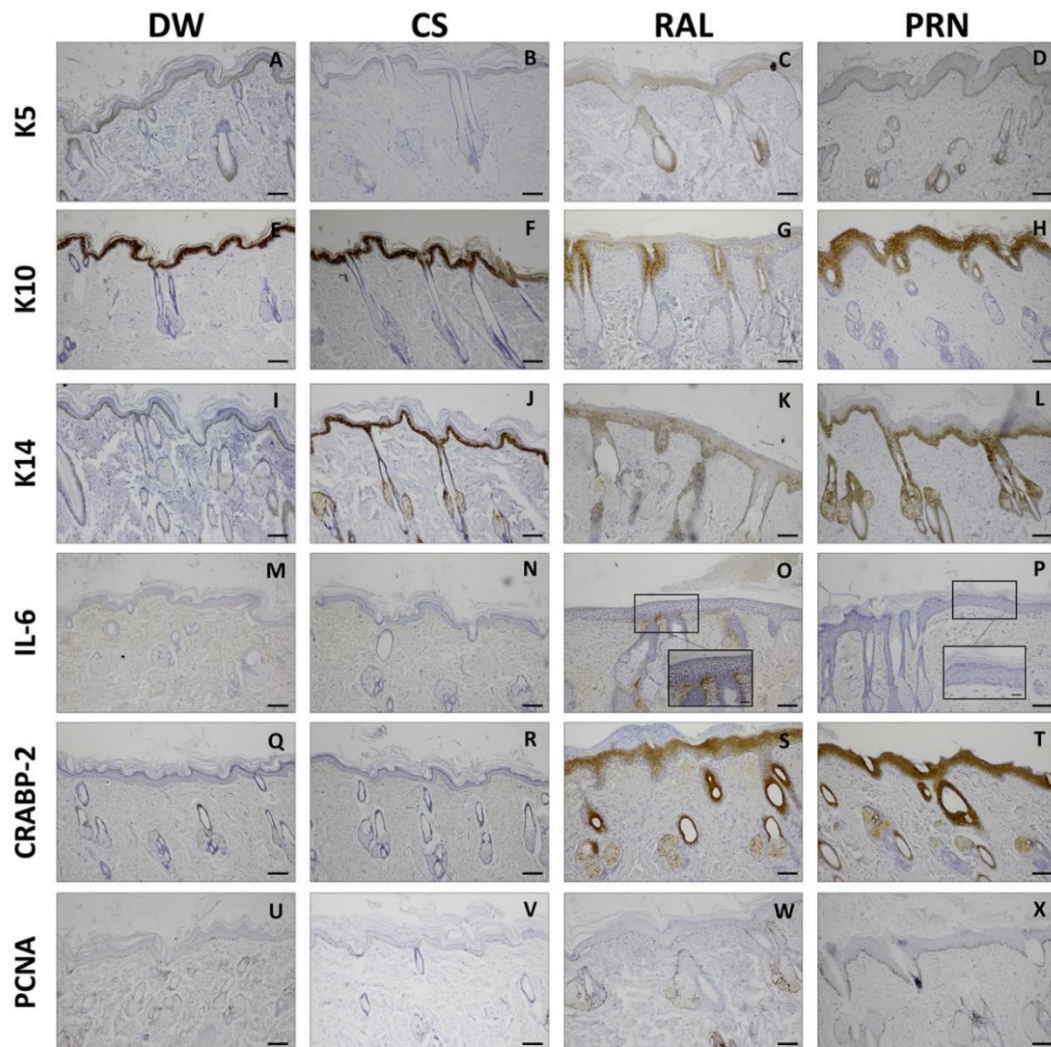
Figure 12 Immunohistochemistry of treated skin at 21 days of topical application. (DW; distilled water, CS; unloaded nanocarriers, RAL; conv.RAL and PRN; proretinal nanoparticles). Immunohistochemical features of diffuse intracytoplamic **(A-D);** K5, **(E-H);** K10, **(I-L);** K14, **(Q-T);** CRABP-2 in epidermis, **(M-P);** IL-6 in dermis, and **(U-X);** nuclear labeling of PCNA in basal epidermal layers in all groups at 21 days of daily topical application (bar = 100 µm). Insets show in higher magnification (bar = 50 µm). Topical application of PRN induces expression of K5, K10, K14, CRABP-2 and PCNA meanwhile slightly expression of IL-6 immunoreactivity compares to DW, CS and RAL-treated groups.

CHAPTER III

Intercellular and follicular penetration of retinal by topical application of proretinal nanoparticles

This work has been published in the topic of

Increasing the percutaneous absorption and follicular penetration of retinal by topical application of proretinal nanoparticles

(Appendix A)

Benchaphorn Limcharoen, Pattrawadee Toprangkobsin, Wijit Banlunara, Supason Wanichwecharungruang, Heike Richter, Jürgen Lademann, Alexa Patzelt

Highlight

- Topical proretinal nanopartilces, a novel formulation of topical retionids, can penetrated effectively into the hair follicles with the time-independent manner.
- The recovered retinal concentration delivered to the stratum corneum and the hair follicles was significantly higher when retinal was applied in the particulate form.

3.1 Abstract

Topical retinoids are frequently applied for therapeutic and cosmeceutical reasons although their bioavailability is low due to their chemical and photochemical instability. Moreover, skin irritation is a common side effect. Therefore, proretinal nanoparticles (PRN) as a novel formulation of topical retinoids, which are based on chitosan grafted with retinal through reversible linkage, were developed and their skin penetration behavior was studied. As nanoparticles preferably penetrate into the hair follicles, the follicular penetration depths of PRN at different time points were investigated. Moreover, the release capacity of the nanoparticulate system was studied using fluorescein as a model drug. Additionally, the concentration of retinal in the stratum corneum and in the hair follicles was quantified after application in particulate and non-particulate form. The results showed that the nanocarriers reached the infundibular area of the hair follicles, irrespective of the incubation time. The nanoparticles were able to release their model drug within the hair follicle. The retinal concentration delivered to the stratum corneum and the hair follicles was significantly higher when retinal was applied in the particulate form. In conclusion, the presented proretinal nanoparticle system may help to overcome the main problems of topical retinoid therapy, which are skin irritation, chemical and photochemical instability and low bioavailability, thus improving the topical retinoid therapy.

Keywords: Retinaldehyde, nanoparticles, follicular penetration, tape stripping

3.2 Introduction

Vitamin A and its derivatives (retinoids) are known as crucial natural regulators in skin proliferation and differentiation. In order to reduce the side effects related to systemic administration, such as teratogenicity, skin and mucous membrane dryness [109] which limit the use of retinoids in therapeutic purposes, topical application of retinoids is often the preferred method of administration for dermatological or cosmeceutical indications.

Retinaldehyde (retinal) is one of the natural intermediate precursors of retinoic acid, which exerts the biological retinoid effects [110]. Unfortunately, topically applied retinal is still irritative to human skin [111] and moreover, chemically and photochemically unstable. Topically applied retinal can induce a retinoid dermatitis [112]. This inflammation is induced by an overload of non-physiological amounts of exogenous retinoic acid in the skin [113]. Therefore, the aim is to eliminate this dose-related side effect and the instability of the chemical by developing a topical nanoparticulate controlled-release drug delivery system, which releases retinal continuously to prevent an excessive amount of retinal on the skin immediately after application. Polymer-based nanoparticulate drug delivery systems have already been considered and evaluated as topical carriers for different drugs [33]. Especially chitosan-based nanoparticulate drug delivery systems have been used as transdermal drug carriers [114]. They are assumed to provide several advantages in transdermal drug delivery via their mucoadhesive, permeation enhancement and controlled-release properties by the degradation of the polymer, which may enhance the drug bioavailability [115, 116].

Next to dose-related side effects, also the penetration of topically applied retinal itself represents a challenge. In general, most topically applied drugs provide extremely limited bioavailability rates, which are often below 1%. The bioavailability for retinoids is also less than 1% after single topical application [117, 118]. The low bioavailability of most topically applied drugs is due to the strong barrier properties of the skin and mainly the stratum corneum, the outermost layer of the skin. Three potential penetration pathways, in general, provide access to the skin: the intercellular

penetration pathway [119], the follicular penetration pathway and transcellular penetration pathways [120]. Topically applied substances can try to overcome the skin barrier via the intercellular penetration pathway, which is located within the lipid layers that are surrounding the corneocytes of the stratum corneum or they can - at least theoretically - pass the skin barrier by intracellular penetration, which, however, is probably of minor importance. In addition, the hair follicles represent an interesting entry port into the skin, which is especially of importance for particulate substances. Previous studies could demonstrate that nanocarriers penetrate very efficiently into the hair follicles, which was hypothesized to be due to a mechanical transport mechanism induced by hair movement. Due to rhythmic movement of the hair in the hair follicle, the nanocarriers can be transported deeply into the hair follicle comparable to a ratchet mechanism. This effect was shown to be dependent, inter alia, on the size of the nanocarriers and on the frequency of hair movement [121].

Although nanocarriers show an effective follicular penetration, they are not able to overcome the stratum corneum directly due to their increased size. Already in 2000, the 500-Dalton rule was established which clarifies that substances, which have a molecular weight more than 500 Dalton, are not able to penetrate via the intercellular pathway [122]. Nevertheless, there are several studies that report an increased penetration of topically applied substances delivered by particulate systems, although the particles are not able to penetrate themselves. Here, the concentration gradient and other, partially unclarified mechanisms seem to play the major roles [123, 124] .

By grafting retinal onto chitosan polymer, a biocompatible and bioabsorbable polymer derived from the natural chitin polymer, and inducing self-assembly of the grafted polymers, proretinal nanoparticles showed sustained release of retinal *in vitro* [125]. Abilities of the proretinal nanoparticles to produce physiological effects without skin irritation side effects were already demonstrated both, in an animal model and also in human volunteers [125]. Nevertheless, the journey of the particles on skin, together with their location are unknown. Therefore, the aim of the present study was to investigate and quantify the skin and hair follicle penetration behavior of topically

applied proretinal nanoparticles and the release of retinal from this system or of a model drug, respectively, in order to improve topical retinoid therapy in the future. It was hypothesized that proretinal nanoparticles penetrate very effectively into the hair follicles and might be able to increase the bioavailability of retinal in the skin.

3.3 Materials and methods

3.3.1 Materials

3.3.1.1 Nanoparticles

PRN: PRN was prepared as previously described [125]. Briefly, chitosan (CS, molecular weight of ~40,000–50,000 Da, Taming Enterprise, Samut Sakhon, Thailand) was dissolved in 0.1% acetic acid, and the pH of the obtained solution was adjusted to 5.9 using NaOH. The final solution contained 45 mg CS in 19.0 mL solution. Then retinal (15 mg in 1.0 mL of ethanol) was slowly added dropwise into the CS suspension at 5°C in the dark, under ultrasonic (40 kHz) and N_2 atmosphere. After 2 h, the suspension was dialyzed against water under N_2 atmosphere and lightproof condition to obtain PRN suspension in water. The suspension was then freeze-dried. The size of PRN was 240.1±29 nm.

Rhodamine labelled-PRN: 5(6)-Carboxytetramethylrhodamine (6.34 mg) was dissolved in dimethyformamide (DMF, 0.5 mL) at 0 °C under N_2 atmosphere. 1-Ethyl-3-(3-dimethylaminopropyl)carbodiimide (EDCI, 8.45 mg, Sigma Aldrich) was added to the solution and stirred for 30 min at 0 °C. Then N-hydroxysuccinimide (NHS, 3.5 mg, Sigma Aldrich) was added, followed with PRN suspension (120 mg in 20 mL water) and the mixture was stirred for another 4 h. The suspension was then dialyzed against water under N_2 and lightproof condition. Suspension in the dialysis bag was then freeze-dried.

Rho-Flu-Chitosan nanoparticles: On ice, 5(6)-carboxytetramethylrhodamine (4.0 mg) was dissolved in DMF (0.3 mL) under N_2 atmosphere. EDCI (6.0 mg) was added to the solution and stirred for 30 min. Then NHS (3.5 mg) was added, followed with N-succinylchitosan suspension (120 mg in 20 mL water) and the mixture was stirred for another 4 h before being dialyzed against water. Then the obtained suspension was

stirred with the activated 5-carboxyfluorescein solution (prepared by dissolving 5-carboxyfluorescein (4.0 mg in 0.3 mL DMSO) and mixed with EDCI (6.0 mg) and NHS (3.5 mg) on ice) for 4 h and then dialyzed against water. The obtained suspension was freeze-dried.

RAL: Moreover, all-trans-retinal (RAL) (Sigma Aldrich, St. Louis, USA) was prepared in the solution as the same retinoid concentration corresponding to PRN and served as control.

3.3.2 Methods

3.3.2.1 *Ex vivo* skin preparation

The studies were performed *ex vivo* on porcine ear skin. Porcine ear skin is as an appropriate model for human skin [126] and very suitable for investigating the follicular penetration process as hair follicle size and density are well comparable. Other than excised human skin, porcine ear skin remains fixed to the cartilage during the experiments. Thus, any contraction of the skin and the hair follicles can be excluded [127]. Fresh pig ears (6-month-old German domestic pig) with no abnormal external appearances and no skin lesions were obtained from a local slaughter house in Niederlehme, Germany. The protocol for this study adhered to the ethical principles of the Veterinary Board of Control, Dahme-Spreewald. The porcine ears were cleaned and rinsed with cold water, dried with paper towels and fixed on a polystyrene board. The topical substances were applied to the well-demarcated skin areas using a silicon barrier (Marabu Window Color, Marabu GmbH, Bietigheim-Bissingen, Germany) to prevent any lateral spreading of the applied formulations from the designated skin areas. 20 µL per cm^2 of each formulation was applied to the skin areas, distributed homogeneously with 2 min of 50 Hz massage appliance (Novafon Pro soundwave appliance, Weinstadt, Germany) and incubated following the indicated penetration times following each application protocol at room temperature in a moisture chamber. Each experiment was performed on 6 independent pig ears. Due to the light sensitivity of retinoids, all experiments were carried out in a darkened room.

3.3.2.2 Application of topically applied substances

*3.3.2.2.1 **Experiment A** Determination of the follicular penetration depths of PRN*

In experiment A of the study, the follicular penetration depths of PRN were investigated using 5(6)-carboxytetramethylrhodamine labelled-PRN for visualization by confocal laser scanning microscopy. Therefore, two skin areas of 2x3 cm^2 for each pig ear were demarcated as described above. One skin area was treated with PRN, the other skin area remained untreated and served as control. After the topical application and an incubation time of 2 h, skin biopsies were excised.

*3.3.2.2.2 **Experiment B** Determination of the time dependency of the follicular penetration depth and the release of the 5-carboxyfluorescein from the 5(6)-carboxytetramethylrhodamine-labelled chitosan nanoparticles*

In experiment B of the study, 4 areas of 2x3 cm^2 were prepared as described above. The chitosan nanoparticles double labelled with 5(6)-carboxytetramethylrhodamine and 5-carboxyfluorescein were applied to three of the marked areas. The fourth area remained untreated and served as control. Each of the three treated skin areas was designated to have a different penetration time of 2, 4 or 24h, respectively.

*3.3.2.2.3 **Experiment C** Modified differential stripping technique to estimate the amount of retinal in the stratum corneum and the hair follicle after topical application of RAL and PRN*

In experiment C of the study, three areas of 4 x 3 cm^2 were marked. PRN and RAL were topically applied and one skin area remained untreated and served as control. The incubation was determined to be 4 h according to the deepest follicular penetration depths in experiment B and according to the previous in vitro study determining the release efficacy of free retinal from chitosan nanoparticles, which was approximately 60% at this time point [125].

3.3.2.3 Analytical methods

3.3.2.3.1 Investigation of follicular penetration depths (experiment A and B)

In experiment A and B, skin samples were processed after the different incubation times as follows: full thickness skin biopsies were cut into probes of 5 x 5 mm in size using a surgical blade. The subcutaneous fat tissue was removed, and the probe was immediately fixed with cryospray (Solidofix-cryospray, Carl Roth, Karlsruhe, Germany), snapped in liquid nitrogen and kept in -20°C. Subsequently, cryosections of hair follicles of 10 μm thickness were prepared using a cryostat (Microm Cryo-Star HM 560, Microm International GmbH, Walldorf, Germany). At least 10 hair follicles per investigated skin area were prepared.

3.3.2.3.2 Confocal laser scanning microscopy

The hair follicle sections were examined with confocal laser scanning microscopy (CLSM0700 Zeiss, Oberkochen, Germany) without additional tissue processing. Laser excitation wavelengths of 488 and 555 nm were used to scan the hair follicle sections. Untreated skin samples were used as controls to avoid any autofluorescence measurement.

The CLSM provided dual-colored images of the fluorescent signals of 5-carboxyfluorescein ($\lambda_{ex/em}$ = 488/518 nm) and 5(6)-carboxytetramethylrhodamine ($\lambda_{ex/em}$ = 555/580 nm), respectively. The images were studied using 100x magnification. Once the images were obtained, follicular penetration depths were measured in micron for each formulation using ZEN 2012 software program (Carl Zeiss, Oberkochen, Germany). The release properties of 5-carboxyfluorescein dye from the chitosan nanoparticles in experiment B were also calculated as a percentage of the number of hair follicles that had deeper follicular penetration depths of 5-carboxyfluorescein than 5(6)-carboxytetramethyl rhodamine at each time point against all hair follicles of that time point.

3.3.2.3.3 Modified differential stripping protocol (experiment C)

In experiment C, the modified differential stripping protocol according to Knorr and colleagues in 2013 [128] was used to estimate the amount of retinal penetrating into the stratum corneum and into the hair follicles after topical application of RAL and RPN. Based on the assumption that most of the topical applied retinal is located on the skin surface and in the stratum corneum, the stratum corneum was removed by 70 tape strips. Subsequently, split skin of 600 µm in thickness was removed with an electronic dermatome (Acculan 3Ti Dermatome, Aesculap, B Braun, Tuttlingen, Germany). As tape stripping did not show any penetration of retinal into the inferior part of the stratum corneum, it was assumed that retinal extracted from the remaining split skin can only originate from the hair follicles.

The tape stripping procedure was performed as described by Weigmann and colleagues in 1999. For the described experiment, adhesive tapes of a width of 18 mm (TESA film No.5529, Beiersdorf, Hamburg, Germany) were used. After incubation of the topically applied substances, tape stripping was started. Seventy consecutive tapes were collected from each skin area. Immediately after tape stripping, the split skin was removed.

3.3.2.3.4 UV/Vis spectroscopy and extraction protocol

At first, the transmission spectrum was determined for each removed tape strip by UV/Vis spectroscopy (Perkin Elmer Lambda 650 S, Uberlingen, Germany) with an empty tape in the reference beam. The absorption measured at 600 nm was used as measure for the mass of the corneocyte aggregates placed on the individual tapes [129]. Subsequently, all tape strips, and the tiny pieces of dermatomized skin were extracted in ethanol. Therefore, the tapes were cut to a size of 1.5 x 3 cm^2. Each single tape strip of No. 1-10 and the dermatomized skin were placed in a single test tube, which was filled with the amount of 3.14 ml ethanol (Ethanol UVASOL, Merck, Darmstadt, Germany) as extraction solvent. The tapes 11-70 were placed, each 5 consecutively together, in a test tube avoiding any overlapping and adhering to the test tube and other tapes. Then, all tubes were ultrasonicated for 10 min (Sonorex

Super RK102H, Bandelin Electronic, Berlin, Germany) and centrifugated at 4,000 rpm for 10 min at 20°C (Hettich® Universal 320/320R centrifuge, Sigma Aldrich, St. Louis, USA). After the extraction, the absorption spectra of retinal were recorded on the UV-visible spectrometer at 25°C in the range of 250 - 500 nm using a quartz cuvette with 10 mm path length (Quartz Suprasil, Hellma Analytics,). The band maxima of the retinal is at 380 nm. The concentration of free retinal in the extracted tapes and the dermatomized skin was calculated using the standard reference curve, which had been prepared of retinal standards. The results obtained from the PRN and retinal were compared with the untreated skin areas as control.

3.3.2.4 Statistical analysis

To analyze the data, unpaired t-test for comparison of two pairs of samples and Kruskal Wallis One-way ANOVA were used to investigate the differences between the groups (GraphPad Software, San Diego, California, USA). Differences were considered significant at $p < 0.05$.

3.4 Results

3.4.1 Experiment A Determination of the follicular penetration depths of PRN.

The follicular penetration depth of 5(6)-carboxytetramethylrhodamine-labelled PRN was determined by confocal laser scanning microscopy. The red fluorescent signal emitted by the topically applied PRN was detected in the hair follicles and also on the skin surface. In total, 60 hair follicles from 6 independent skin samples were analyzed, the mean follicular penetration depth was 411±60 µm (max=725; min=209) **(Fig.13A)**. No red fluorescent signal was detected in untreated skin areas **(Fig.13B)**.

5(6)-carboxytetramethylrhodamine-labelled PRN   Untreated skin
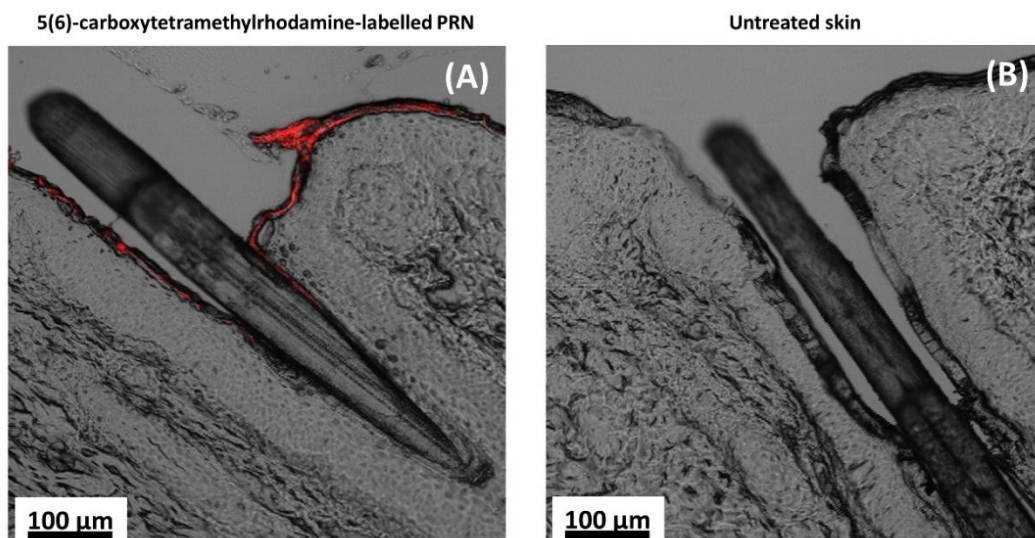
Figure 13 Representative figures of hair follicle cross sections showing the follicular penetration of 5(6)-carboxytetramethylrhodamine-labelled PRN.

(A) and untreated skin as control (B). The distribution of the red fluorescent signals reflects the PRN distribution in the hair follicle after 2 h.

3.4.2 Experiment B Determination of the time dependency of the follicular penetration depth and the release of the 5-carboxyfluorescein from 5(6)-carboxytetramethylrhodamine-labelled chitosan nanoparticles

The CLSM images of the hair follicle cross sections after topical application of 5(6)-carboxytetramethylrhodamine-labelled chitosan nanoparticles loaded with 5-carboxyfluorescein after different incubation times are depicted in **Fig.14**. The fluorescence of 5(6)-carboxytetramethylrhodamine could be visualized at laser line 555 in red and the fluorescence of 5-carboxyfluorescein at laser line 488 in green. In the right column, a merge of both fluorescence signals is demonstrated. The untreated skin showed no fluorescent signal. The corresponding penetration depths of the 5(6)-carboxytetramethylrhodamine-labelled chitosan nanoparticles, of the 5-carboxyfluorescein and of the PRN are summarized in **Fig.15**. Both figures demonstrate that 2 h after topical application, the follicular penetration of 5-carboxyfluorescein (445±21 μm) was deeper than that of 5(6)-carboxytetramethylrhodamine (408±25 μm).

Therefore, it can be assumed that 5-carboxyfluorescein has been successfully released from the 5(6)-carboxytetramethylrhodamine-labelled nanoparticles. After 4 h of incubation time, the deepest follicular penetration of 5(6)-carboxytetramethylrhodamine (474±31μm) and of 5-carboxyfluorescein (509±34 μm) was detected. After an incubation time of 24 h, 5(6)-carboxytetramethylrhodamine (369±28 μm) and 5-carboxyfluorescein (413±28 μm) showed the lowest follicular penetration depths. The follicular penetration depths of 5-carboxyfluorescein were significantly deeper than those of 5(6)-carboxytetramethylrhodamine at every time point for the majority of the hair follicles (2h: 80%, 4 h: 70% and 24 h: 87%) ($p<0.05$).
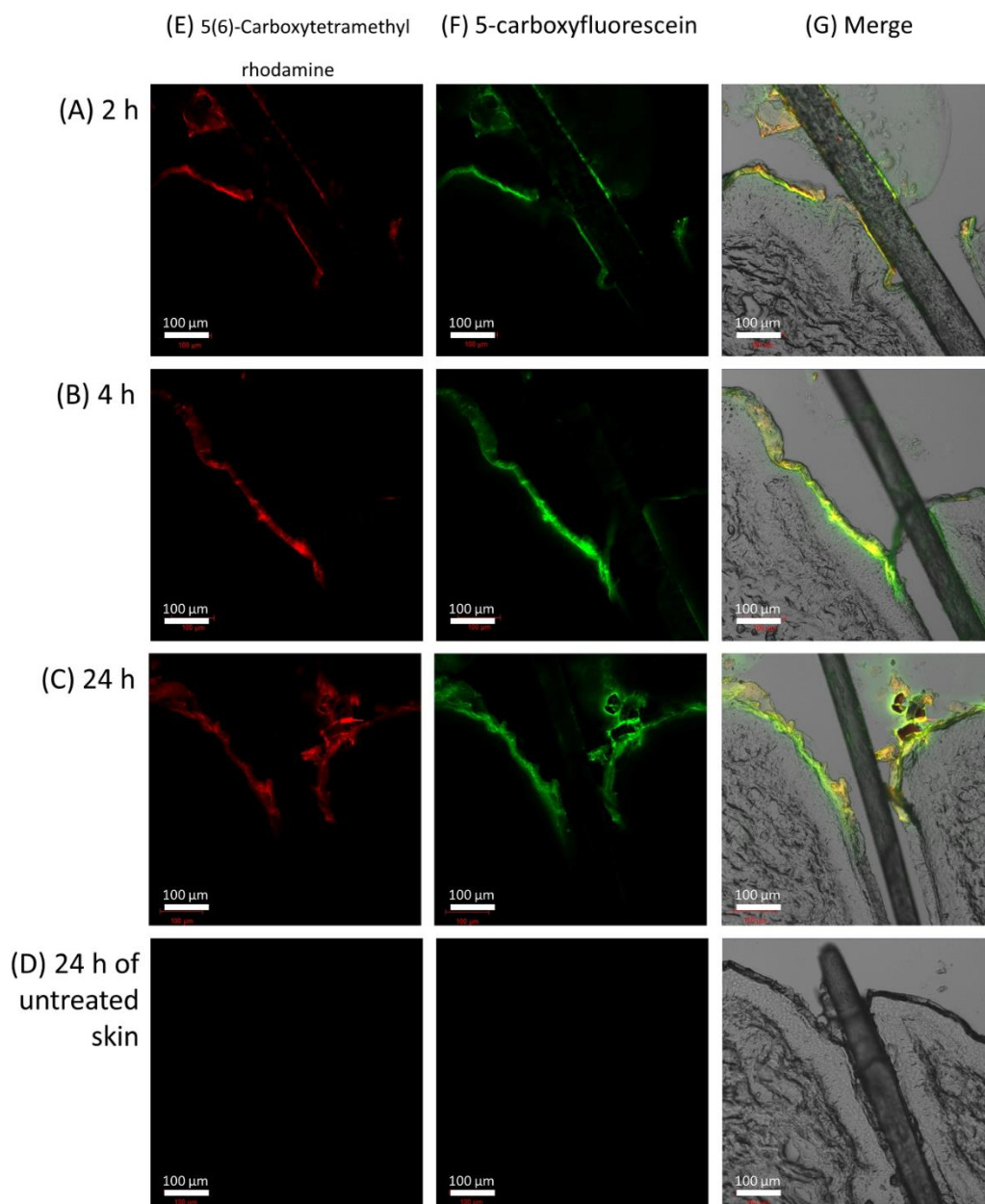
Figure 14 CLSM images of hair follicle cross sections prepared at different time points (A) 2h (B) 4h (C) 24h) after topical application of 5(6)-carboxytetramethylrhodamine-labelled chitosan nanoparticles loaded with 5-carboxyfluorescein. Column E presents the distribution of 5(6)-carboxytetramethylrhodamine in the hair follicles, column F the distribution of 5-carboxyfluorescein. Column G is the merge of both fluorescent signals and the transmission mode. The last row represents hair follicle cross sections of untreated skin. Here, no fluorescent signal was detectable.
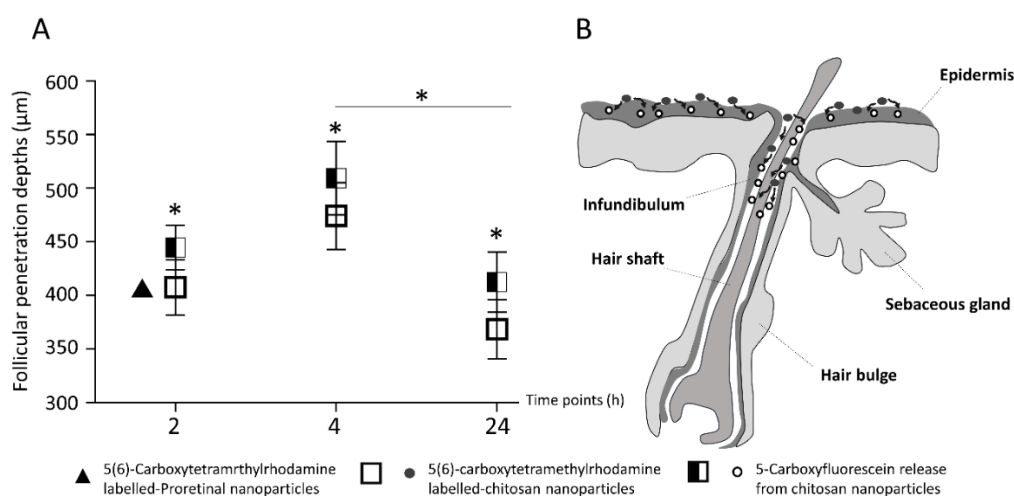
Figure 15 Presentation of the mean follicular penetration depths in μm of 5(6)-*carboxytetramethylrhodamine and 5-carboxyfluorescein, at different time points.*

(A) The black triangle represents the follicular penetration depth of 5(6)-carboxytetramethylrhodamine-labelled PRN after 2 h of incubation. The box plot graph shows the mean follicular penetration depth of 5(6)-carboxytetramethylrhodamine at different time points (which was linked to the chitosan nanoparticles). Due to the significantly deeper follicular penetration depths of the model drug 5-carboxyfluorescein ($*p<0.05$), it can be assumed that 5-carboxyfluorescein has been released from the 5(6)-carboxytetramethylrhodamine-labelled chitosan nanoparticles. (B) Schematic illustration of a hair follicle and follicular penetration depths for 5-carboxyfluorescein dye as a drug model release (clear dots), 5(6)-carboxytetramethylrhodamine as the indicator for penetrated particles (black dots) and 5(6)-carboxytetramethylrhodamine-labelled chitosan nanoparticles 2 h after topical application. After the investigated time points, chitosan nanoparticles and PRN were found mainly in the infundibulum of hair follicle.

3.4.3 Experiment C Modified differential stripping protocol

After topical application of PRN and retinal, the concentration of retinal was quantified in the stratum corneum and in dermatomized skin as shown in the **Table 7** and **Fig. 16**. As the tape stripping revealed only very low or absent concentrations of retinal in the middle and lower stratum corneum, respectively, the modified differential stripping technique was applied analogously to previous study of Knorr and colleagues in 2013 . This technique is based on the assumption that if no substance is located in the lower stratum corneum by tape stripping (as could be demonstrated for PRN and retinal, see **Fig. 16E and F**), the concentration found in the residual epidermis and dermis highly probably originates from the hair follicles. Therefore, the concentrations of retinal extracted from the dermatomized skin are referred to hereinafter as follicular content.

The results revealed that the retinal concentration was higher in the PRN than in the retinal-treated group, which was statistically significant for tape 1 and the follicular content (p<0.05) **(Fig. 16A-C)**. Although the concentration of retinal in tapes 2-10 and tapes 11-70 of PRN-treated group was not significantly different to the retinal group, there is still a clear tendency for a higher concentration in the PRN group. After 70 tape strips, the cumulative concentration of retinal of PRN group was 3-fold higher than in the retinal group **(Fig. 16D)**.

The penetration profile of PRN in **Fig. 16E** demonstrates that retinal is located approximately in the upper 75% of the horny layer. In contrast, the retinal from RAL is located only in the upper 25% of the horny layer **(Fig. 16F)**.

Table 7 The summary of recovered retinal amount found in PRN and retinal-treated groups in each tape stripping compartment and follicular content. Data were represented as the mean values and the standard deviations of 6 replicated experiments. [†]$p<0.05$

Treatment groups	Tape1	Tape2-10	Tape11-70	Follicular content	total
PRN					
Concentration of recovered retinal $(\mu g/cm^2)$	14.5±7.7[†]	5.3±2.0	1.5±1.7	2.6±1.2[†]	23.8±8.4
Percentage of recovered retinal (%)	16.1±8.6	5.9±2.2	1.7±1.9	2.9±1.3	26.4±9.3
Percentage of relative amount of recovered retinal (%)	59.5±19.0	23.5±9.3	6.4±8.7	11.2±6.0	100
Retinal					
Concentration of recovered retinal $(\mu g/cm^2)$	2.9±1.4	3.5±2.0	0.4±0.5	0.2±0.2	7.0±2.5
Percentage of recovered retinal (%)	3.2±1.6	3.9±2.2	0.5±0.5	0.2±0.3	7.7±2.7
Percentage of relative amount of recovered retinal (%)	43.4±15.1	50.2±15.6	5.5±4.7	2.5±2.9	100
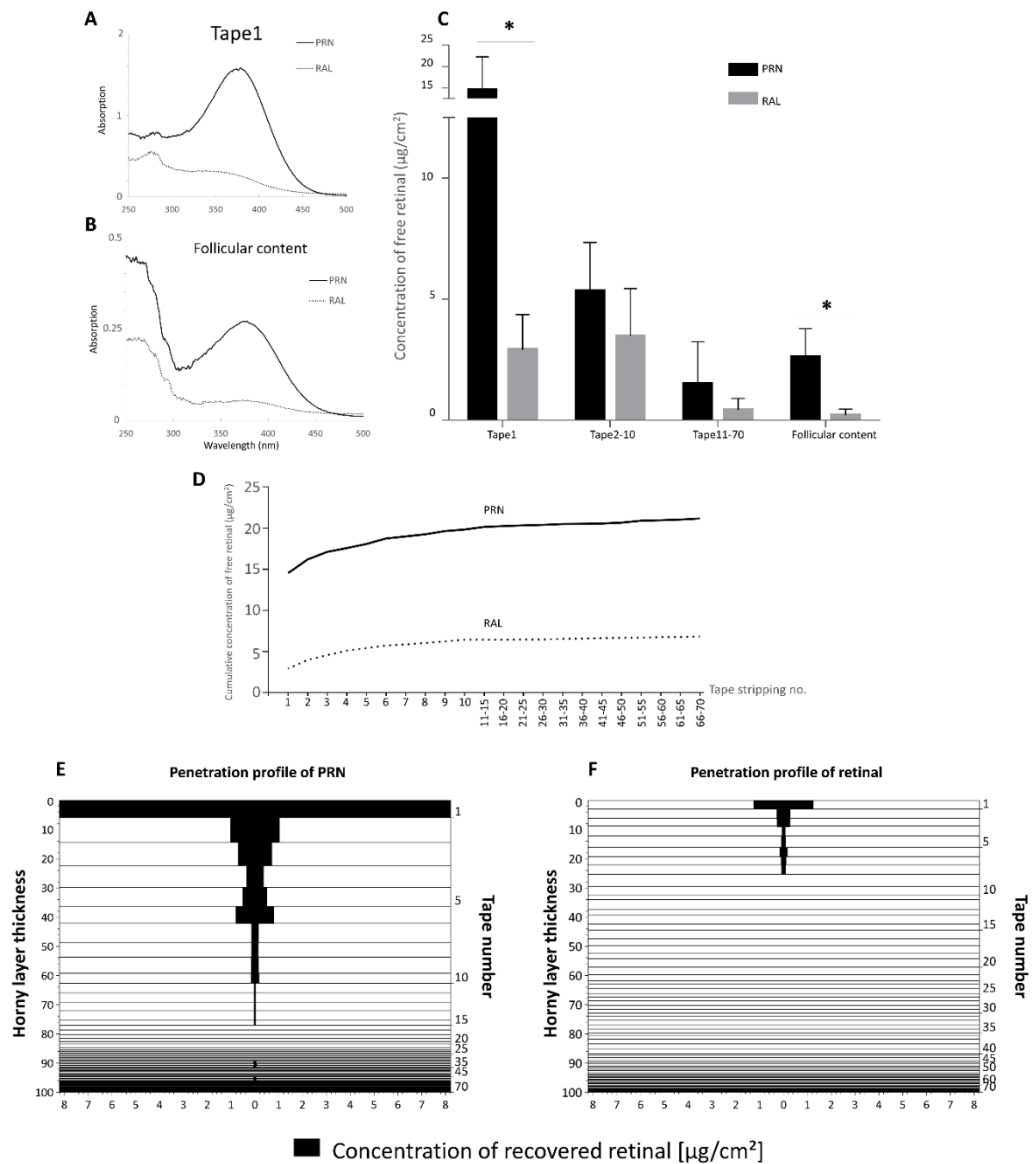
Figure 16 UV-absorption spectra of recovered retinal (λ_{380nm}) from PRN (---) and RAL (⋯) in the region of 250-500 nm (A) tape1 (B) follicular content. (C) Comparison of the concentration of retinal in PRN and RAL-treated groups (μg/cm2) for tape 1, tape 2-10, tape 11-70 and the follicular content after 4 h of incubation (* p<0.05). (D) Cumulative concentration of retinal (μg/cm2) after topical application of PRN and RAL in the stratum corneum. (E-F) Distribution of retinal in (E) PRN- (black fill) and (F) RAL-treated skin (black fill) inside the stratum corneum.

3.5 Discussion

The usefulness of retinoids is widely recognized in dermatology for the therapy of acne and other retinoid responsive disorders, but also as an anti-aging cosmeceutical. Due to its susceptibility, the development of topical retinoid preparations requires improvement in stability and controlled release properties. Therefore, the utilization of particulate drug delivery systems seems to be a promising approach as nanoparticle systems can provide a better chemical and physical stability of drugs and moreover, offer a sustained release. Unfortunately, nanoparticles are rarely able to ov ercome an intact skin barrier directly, but they have been described to penetrate very efficiently into the hair follicles and to improve skin absorption of actives by maintaining a concentration gradient and by other partly still unclarified mechanisms [123, 124].

Previous studies clearly demonstrated that the follicular penetration mechanism is mainly mechanically driven and comparable to a ratchet [121]. Due to the movement of the hair, whereby movement direction and frequency also play significant roles, the nanoparticles are transported deeply into the hair follicle. This process is facilitated if nanoparticle size and the thickness of the cuticula cells, which cover the hairs, are comparable in size. In an earlier study it was shown that, by selecting a specific particle size, different target sites within the hair follicle can be reached. For nanoparticles with a diameter of 643 nm, the follicular penetration depth was significantly deeper than for nanoparticles of smaller or larger sizes. Whereas the 643 nm nanoparticles reached follicular penetration depths of more than 1000 μm, smaller or larger particles remained only in the infundibulum. The authors could reproduce their findings for different particle types [130]. In the present study, nanoparticles of a size of about 240 nm were utilized. The deepest follicular penetration depth for PRN was around 470 μm after an incubation time of 4 h, meaning a penetration down to the inferior infundibulum part of the hair follicle. When comparing the data of the present study with data obtained for the PGLA particles with a comparable size [131], the 230 nm PGLA particles penetrated approximately 800 μm into the hair follicle. The detected differences could be due to an aggregation

effect of the particles used in the present study, which can affect the penetration behavior [132]. Nevertheless, it can be stated that the target site of interest for retinal in the therapy of acne, which is the infundibulum, can be successfully reached in order to affect the main problems of acne, which are inflammation and abnormal keratinization [133]. If deeper areas of the hair follicle have to be targeted in further clinical indications, probably other vehicles have to be selected to avoid the aggregation effect and to enhance the follicular penetration. Actually, the slightly different follicular penetration depths can also be due to different vehicle formulations as has been reported by Patzelt et al [130]. The PRN were prepared as an aqueous suspension, which might support the aggregation effect [132]. Patzelt et al. also reported that the same type of particles penetrated slightly deeper into the hair follicles when applied in gel formulation than in aqueous suspension [130] .

Double fluorescent-labelled chitosan nanoparticles were used to investigate the time dependency of the follicular penetration depth and the potential release of the model drug fluorescein. Although many studies have succeeded in encapsulating retinoids into nanocarriers [134, 135], especially the follicular penetration of these nanocarriers at different time points has not been investigated so far to our knowledge.

For the investigation of the potential release, retinal was replaced by 5-carboxyfluorescein for the visualization of the release by confocal laser scanning microscopy. Although, 5-carboxyfluorescein is not able to replace retinal completely as the chemical bond to the chitosan nanocarriers was changed from imine to ester bond for fluorescein, both nanocarriers (PRN and double-labelled chitosan nanocarriers) at least provided the same follicular penetration depth at 2 h. Therefore, it can be concluded that the follicular penetration behavior of both particle types is comparable.

Therefore, the fluorescent signal of 5(6)-carboxytetramethylrhodamine was used to study the penetration behavior of the nanocarrier and the fluorescent signal of 5-carboxyfluorescein was used to study the release properties of the nanocarriers. Due to the solubility of chitosan, chitosan nanoparticles possess pH-dependent drug

release [136]. The skin pH could control the grafted active substance sustainably releasing from the chitosan nanoparticles. The sustain release character of the chitosan nanoparticles at the skin pH was hypothesized to deliver the grafted active substances on chitosan nanoparticles after single application [125]. Although the ester linkage between 5-carboxyfluorescein and chitosan is not as labile as the imine linkage between retinal and chitosan, ester bond hydrolysis is expected in hair follicles due to the lipase presence in in the sebaceous glands and in the external root sheath of the hair follicle [137, 138]. Faster release of 5-carboxyfluorescein as compared to that of the 5(6)-carboxytetramethylrhodamine is likely the result of a more hydrophobicity of the latter comparing to that of the former. Therefore, here the release of 5-carboxyfluorescein was expected to be representative of drug release from the penetrated particles in hair follicles. The follicular penetration depths of 5(6)-carboxytetramethylrhodamine and 5-carboxyfluorescein were significantly different at all time points, whereby 5-carboxyfluorescein could be detected approximately 50 μm deeper inside the hair follicle than 5(6)-carboxytetramethylrhodamine. Therefore, it can be assumed that the model drug fluorescein was transported into the hair follicle by the nanocarrier, then it was released from the nanocarrier within the infundibulum of the hair follicle, as expected, and subsequently, penetrated deeper into the hair follicle independently from the nanocarrier.

The follicular penetration depths of the chitosan nanoparticles were found to be not time dependent. There was no significant difference in the follicular penetration depths after 2 h and 4 h, meaning that the maximum penetration depth can already be reached at early time points. Based on the *in silico* data [121], it can even be assumed that the maximum follicular penetration depth in *ex vivo* skin models can be reached already within a couple of minutes during the massage application as the results suggest that the follicular penetration process has to be mechanically stimulated. As previous studies [125], however, demonstrated that more than 50% of the release occurs after 4 h, this incubation time was selected. Surprisingly, the follicular penetration depth was shown to be significantly reduced after 24 h. This effect is probably due to a reduction of the fluorescence signal of 5(6)-

carboxytetramethylrhodamine and 5-carboxyfluorescein over time as a retrograde penetration cannot be expected in an *ex vivo* skin model. For the in vivo situation, it is known that the particles are transported out of the hair follicle by sebum flow and hair growth, which are lacking in *ex vivo* skin [139].

Additionally, the intercellular and follicular penetration of retinal was investigated for retinal either released from a conventional RAL formulation or from PRN. Most topically applied substances only show a very limited skin penetration due to the strong barrier function of the skin. The results of the study showed that the cumulative concentration of retinal in the stratum corneum was 3fold higher when retinal was delivered by PRN than by a conventional RAL formulation. Moreover, the penetration of retinal was significantly deeper when applied as PRN. Retinal released from conventional RAL was only detected in the upper 10 tape strips, whereas retinal from PRN was also detected in the lower part of the SC. The penetration profiles clearly demonstrate these effects. It can be supposed that due to the good encapsulation efficacy, retinal can be continuously delivered from the PRN reservoir located on the skin surface and upper stratum corneum layers, whereas retinal from conventional RAL is easily degrading due to its chemical and photochemical instability.

According to the Fick's law explaining the passive transport of substances through the skin [140], the flux of a substance is positively correlated to the concentration gradient. Due to the increased concentration of retinal on the skin surface when applied as PRN, a high concentration gradient exists resulting in a high flux of retinal into the stratum corneum. These results are in agreement with [141] who explained that nanoparticles would rather enhance the drug diffusion through the skin barrier and increase the drug gradient than penetrating through the healthy stratum corneum. Moreover, as already reported in other studies, it has to be taken into consideration that the amount of retinal recovered from the middle and lower part of the stratum corneum could already originate from the hair follicle openings [142], which are also removed by the tape stripping procedure. This assumption can be emphasized by the fact that especially retinal from PRN is localized at higher concentrations in the lower stratum corneum. The better penetration of retinal from

PRN application observed here agrees well to the more pronounced in vivo biological effect observed for the PRN as compared to the RAL reported earlier [125].

In the present study, this assumption was the basis for the method to quantify the follicular content. It was suggested that unless retinal is available in the lower stratum corneum, it will likewise not be detectable in the rest of the epidermis but only in the hair follicles. This assumption is also according to the well-established method of differential stripping that is used to quantify the follicular content [143]. As the removal of the follicular content was not possible by cyanoacrylate skin surface biopsies in the porcine ear skin model as suggested by the differential stripping method, subsequently to the removal of 70 tape strips, split skin was removed, extracted and quantified to determine the follicular content. The follicular content was around 5% of the applied retinal, which is in the same range reported by other studies, which used the unmodified differential stripping technique [143].

Acknowledgements

Declarations of interest

None.

CHAPTER IV

Microneedle-facilitated intradermal proretinal nanoparticles delivery

Manuscript in preparation in the topic of

Microneedle-facilitated Intradermal Proretinal Nanoparticles delivery

Benchaphorn Limcharoen, Pattrawadee Toprangkobsin, Titiporn Sansureerungsikul, Marius Kröger, Supason Wanichwecharungruang, Wijit Banlunara, Maxim E. Darvin and Alexa Patzelt

Highlight

- Proretinal nanoparticles loaded microneedle is possible to deliver retinal to dermis by piercing through stratum corneum

- Several non-invasive imaging techniques could demonstrate the presence of proretinal nanoparticles loaded-microneedle in the dermis.

- We could have the opportunity to deliver retinal directly to dermis using two combinations of drug delivery strategies to treat some skin conditions

4.1 Abstract

Topical retinoid treatments exert biological activities of skin both epidermis and dermis. The topical application of retinoids targets multiple aspects in dermal improvements including dermal collagen synthesis either treatment of skin aging or scar-smoothing benefits in atrophic acne scar. Retinaldehyde has been well known to be useful in these conditions. The main primary biological barrier to deliver topical drug which limits the efficacy of transdermal drug delivery system is stratum corneum which is formed by compact corneocytes. Proretinal nanoparticles (PRN), a polymeric nanoparticulate form of retinaldehyde, has been proved to efficiently deliver and supply retinal mainly in epidermis which is the upper part of skin. The use of two combinations transdermal drug delivery strategies were developed and investigated in this study by non-invasive imaging techniques as dermoscopy, optical coherence tomography and multiphoton microscopy. The insertion array, microchannel characteristics, PRN localization in microchannels and skin closure kinetic have been studied and visualized successfully over the time following the application. Finally, the skin depositions of retinaldehyde concentration in different topical application were compared. The recovered retinaldehyde concentration in dermis was significantly higher in microneedle loaded with PRN treated skin. We hypothesized that this platform of PRN-loaded microneedle would provide rapid administration through short time after microneedle insertion, assist a long-term releasing retinaldehyde from PRN depots and supply dermis. Finally, it could be beneficial in some skin condition as atrophic scar and photoaging in the future.

Keywords; Microneedle, retinaldehyde, nanoparticles, dermis

4.2 Introduction

Topical application of retinoids targets multiple aspects in dermal improvements including dermal collagen synthesis [144] either treatment of skin aging [145-147] or scar-smoothing benefits in atrophic acne scar [148, 149] by enhancing fibroblast in UV-damaged skin [150], improving skin texture and reducing discoloration [151]. Retinaldehyde, a natural precursor of retinoic acid and a metabolite of vitamin A, is shown to exert the biological activities of retinoids and beneficial for the treatment of photoaging [10] and acne scarring [152]. Although topical application of retinaldehyde is useful in clinical dermatology, there are still some limitations of the topical usages such as its photochemical instability and irritation in long-term application. Moreover, when focus on cutaneous concentrations of retinoids, *all-trans*-retinoic acid has steep concentration gradient with high concentration in the epidermis and relatively low concentration in the dermis [153]. The skin permeability of the commercially available all-trans-retinoic acid is quite low as 5% [154]. The main primary biological barrier to deliver topical drug which limits the efficacy of transdermal drug delivery system is stratum corneum which is formed by compact corneocytes as the thickness of 10-15 µm [155]. New growing microneedle technologies have been purposed to tackle the limitation of customary transdermal drug delivery. Microneedle (MN) is minimally invasive technique employed the array of micron-sized needles and the length up to 1000 µm [156] to penetrate through stratum corneum and facilitate the active substances to viable epidermis or dermis. Different biodegradable and water-soluble polymer such as sodium hyaluronate [157, 158], polyvinylpyrrolidone (PVP) [159] and polyvinyl alcohol (PVA) [160] have been used to fabricate dissolvable MN. Then, it can manage the rate-controlling release of nanoparticles-loaded MN into target area. Recently, proretinal nanoparticles (PRN) has shown promising capability to overcome the instability of retinaldehyde and possess the controlled release of retinal at skin pH [13]. However, nanoparticulate system has been proved to efficiently deliver and supply retinal mainly in epidermis which is the upper part of the skin [13]. To improve efficacy of delivery for further dermatological treatment in the dermis aspects, the application of PRN-loaded microneedle has been purposed to overcome the stratum corneum which is the natural barrier of the skin. Since retinaldehyde has many

significant biological effects to dermis. The dissolvable PRN-loaded microneedle has been developed to bypass PRN to dermis directly. Thus, the aim of this investigation is to visualize the ability of insertion of PRN-loaded microneedles by non-invasive techniques including dermatoscopy, optical coherence tomography (OCT) as well as multiphoton microscopy (MPM) and to quantify recovered retinal concentration in both epidermis and dermis. All of these imaging techniques enabled real-time functional images of skin penetration in the natural state and provided the penetration depth data without the need for tissue sections.

4.3 Materials and methods

4.3.1 Fabrication of the dissolving PRN-loaded microneedles

PRN was prepared as previously described with some minor adjustment [19]. Briefly, chitosan (CS, molecular weight of ～40,000–50,000 Da, Taming Enterprise, Samut Sakhon, Thailand) was dissolved in 0.05 % acetic acid, and the pH of the obtained solution was adjusted to 5.9 using NaOH. The final solution contained 45 mg CS in 19.0 mL solution. Then cold retinal (15 mg, Sigma Aldrich, in 1.0 mL of ethanol) was slowly added dropwise into the cold CS suspension (5°C) under light-proof condition while the mixture was continuously ultrasonicated (40kHz) under N_2 atmosphere. The obtained PRN suspension was then freeze-dried. The size of PRN was 240.1±29nm.

The microneedles were fabricated using micro-molding technique with sodium hyaluronate as the base material. Sodium hyaluronate (injection grade, Shandong Focuschem Biotech Co., Ltd., Shandong Sheng, China), maltose and PVP (Sigma-Aldrich, Missouri, USA) were dissolved and mixed with proretinal nanoparticles (PRN). The obtained suspension was cast on micromoles and dried in a desiccator at room temperature. The PRN-loaded microneedles were obtained by removing them from the micromoles. The microneedle patch obtained here is the 10 × 10 needle array patch with tetragonal pyramidal shaped needle of 200 × 200 µm base and 650 µm needle height. The amount of retinaldehyde loaded in the 10 × 10 needle part of

each microneedle patch was 2.08 $\pm$ 0.55 μg. A stereomicroscope (Olympus DP22, Japan) was used to observe the morphologies and dimension of the MN.

4.3.2 Experimental designs of topical applications

Fresh porcine ears without any skin lesions from 6-month-old German domestic pigs were obtained from local abattoir. The used protocol was approved by the Veterinary Board of Control, Dahme-Spreewald. The porcine ears were cleaned up under running tap water and dry with papers. Hairs were trimmed. Four areas of 1.5x3 cm^2 were defined. The test samples were untreated skin as a control, PRN-loaded microneedles, PRN and RAL suspension.

The topical substances were applied to the well-demarcated skin areas using a silicon barrier (Marabu Window Color, Marabu GmbH, Bietigheim-Bissingen, Germany) to prevent the lateral spreading of applied substances in each pig ear. The 20 μL of liquid substances per cm^2 of treated area were applied (equivalent to 12 μg of retinaldehyde/ 4.5 cm^2), distributed homogeneously with 2 min of 50 Hz massage appliance (Novafon Pro soundwave appliance, Weinstadt, Germany) and were incubated following the indicated penetration times of 4 h at room temperature. PRN-loaded MN patches were inserted to the tested area using hand pressure to press the needle patch into the skin, the patch was held in place for 5 min with some massage motion and pressure through the finger tip, then the base of the patch was peeled off. Six patches of MN were used on the area of 4.5 cm^2. The peeled off base was subjected to microscopic examination to make sure that all needles have been detached and left in the skin. Each experiment was performed on 6 independent pig ears (N=6). Due to the light sensitivity of retinoids, all experiments were handled to avoid the light.

4.3.3 *Ex vivo* skin penetration studies

4.3.3.1 Dermoscopy

To investigate the ex vivo insertion capability of PRN-loaded MN, dermoscopic examination was performed immediately, 4h and 24h after microneedle administration by a computerized polarized light videodermatoscope (FotoFinder Dermoscopy equipped with Medicam 800 HD; FotoFinder Software, Bad Birnbach, Germany) with

magnification factors of X20 to X70 at X10 increment lens. As polarized light was used, no preparation of the area under examination was necessary.

4.3.3.2 Optical Coherence Tomography (OCT)

OCT was used as adjunct to dermoscopy to visualize the morphologic changes of superficial layers of skin and to confirm the insertion and creation of microchannels following the application of MN to porcine skin. Test areas of MN insertion were scanned with OCT (VivosightOCT Scanner, Michelson Diagnosis Ltd., Kent, UK) after dermoscopy over an area of 6x6 mm, depth 1 mm, with an optical resolution of < 7.5 μm laterally and < 5 μm axially at the same time points as dermoscopic examination. No preparation of the skin surface, oil or ointment of test areas were required in OCT scan. The function 'multi-1' setting automatically generated 60 lateral scans of 6-mm length every 100 μm of lateral scanning of the axial OCT scans resulting in two-dimensional cross-sectional images and en-face views. The OCT images were assessed by naked eye for features affecting the epidermis and the dermis immediately, 4h and 24 h after single insertion. The penetration capability of MN was immediately investigated without histological processes or sections.

4.3.3.3 Multiphoton microscopy (MPM) with fluorescence lifetime imaging microscopy (FLIM)

In order to verify the location of PRN dissolved from MN, images of the epidermis and dermis were acquired by means of the two-photon laser microscopy *Dermainspect* (JenLab GmbH, Jena, Germany) consisting of a tunable femtosecond titanium sapphire laser (Mai Tai XF, Spectra Physics, USA). The full thickness of skin samples after MN insertion in the size of 1 x 1 cm^2 were prepared for the experiment.

To detect autofluorescence, the excitation wavelength used for this study was at 760 nm. The laser was generated 100-fs pulses at a repetition rate of 80 MHz. Te 410–680 nm bandpass filter was utilized. The combination of TPM and FLIM was applied for the detection of subtle changes in fluorescence lifetime of intrinsic autofluorescent compound intentionally in microchannels in the treated skins created by the insertion of PRN-loaded MN. Fluorescence lifetime data were analyzed by the

SPCImage software (Becker&Hickl, Berlin, Germany) incorporated into the Dermainspect system. Fluorescence decay in each pixel was fitted with a sum of two exponentials (fast and slow) with a fixed shift value, and the intensity threshold was chosen depending on the image quality. To obtained lifetime (τ1 and τ2) and amplitude (a1 and a2) values were further exported and used for the evaluation of lifetime distributions and image segmentation. The average lifetime was defined as τm=(a1τ1+a2τ2)/(a1+a2). The scanning modality of MPM-FLIM images was x-y scanning, resulting in z-stack of horizontal images from the stratum corneum to the dermis. The z-stack were taken by moving the objective in the z-direction, thus scanning at different depths in the skin with steps every 10 μm.

4.3.4 Skin deposition of retinaldehyde from PRN-loaded MN

Skin deposition of retinaldehyde was performed after designated time of incubation of all topical applications of ex vivo porcine model.

4.3.4.1 Extraction of epidermis and dermis treated with retinoids

To separate epidermis from dermis, full-thickness skin was dissected from the underlying cartilage by using a scalpel and heated for 1 min on stainless steel heating plate at 60 ℃ [161]. Epidermis could be entirely peeled from dermis with forceps. Recovered retinaldehyde concentration in the skin was determined by UV-vis spectroscopy

4.3.4.2 UV-vis spectroscopy for quantification of recovered retinal in the skin

After epidermis and dermis from all test groups were subjected to be extracted for the recovered retinal. Epidermis and dermis from each treatment group were disrupted separately into tiny pieces and placed into a sterile 2 mL round-bottom tube containing a 0.5 cm diameter stainless steel bead. All samples were mechanically disrupted using a TissueLyser II (Qiagen, Venlo, Netherlands) for 1 min at 30 Hz. and another 1 min with 1 ml of extracted buffer (10% distilled water in acidic ethanol pH 3 (Ethanol UVASOL, Merck, Darmstadt, Germany). Each sample was placed in a single test tube which was filled with the amount of 2.14 ml extracted buffer. Then, all tubes

were ultrasonicated 10 min (Sonorex Super RK102H, Bandelin Electronic, Berlin, Germany) and centrifugated at 4,000 rpm for 10 min at 20 $^\circ$C (Hettich$^{®}$ Universal 320/320R centrifuge, Sigma Aldrich, St. Louis, USA).

After the extraction, the absorption spectra of recovered retinal in supernatant were recorded on a Perkin Elmer Lambda 650 S UV-visible spectrometer (Uberlingen, Germany) at 25 $^\circ$C in the range 250-500 nm using a quartz cuvette with 10 mm pathlength (Quartz Suprasil, Hellma Analytics,). The band maxima of the retinal is at 380-400 nm. The results obtained from the recovered retinal concentration of PRN-loaded MN, PRN and RAL which were different formulations were compared with the untreated skin areas as a control. The amount of recovered retinal in epidermis and dermis from all formulations was calculated using the standard reference curve by the fresh preparation of retinal standards.

4.3.5 Statistical analysis

To analyze the data, one-way ANOVA test was studied the difference of recovered retinaldehyde concentration in epidermis and dermis between groups using GraphPad Software (San Diego, California, USA). Significant differences were considered significant at p-value < 0.05.

4.4 Results

4.4.1 Morphology of PRN-loaded MN

After fabrication, microscopy confirmed the MNs array had a dimension of 0.5 x 0.5 cm with 10 x 10 needles in each patch. Each needle is a tetragonal pyramidal shape needle with sharp-pointed end of the pyramid as a tip. The dimension of each tetragonal pyramindal needle is 200 x 200 μm at the base and 650 μm height of each needle **(Fig.17A)**. Prominently, the yellow-orange PRN [13] were highly concentrated at the needles, forming a yellowish orange tip on each MN **(Fig.17A)**. After application, the complete array of MN detached from the base and remained in the skin**(Fig.17 B)**.
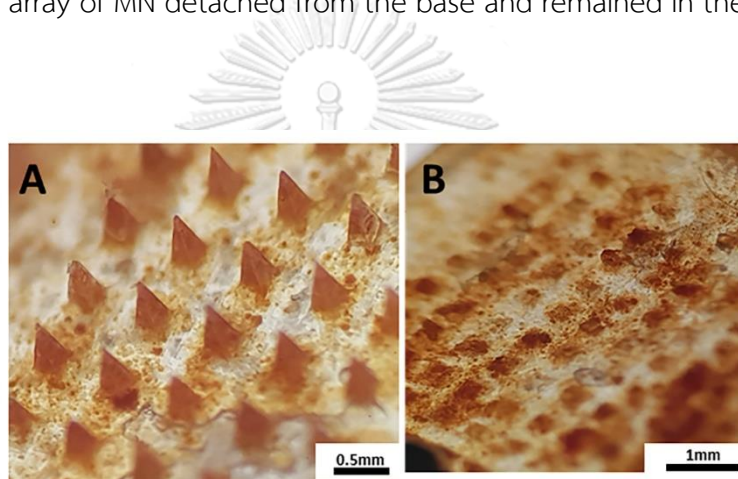
Figure 17 Characterization of PRN-loaded MN

(A) optical image of MN patch and the array of microneedles in higher magnified view of the MN array on the patch under optical microscope represents microneedles before application **(B)** PRN-loaded MN patch after ex-vivo application to the porcine ear skin.

4.4.2 *Ex vivo* skin penetration studies

2.1 Dermatoscopy

Dermatoscopic examination of test area immediately and 4 h after application of MN. After removing MN, dermoscopic images of the porcine skin after application are shown in **Fig.18**. The PRN-loaded MN could easily penetrate the fresh porcine skin as observed from dermoscopy. There are yellow dots which were visible on the dermal

side of MN-treated skin samples indicating the tip of MNs located with the porcine skin immediately until 4 h after application in array of 10 x 10 **(Fig.18A-F)**. These dots confirm the creation of microchannels or conduits by the application of PRN-loaded MN. The treated skins were subjected to continue to observe disappearance of microneedles in the skin within 24 h. The remainder of the skin examination findings after 24 h of MN application were unremarkable **(Fig.18G-H)**.
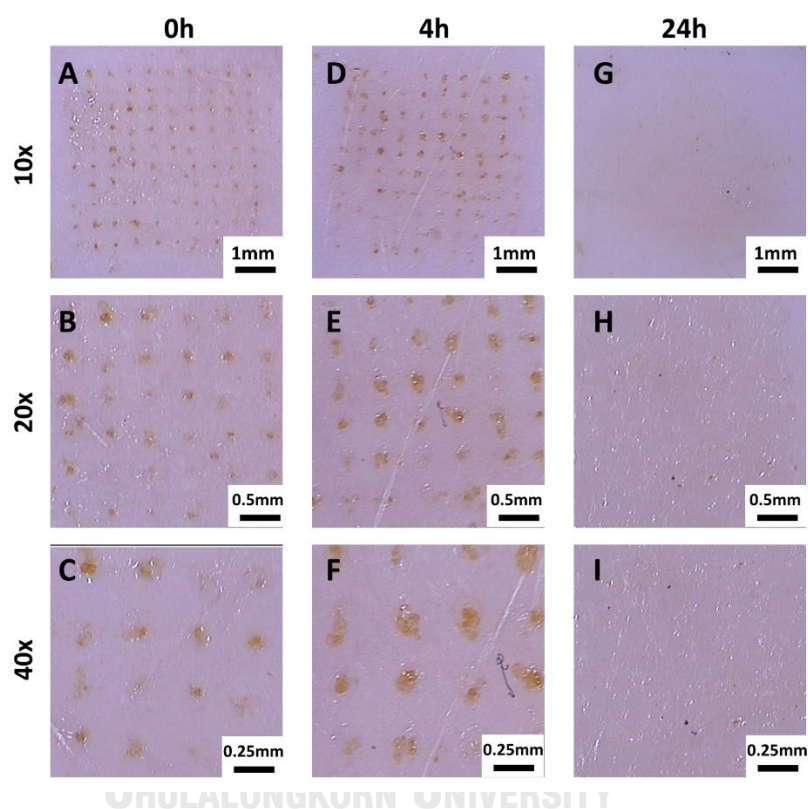
Figure 18 Dermoscopic images of representative porcine skin treated with PRN-loaded MNs patch at different magnification. Application test of PRN-loaded MN into porcince skin. Top views of the skin surface were imaged by dermoscopy of which area showed the effect of application times in different time points; (left column) immediately, (middle column) 4h and (right column) 24h. **(A-F)** The 10x10 array of yellow dots showed the successful insertion of MN in skin. **(G-I)** after 24 h, the disappearance of microneedle in the skin.

2.2 Optical Coherence Tomography (OCT)

For visual inspection of real-time and non-invasive technique MN-treated skin, representative optical coherence tomography images of PRN-loaded MN array after insertion into porcine skin immediate until the period of 24 h. The images are shown in **Fig.19**. The en-face images and cross-sectional images of MN-inserted skin in a series of time are shown in **Fig.19A** and **19B** respectively. In en-face view, the microchannels formed by PRN-loaded MN in the array of 10x10 could be obviously visualized from the depth of 100 µm until 600 µm of skin surface prominently immediately until 4 h after insertion and less noticeably after 24 h of insertion in every depth **(Fig.19A)**.

In the cross-sectional views of porcine skin from OCT following time points after single MN insertion, PRN-loaded MN could puncture the stratum corneum as penetrate efficiently the skin in which MNs tip reached the dermis layers **(Fig.19B)**. PRN-loaded MNs were able to insert the porcine skin reaching the depth of insertion approximately 600 µm in dermis. The high intensity of stratum corneum was indented at the concave injection sites directly after pressed MN and the microchannels were created **(Fig.19B; 0 h)**. In addition, the hyperreflectivity of tips of MNs were found within the microchannels than the intensity of adjacent normal dermal **(star in Fig.19B)**. The pattern of microchannels on the skin surface which the center to center spacing of microchannel is 100 µm broadly reflected the arrangement and dimension of the MN array both in en-face and cross-sectioned views at all time point. The closure kinetics of microchannels and skin indentations become shallower within the time starting from 4 h. After 24 h, the stratum corneum could reseal almost to its initial condition. Nonetheless, a slight discontinuity of the skin surface could be still visualized at the end of the experiment **(Fig.19B: 24 h)**.
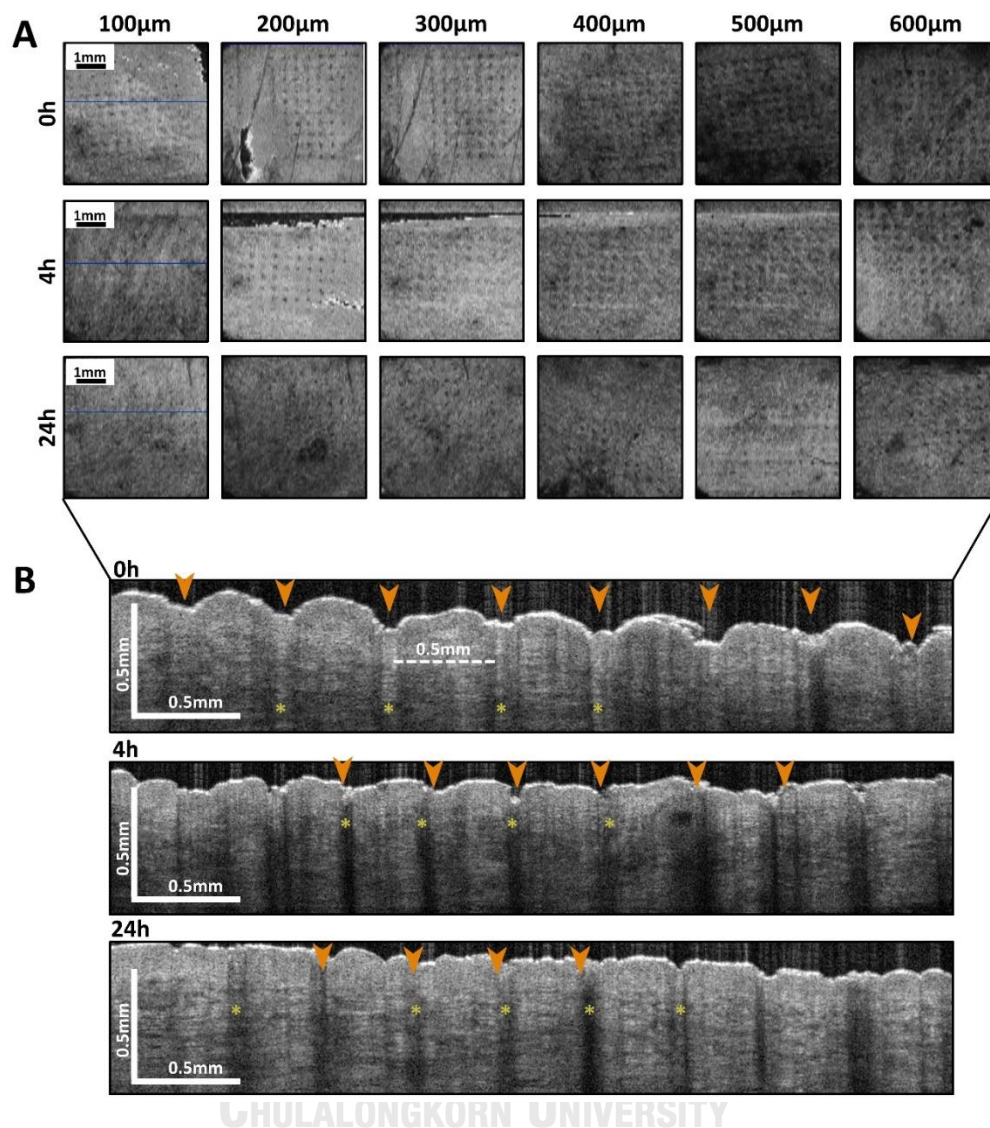
Figure 19 Representative optical coherence tomography images after insertion PRN-
loaded MN of in different time point as immediately, 4 h and 24 h consecutively.
(A) En-face OCT images (XY plane) in projection view of the skin surface of skin after
MN insertion obtained from different depth ranges from 100-600 μm beneath the skin
surface. Scale bar represents 1 mm. **(B)** Cross-sectional OCT images (XZ plane) highlight
the ability of MN to penetrate to ex-vivo porcine skin approximately 600 μm.
Arrowhead; the disrupted stratum corneum as the concave indentation of skin and the
MN-forming microchannels. *; tips of MN and become dissolvable within series of time.
Scale bar represents 0.5 mm.

2.3 Multiphoton microscopy (MPM) with fluorescence lifetime imaging (FLIM)

The fluorescent lifetime is usually reported in picosecond and nanosecond units. Fluorescent lifetimes can change with the microenvironment and be optimal to separate PRN and dissolved polymer in microchannels.

Following the insertion of PRN-loaded MN in the skin, certain area of the microchannels through the skin surface (z=0 µm) until the depth of 150 µm (z = 150 µm) were observed to have nanoparticle deposition in the pattern similar to the aggregation of PRN in the tips in the designed MN array. Each representative MPM image corresponding to 1 microchannel is shown in the **Fig.19-20** both in Two photon excited autofluorescence (TPEAF) and FLIM modes. The main MPM-FLIM features associated with microchannels included microchannel, dissolved polymer and PRN. A well-demarcated stratum corneum as a microchannel were seen at the skin surface until the dermis. The size of the opening of microchannels became slightly smaller within series of time. There were approximately 90 µm in diameter until 4h and smaller as 60 µm in diameter at 24h after insertion at the treated skin surface and in dermis. The delivery of PRN into the microchannel could by observed by MPM-FLIM as PRN has a strong signal from MPM-FLIM. PRN luminescence is shown in orange in **Fig.20B-G**. PRN signal can be observed primarily in the microchannel of MN treated skins. The MPM-FLIM was intended to separate PRN from dissolved polymer. In each microconduit, dissolved polymer from tip of MN was pseudocolored from yellow to green **(Fig.20B-G)**. These false colors are in agreement to relatively slow autofluorescence lifetime and instant nature of PRN luminescence relatively.
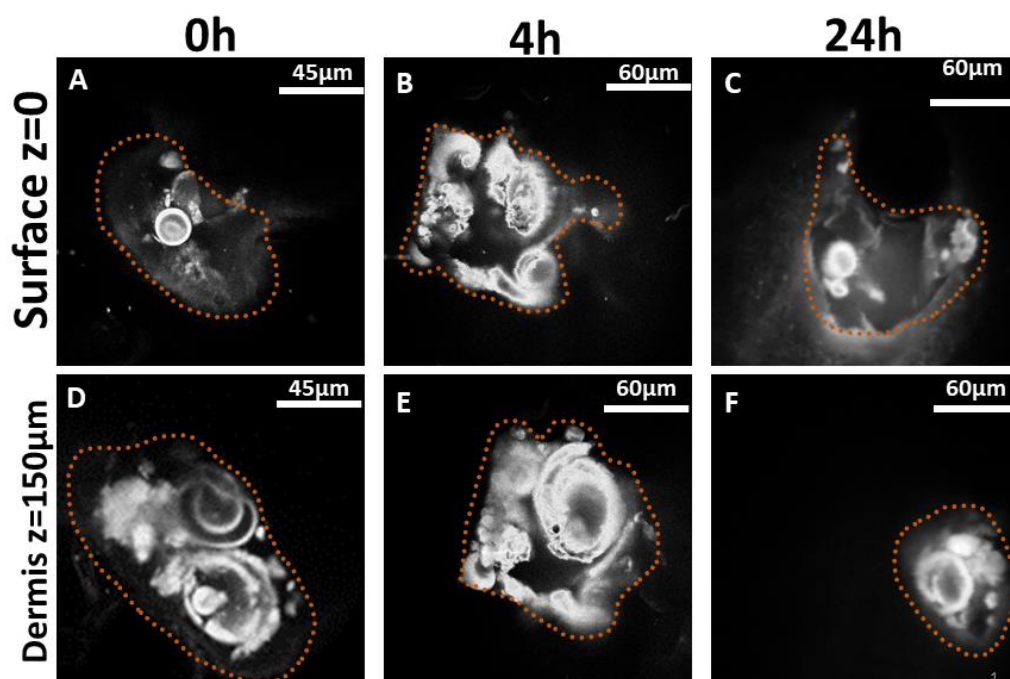
Figure 20. En-face multiphoton microscopy (MPM) with two photons excited autofluorescent mode (X-Y scans) of microchannel-creating MN following time points (0 h, 4 h and 24h) at two different depths. The orange draw line represents the microchannels. **(A-C)** Surface of the skin z=0. **(D-F)** Dermis at the depth of 150 μm from skin surface (z=150 μm). PRN and dissolved polymer from MN deposition in microchannels (760 nm excitation wavelength) following time point in columns.
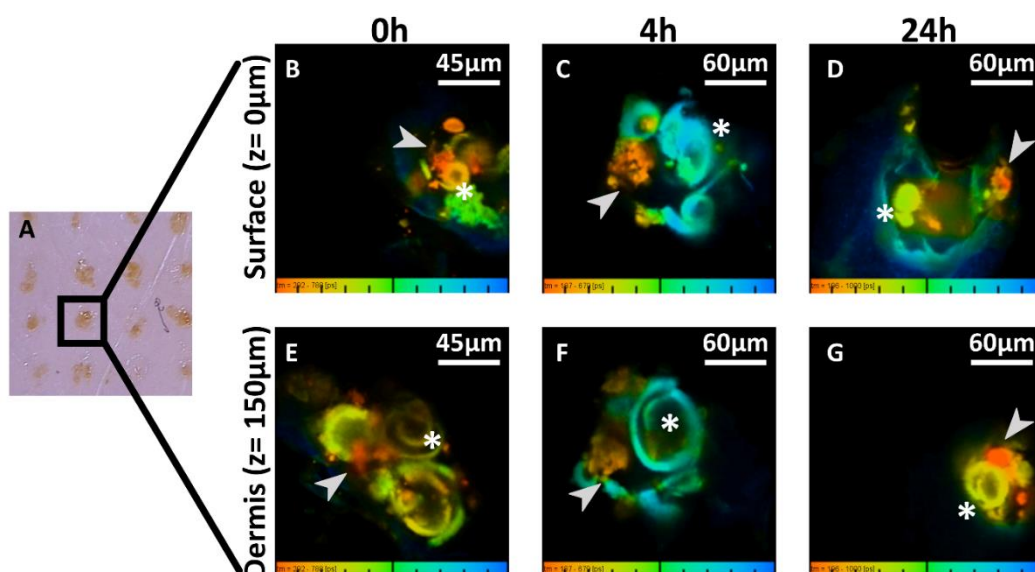
Figure 21. En-face multiphoton microscopy (MPM) with fluorescence lifetime imaging (FLIM) images (X-Y scans) of microchannel-creating MN following time points (0 h, 4 h and 24h) at two different depths. **(A)** The black square marker represents the location wherein the image was shown in **B-G**. **(B-D)** surface of the skin z=0. **(E-G)** dermis at the depth of 150 μm from skin surface (z=150 μm). PRN and dissolved polymer from MN deposition in microchannels (760 nm excitation wavelength) following time point. Orange coloration indicates the nest of PRN (arrowhead) surrounded by a dissolved polymer (yellow-green).

4.4.3 Skin deposition of retinaldehyde from PRN-loaded MN

To compare the retinaldehyde delivery to each skin compartment by different topical formulations, the recovered retinaldehyde concentration from epidermis and dermis was quantified as shown in Fig.5. The amount of retinaldehyde recovered from epidermis was highest in the group of topical application of retinaldehyde in nanoparticulate system, then in conventional RAL and lowest from PRN-loaded MN group. The recovered amount of retinaldehyde from PRN, conventional RAL and PRN-loaded MN was 0.86 μg/ cm^2, 0.20 μg/ cm^2 and 0.08 μg/cm^2 or 32.1%, 7.6% and 2.9% from the total amount of each formulation respectively. Notably, the recovered

concentration of retinaldehyde in epidermis from nanoparticulate system is significantly different to another two topical formulations ($p<0.05$) **(Fig.22)**.

For retinaldehyde delivery in the dermis, where it can affect the biological activities of dermis. The recovered retinaldehyde deposition in the dermis from topical formulation of PRN-loaded MN as compared to conventional RAL and PRN significantly increased ($p<0.05$). The amount of retinaldehyde recovered from dermis of the microneedle-treated skin was 0.85 µg/cm^2 or 31.7% from the total load in MN while 0.35 µg/cm^2 or 13.2% from PRN-treated group and 0.22 µg/cm^2 or 8.2% in conventional RAL-treated group.
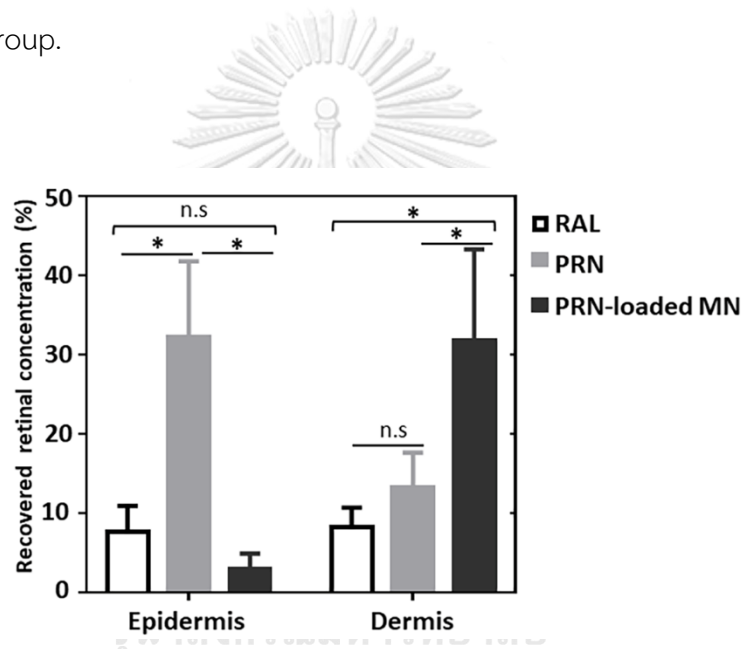
Figure 22. The percentage of recovered retinaldehyde concentration in epidermis and dermis from different topical formulations as proretinal nanoparticle (PRN), conventional retinaldehyde (RAL) and PRN-loaded microneedle. (*$p<0.05$ and n.s.; $p>0.05$)

4.5 Discussion

Stratum corneum, an outermost layer of the skin, is consisted of dense corneocyte and intercellular lipids and acts as the rate-limiting barrier of topical substances. Microneedle is one of the new approaches which intends to alter the barrier of intact stratum corneum. It was firstly introduced by Gerstel and Place in 1976. They suggested that microneedle length should be long enough to puncture through the stratum corneum and create the bypass to transport the drug. Until now, microneedle technology has been developed in order to facilitate the intradermal delivery of interested substances and enhance the skin permeability of nanoparticles [163-165].

It has been long known that retinoids have the profound effects to dermis especially in collagen synthesis stimulation. There were few attempts developing all-trans retinoic acid (ATRA)-loaded microneedle and confirming the biological activities of ATRA [166, 167]. Earlier in the previous study [13], PRN was shown to have promising physicochemical stabilities and less skin irritation. This accomplishment drives us to extend the study into intradermal delivery using the combination of dissolvable microneedle and PRN. The hypothesis is that PRN could be dissolved from the microneedle and slowly release retinaldehyde supplied dermis as a new approach for some retinoid-responsive dermatological conditions. The use of ex vivo porcine skin model is suitable in this study as a representative of human model since the structures of it are similar to those in human [15]. The accomplishment of intradermal retinaldehyde delivery consisted of a set of interacting phenomena. Firstly, the capability of PRN-loaded MN can be inserted through the stratum corneum in ex-vivo porcine skin model in the complete array of microneedle patch. The disappearance of the array embedded in the skin was observed by dermoscopy. This was because of the water solubility of polyvinylpyrrolidone and sodium hyaluronate as the casting materials of microneedle in the interstitial fluid of the skin. The dermoscopy was only able to visualize the sub-surface morphological disappearance of PRN-loaded MN array and its natural state of skin. This can predict for further clinical use when it would become invisible clinically.

For the penetration depths of this PRN-loaded MN, OCT images were evaluated. From the result, the observed penetration depth was at 600 μm. The concave injection site caused by the MN pressing force indicates that NP can be delivered at the depth of 600 microns which meets the required penetration depths. As the array of PRN-loaded MN was 400 needle/cm^2 in this study, it was supposed to be enough for effective intradermal drug delivery. According to Yan et al. in 2010 who studied the effective the needle length and density, they suggested that microneedle with more than 600 μm length and lower needle density less than 2000 needles/cm^2 efficiently penetrated through the skin and enhanced the drug flux [168]. Moreover, the elasticity of the skin could influence the difference or the displacement between the needle length and the actual penetration depth [169]. As we could observe some difference of those in the cross-sectional OCT images.

After the disruption of stratum corneum barrier by MN insertion resulting in the microchannels, the skin needs to reseal. The microchannels generated by MN are naturally impermanent [170]. There was a study performing in vivo suggesting that in an absence of occlusion condition of the skin could lead rapidly skin recovery process within 2 h [171]. Although the insertion array which were examined by dermoscopy became invisible, it still could be observed and remained by OCT and MPM investigations within 24 h after insertion and the microchannels in our study was in an absence of occlusion condition. when comparing ex-vivo model to the living skin, interstitial fluid could be over or under estimated due to blood perfusion, fluid dynamics or physiological osmotic gradients in dermis [172]. These could influent the dissolubility of casting polymer. Since this property of the polymer is depended on interstitial fluid in dermis. Nonetheless, Park and colleagues [173] suggested that the biodegradable polymer microneedles could be inserted and remained in the skin from several days in order to employ their controlled-release degradation properties and then offer the controlled-release delivery in skin for up to months. To perform label-free MPM imaging as an emerging technology in clinical dermatology, MPM provide the possible scanning through the skin from stratum corneum until 400 μm. In fact, useful data in the experimental situation could only be obtained from the depth of the scan

not exceeding 250 μm [174]. In this study we successfully demonstrate the existing of PRN in the microchannels after PRN-loaded MN application until 24 h after application. We hypothesized that the existing of PRN could provide the slow release properties of the retinaldehyde over time to dermis, then it can reduce the frequency of topical retinaldehyde application. The difference in the amount loaded to the amount of recovered retinaldehyde delivered into dermis could be attributed to slow degradation of two combinations of transdermal delivery systems as polymeric microneedle and nanoparticulate system of retinaldehyde. Moreover, the possibility of all trans retinoic acid (a retinoid) with hyaluronic acid- a high molecule polymer and a component of MN is slow [167]. Concerning drug delivery strategies, the selection of microneedle designs for applications should be taken into consideration. Comparing dissolving microneedle patch with other different microneedle designs, its maximum possible drug dose is considerably lowest [175].

Previously, retinoids have been formulated and topically applied in many different forms [42, 44, 49, 51] including retinaldehyde in nanocarriers [13]. In this study, PRN are taken as the model drugs for microneedle mediated transdermal delivery. Ex-vivo retinaldehyde deposition in dermis in this study showed enhanced administration of microneedle compared to other topical retinaldehyde formulation. Although PRN have shown to improve the skin conditions of patients [13], theoretically nanoparticles remained deposited on the outermost layers of the skin [176] and hair follicles [177, 178]. The cutaneous pharmacokinetics of typical retinoids and their biological activities are depended on the steep concentration gradient [153] as high concentration are achieved in the epidermis especially the stratum corneum because of their lipophilicity properties, in the hair follicles [179] resulting in the lower concentration in dermis. Thus, it is possible to modulate PRN as the drug-loaded polymeric particles into the MN tips for directly intradermal delivery and targeting to the deeper layers of skin for sustained delivery. The use of combination of two transdermal drug delivery systems bypass retinaldehyde in nanoparticulate forms to dermis. PRN could be used as intradermal potential therapeutic agent to help atrophic acne scar and anti-aging conditions by stimulating events in the dermis leading to the repair of the damaged

skin. Although, our proposed system demonstrates a potential benefit, the suggestions for the further investigations are to evaluate the efficacy of retinaldehyde actively in vivo after MN application and the safety aspects.

CHAPTER V

General conclusion, discussion, and future recommendations

The therapeutic efficacy of retinoids is limited by the side effect of retinoids dermatitis and their physicochemical instability. To overcome these limitations, the development of novel drug delivery system has been purposed. Retinaldehyde (retinal) in chitosan as nanocarriers is appropriate in regulating and providing better bioavailability of retinal. Proretinal nanoparticles (PRN) provide the sustain release of retinal and then supplying the skin continuously. In chapter II, we have shown that PRN could serve as an excellent retinal reservoir with effective skin penetration and induction of skin proliferation. In vitro Increased expression of CRABP-2 by PRN with no short-term cytotoxicity was clarified in HaCaT cells. Topical application of PRN for 28 days clearly increased cell proliferation and differentiation in rat epidermis resulting in the thickening of the epidermis and increased levels of various retinoid associated biochemical markers such as K5, K14, K10, PCNA, IL-6 and CRABP-2, with no side effect of retinoid dermatitis. Penetration into hair follicles of the PRNs were verified and their time-independent localization was observed. According intercellular and follicular pathways as the major pathways of topical substances penetrating through the epidermis, PRN was investigated following this concept. The findings of the chapter III provide a novel nanoparticle-based system, which is able to increase the stratum corneum and hair follicle concentration of retinal significantly. This system might be able to improve the therapy of retinoid-responsive and hair follicle-associated skin diseases such as acne. Moreover, the utilized model drug was able to reach the lower infundibulum, which is surrounded by antigen-presenting cells [180]. If the released retinal is able to translocate transfollicularly and independently from the nanocarriers, this might be beneficial as retinoids can also effect the development of immune cells [181] and possess anti-inflammatory properties. Although further investigations are necessary to clarify the required doses and dose intervals in clinical settings, the suggested system may help to overcome the main problems of topical retinoid therapy, which are skin irritation, chemical and photochemical instability and low bioavailability.

Besides targeting epidermis, dermis has been studied to investigate the possibility of the use of PRN-loaded microneedle in delivery retinal to dermis, In chapter IV, we demonstrated the use of combination of transdermal drug delivery system as polymeric microneedles loaded with proretinal nanoparticles- a particulate form of retinaldehyde could enhance dermal deposition of retinaldehyde and nanoparticles remaining in microchannels the dermis following the designated of application times through all non-invasive imaging techniques. These findings could shed light on the possibility of effective delivering nanoparticles to the dermis reaching the maximum therapeutic effects and patient compliance. We hypothesize that this platform of PRN-loaded microneedle would provide rapid administration through short time after microneedle insertion, assist a long-term releasing retinaldehyde from PRN depots and supply dermis. Finally, it could be beneficial in some skin condition as atrophic scar and photoaging in the future. The use of drug delivery system for retinal are different in term of the different target site in skin. To supply epidermis continuously, proretinal nanoparticles (PRN) or retinal in nanoparticulate form is efficient and safe and has biological activities of retinoids. For dermal aspect, the use of PRN-loaded microneedle is possible to deliver and by pass retinal to dermis directly.

Although PRN has shown to overcome the limitation of topical retinoids, all results from this present study demonstrated in the intact skin models from *in vitro*, *in vivo* and *ex vivo*. The skin disease models should be considered for the further investigation in the use of topical application of PRN. Skin disease models could be in different types of *in vitro* or *in vivo* models such as psoriasis, seborrheic dermatitis, eczema, or UV-radiated keratinocyte because the microenvironment or the disruptive barriers in skin disease models might affect the response of PRN. The roles and subpopulation of keratinocytes which are responsible for topical application of retinoids in epidermal thickening, proliferation and differentiation still need to be explored. In this research, the protein-based immunohistochemical study of PRN-treated skin needs other functional approaches to confirm these initial observations. The further investigations for PRN-loaded microneedle would be the safety aspects

firstly, the *in vivo* efficacy evaluation of active retinal after microneedle application secondly and finally the clinical study on disease models.

The present study showed that topical application proretinal nanoparticles are safe, non-irritative, successfully penetrate into hair follicles and possess retinoid biological activities to skin as the ability to induct and regulate epidermal proliferation and differentiation. Finally, it could be beneficial in some retinoid-responsive skin conditions in the future. This suggested system as topical proretinal nanoparticles may help to overcome the main problems of topical retinoid therapy, which are skin irritation, chemical, and photochemical instability and low bioavailability.

จุฬาลงกรณ์มหาวิทยาลัย

CHULALONGKORN UNIVERSITY

Appendix

Graphical abstracts

Chapter II

Topical application of proretinal nanoparticles in biological activities, epidermal proliferation and differentiation, follicular penetration, and skin tolerability
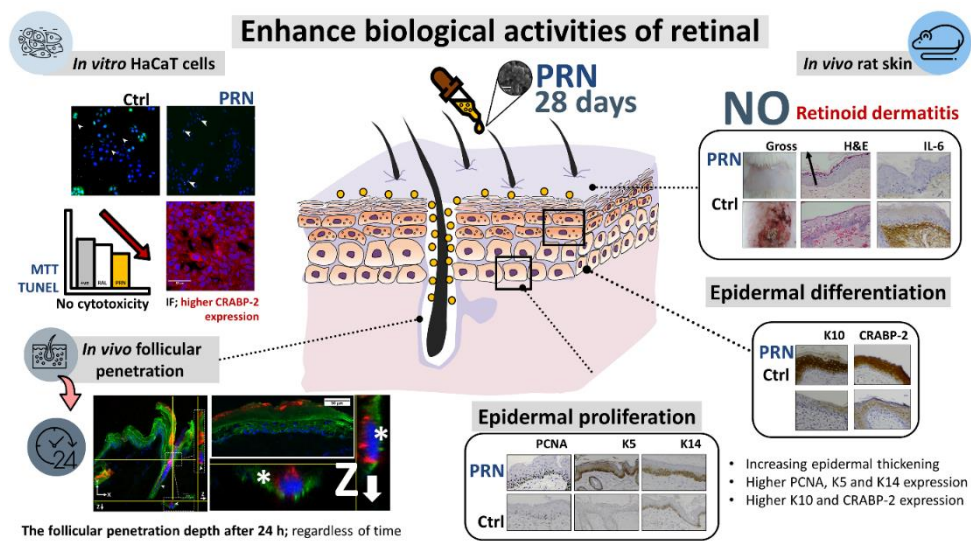
CHAPTER III

Intercellular and follicular penetration of retinal by topical application of proretinal nanoparticles
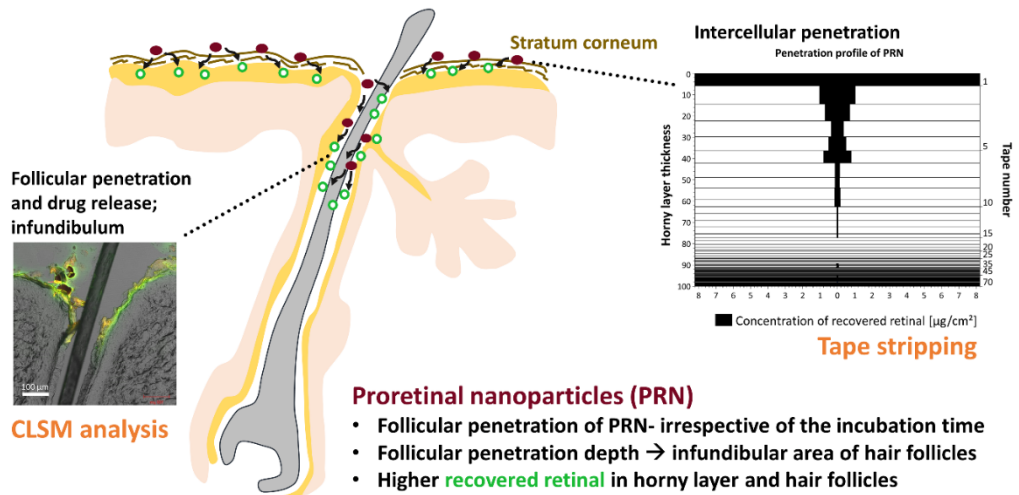
CHAPTER IV

Microneedle-facilitated intradermal proretinal nanoparticles delivery

Microneedle-facilitated Intradermal Proretinal Nanoparticles delivery
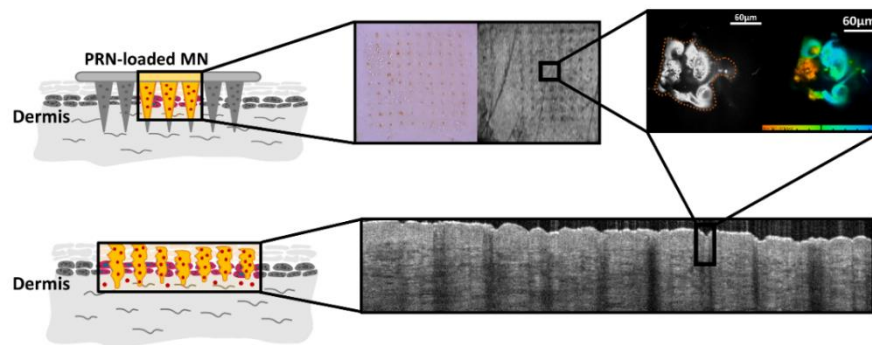
Proretinal nanoparticle (PRN)-loaded microneedles
- Visualization of insertion array, microchannels of PRN-loaded microneedle and skin closure kinetics
- Higher recovered retinal concentration in dermis

จุฬาลงกรณ์มหาวิทยาลัย
CHULALONGKORN UNIVERSITY

Criteria for pathological evaluations

<u>Gross pathology</u>

Scoring system was evaluated by concerning the signs of skin reaction (animal irritation test) followed ISO 10993-10: biological evaluation of medical devices- Part10: Tests for irritation and skin sensitization (Draize test) on Day7, 14, 21 and 28 of treatment **(Table 8)**.

To evaluate the results of the signs of skin reaction (animal irritation test), add together the irritation scores in t**able 9**. of all animals in each experimental group and divide by the total number of animals. This result of the calculated value is the cumulative irritation index. The cumulative irritation index was compared with the categories of irritation response given in **table 9**. And the other adverse pathological changes were recorded for the report.

Table 8 *Scoring system for skin reaction (ISO 10993-10:2010)*

Reaction	Irritation score
Erythema and eschar formation	
No erythema	0
Very slight erythema (barely perceptible)	1
Well-defined erythema	2
Moderate erythema	3
Severe erythema (beet-redness) to eschar formation preventing grading of erythema	4
Edema formation	
No edema	0
Very slight edema (berely perceptible)	1
Well-defined edema (edge of area well-defined by finite raising)	2
Moderate edema (raised approximately 1 mm.)	3
Severe edema (raised more than 1 mm. and extending beyond exposure area)	4
Maximal possible score for irritation	8
Other adverse changes at the skin sites shall be recorded and reported	

Table **9** Cumulative irritation index categories in animals (ISO 10993-10:2010)

Mean score	Response category
0 to 0.4	Negligible
0.5 to 1.9	Slight
2 to 4.9	Moderate
5 to 8	Severe

Histopathology criteria

The routine hematoxylin and eosin (H&E) histological tissue process was performed and then examined under light microscope. The specimen from all experimental groups on each day7, 14, 21 and 28 of treatment will be assessed in terms of epidermal and dermal parameters modified from Machtinger et al., 2004 and ISO 10993-10:2010 as following.

Criteria for histopathological grading system

Epidermal inflammation (Average grade; 0: none 1-4: minimal 5-8: mild 9-11: moderate 12-16: severe)

1.1 Epithelium integrity; 0: Normal or intact 1: Cell degeneration or flatting 2: Metaplasia 3: Focal erosion 4: Generalized erosion

1.2 Presence of inflammatory cell infiltration (per high power field); 0: Absent 1: Minimal (<25) 2: Mild (<50) 3: Moderate (51-100) 4: Marked (>100)

1.3 Hemorrhage; 0: Absent 1: Minimal, 2: Mild 3: Moderate4: Marked with disrupted vessels

1.4 Edema; 0: Absent 1: Minimal, 2: Mild 3: moderate 4: Marked

Epidermal thickness (µm)

The measurement of thickness of the epidermis in micrometers from the base of the stratum corneum to the basement membrane assessed in ten high-power fields will be performed randomly.

The thickness of the granular cell layers (n per N group)

No granular, one cell layer, two or three cell layers and four or more cell layers

The appearance of the stratum corneum (n per N group)

Basket-weave, compact or both

Dermal inflammation (n per N group)

Superficial perivascular, superficial and deep perivascular, diffuse, perifollicular or lichenoid

REFERENCES

[1] C.H. Dicken, Retinoids: A review, J Am Acad Dermatol, 11 (1984) 541-552.

[2] P.M. Amann, D. Schadendorf, R.W. Owen, B. Korn, S.B. Eichmuller, A.V. Bazhin, Retinal and retinol are potential regulators of gene expression in the keratinocyte cell line HaCaT, Experimental dermatology, 20 (2011) 373-375.

[3] E. Trapasso, D. Cosco, C. Celia, M. Fresta, D. Paolino, Retinoids: new use by innovative drug-delivery systems, Expert opinion on drug delivery, 6 (2009) 465-483.

[4] C.C. Zouboulis, Retinoids – Which Dermatological Indications Will Benefit in the Near Future?, Skin Pharmacol Physiol, 14 (2001) 303-315.

[5] L. Didierjean, C. Tran, O. Sorg, J.H. Saurat, Biological activities of topical retinaldehyde, Dermatology (Basel, Switzerland), 199 Suppl 1 (1999) 19-24.

[6] M. David, E. Hodak, N.J. Lowe, Adverse Effects of Retinoids, Med Toxicol Adverse Drug Exp, 3 (1988) 273-288.

[7] L.R. Gaspar, P.M.B.G.M. Campos, Photostability and efficacy studies of topical formulations containing UV-filters combination and vitamins A, C and E, Int J Pharm, 343 (2007) 181-189.

[8] Q. Xia, J.J. Yin, S.-H. Cherng, W.G. Wamer, M. Boudreau, P.C. Howard, P.P. Fu, UVA photoirradiation of retinyl palmitate—formation of singlet oxygen and superoxide, and their role in induction of lipid peroxidation, Toxicol Lett, 163 (2006) 30-43.

[9] O. Sorg, C. Tran, P. Carraux, L. Didierjean, J. Saurat, Retinol and retinyl ester epidermal pools are not identically sensitive to UVB irradiation and anti-oxidant protective effect, Dermatology (Basel, Switzerland), 199 (1999) 302-307.

[10] S. Mukherjee, A. Date, V. Patravale, H.C. Korting, A. Roeder, G. Weindl, Retinoids in the treatment of skin aging: an overview of clinical efficacy and safety, Clin Interv Aging, 1 (2006) 327-348.

[11] M.D. Singh, N. Mital, G. Kaur, Topical drug delivery systems: a patent review, Expert opinion on therapeutic patents, 26 (2016) 213-228.

[12] P.L. Lam, R. Gambari, Advanced progress of microencapsulation technologies: In vivo and in vitro models for studying oral and transdermal drug deliveries, J Control Release, 178 (2014) 25-45.

[13] P. Pisetpackdeekul, P. Supmuang, P. Pan-In, W. Banlunara, B. Limcharoen, C. Kokpol, S. Wanichwecharungruang, Proretinal nanoparticles: stability, release, efficacy, and irritation, Int J Nanomedicine, 11 (2016) 3277-3286.

[14] G.E. Flaten, Z. Palac, A. Engesland, J. Filipović-Grčić, Ž. Vanić, N. Škalko-Basnet, In vitro skin models as a tool in optimization of drug formulation, Eur J Pharm Sci, 75 (2015) 10-24.

[15] U. Jacobi, M. Kaiser, R. Toll, S. Mangelsdorf, H. Audring, N. Otberg, W. Sterry, J. Lademann, Porcine ear skin: an in vitro model for human skin, 13 (2007) 19-24.

[16] M.B. Sporn, N.M. Dunlop, D.L. Newton, W.R. Henderson, Relationships between structure and activity of retinoids, Nature, 263 (1976) 110-113.

[17] J. Reichrath, B. Lehmann, C. Carlberg, J. Varani, C.C. Zouboulis, Vitamins as hormones, Hormone and metabolic research = Hormon- und Stoffwechselforschung = Hormones et metabolisme, 39 (2007) 71-84.

[18] K. Babamiri, R. Nassab, Cosmeceuticals: the evidence behind the retinoids, Aesthetic surgery journal / the American Society for Aesthetic Plastic surgery, 30 (2010) 74-77.

[19] T.C. Roos, F.K. Jugert, H.F. Merk, D.R. Bickers, Retinoid Metabolism in the Skin, Pharmacol Rev, 50 (1998) 315.

[20] R. Darlenski, C. Surber, J.W. Fluhr, Topical retinoids in the management of photodamaged skin: from theory to evidence-based practical approach, The British journal of dermatology, 163 (2010) 1157-1165.

[21] R. Serri, M. Lorizzo, Cosmeceuticals: focus on topical retinoids in photoaging, Clinics in dermatology, 26 (2008) 633-635.

[22] O. Sorg, C. Antille, G. Kaya, J.-H. Saurat, Retinoids in cosmeceuticals, Dermatol Ther, 19 (2006) 289-296.

[23] M. Crettaz, A. Baron, G. Siegenthaler, W. Hunziker, Ligand specificities of recombinant retinoic acid receptors RAR alpha and RAR beta, The Biochemical journal, 272 (1990) 391-397.

[24] G. Allenby, M.T. Bocquel, M. Saunders, S. Kazmer, J. Speck, M. Rosenberger, A. Lovey, P. Kastner, J.F. Grippo, P. Chambon, Retinoic acid receptors and retinoid X receptors: interactions with endogenous retinoic acids, Proc Natl Acad Sci U S A, 90 (1993) 30-34.

[25] J.H. Saurat, L. Didierjean, E. Masgrau, P.A. Piletta, S. Jaconi, D. Chatellard-Gruaz, D. Gumowski, I. Masouyé, D. Salomon, G. Siegenthaler, Topical Retinaldehyde on Human Skin: Biologic Effects and Tolerance, The Journal of investigative dermatology, 103 (1994) 770-774.

[26] L. Didierjean, P. Carraux, D. Grand, J.O. Sass, H. Nau, J.-H. Saurat, Topical Retinaldehyde Increases Skin Content of Retinoic Acid and Exerts Biologic Activity in Mouse Skin, The Journal of investigative dermatology, 107 (1996) 714-719.

[27] S. Chen, J. Ostrowski, G. Whiting, T. Roalsvig, L. Hammer, S.J. Currier, J. Honeyman, B. Kwasniewski, K.-L. Yu, R. Sterzycki, C.U. Kim, J. Starrett, M. Mansuri, P.R. Reczek, Retinoic Acid Receptor Gamma Mediates Topical Retinoid Efficacy and Irritation in Animal Models, The Journal of investigative dermatology, 104 (1995) 779-783.

[28] J.W. Fluhr, M.P. Vienne, C. Lauze, P. Dupuy, W. Gehring, M. Gloor, Tolerance profile of retinol, retinaldehyde and retinoic acid under maximized and long-term clinical conditions, Dermatology (Basel, Switzerland), 199 Suppl 1 (1999) 57-60.

[29] J.H. Saurat, Side effects of systemic retinoids and their clinical management, J Am Acad Dermatol, 27 (1992) S23-S28.

[30] M.J. Day, Immune-Mediated Skin Disease, in: M.J. Day (Ed.) Clinical immunology of the dog and cat, Second Edition, CRC Press2011, pp. 122-171.

[31] T. Welss, D.A. Basketter, K.R. Schröder, In vitro skin irritation: facts and future. State of the art review of mechanisms and models, Toxicol in Vitro, 18 (2004) 231-243.

[32] B.Y.S. Kim , J.T. Rutka , W.C.W. Chan Nanomedicine, New Engl J Med, 363 (2010) 2434-2443.

[33] D. Thassu, Y. Pathak, M. Deleers, Nanoparticulate Drug-Delivery Systems, in: D. Thassu (Ed.) Nanoparticulate Drug Delivery Systems, CRC Press2007, pp. 1-31.

[34] A.H. Faraji, P. Wipf, Nanoparticles in cellular drug delivery, Bioorgan Med Chem, 17 (2009) 2950-2962.

[35] R. Goyal, L.K. Macri, H.M. Kaplan, J. Kohn, Nanoparticles and nanofibers for topical drug delivery, J Control Release, 240 (2016) 77-92.

[36] M. Garcia-Fuentes, M.J. Alonso, Chitosan-based drug nanocarriers: Where do we stand?, J Control Release, 161 (2012) 496-504.

[37] M. Prabaharan, J.F. Mano, Chitosan-based particles as controlled drug delivery systems, Drug delivery, 12 (2005) 41-57.

[38] J.J. Wang, Z.W. Zeng, R.Z. Xiao, T. Xie, G.L. Zhou, X.R. Zhan, S.L. Wang, Recent advances of chitosan nanoparticles as drug carriers, Int J Nanomedicine, 6 (2011) 765-774.

[39] C. Sinico, M. Manconi, M. Peppi, F. Lai, D. Valenti, A.M. Fadda, Liposomes as carriers for dermal delivery of tretinoin: in vitro evaluation of drug permeation and vesicle–skin interaction, J Control Release, 103 (2005) 123-136.

[40] C. Díaz, E. Vargas, O. Gätjens-Boniche, Cytotoxic effect induced by retinoic acid loaded into galactosyl-sphingosine containing liposomes on human hepatoma cell lines, Int J Pharm, 325 (2006) 108-115.

[41] M. Manconi, C. Sinico, D. Valenti, F. Lai, A.M. Fadda, Niosomes as carriers for tretinoin: III. A study into the in vitro cutaneous delivery of vesicle-incorporated tretinoin, Int J Pharm, 311 (2006) 11-19.

[42] J. Liu, W. Hu, H. Chen, Q. Ni, H. Xu, X. Yang, Isotretinoin-loaded solid lipid nanoparticles with skin targeting for topical delivery, Int J Pharm, 328 (2007) 191-195.

[43] V. Jenning, A. Gysler, M. Schäfer-Korting, S.H. Gohla, Vitamin A loaded solid lipid nanoparticles for topical use: occlusive properties and drug targeting to the upper skin, Eur J Pharm Biopharm, 49 (2000) 211-218.

[44] V. Jenning, M. Schäfer-Korting, S. Gohla, Vitamin A-loaded solid lipid nanoparticles for topical use: drug release properties, J Control Release, 66 (2000) 115-126.

[45] A.F. Ourique, A.R. Pohlmann, S.S. Guterres, R.C.R. Beck, Tretinoin-loaded nanocapsules: Preparation, physicochemical characterization, and photostability study, Int J Pharm, 352 (2008) 1-4.

[46] A.C. Williams, B.W. Barry, Penetration enhancers, Adv Drug Deliver Rev, 56 (2004) 603-618.

[47] R. Alvarez-Román, A. Naik, Y.N. Kalia, R.H. Guy, H. Fessi, Skin penetration and distribution of polymeric nanoparticles, J Control Release, 99 (2004) 53-62.

[48] S.-J. Seo, H.-S. Moon, D.-D. Guo, S.-H. Kim, T. Akaike, C.-S. Cho, Receptor-mediated delivery of all-trans-retinoic acid (ATRA) to hepatocytes from ATRA-loaded poly(N-p-vinylbenzyl-4-o-β-d-galactopyranosyl-d-gluconamide) nanoparticles, Mater Sci Eng C Mater Biol Appl, 26 (2006) 136-141.

[49] Y.-I. Jeong, M.-K. Kang, H.-S. Sun, S.-S. Kang, H.-W. Kim, K.-S. Moon, K.-J. Lee, S.-H. Kim, S. Jung, All-trans-retinoic acid release from core-shell type nanoparticles of poly(ϵ-caprolactone)/poly(ethylene glycol) diblock copolymer, Int J Pharm, 273 (2004) 95-107.

[50] Y. Sung Nam, K. Joong Kim, H. Seok Kang, T. Gwan Park, S.-H. Han, I.-S. Chang, Chemical immobilization of retinoic acid within poly(ϵ-caprolactone) nanoparticles based on drug–polymer bioconjugates, J Appl Polym Sci, 89 (2003) 1631-1637.

[51] S. Arayachukeat, S.P. Wanichwecharungruang, T. Tree-Udom, Retinyl acetate-loaded nanoparticles: Dermal penetration and release of the retinyl acetate, Int J Pharm, 404 (2011) 281-288.

[52] S. Higgins, N.O. Wesley, Topical Retinoids and Cosmeceuticals: Where Is the Scientific Evidence to Recommend Products to Patients?, Curr Dermatol Rep, 4 (2015) 56-62.

[53] T.W. Prow, J.E. Grice, L.L. Lin, R. Faye, M. Butler, W. Becker, E.M.T. Wurm, C. Yoong, T.A. Robertson, H.P. Soyer, M.S. Roberts, Nanoparticles and microparticles for skin drug delivery, Adv Drug Deliver Rev, 63 (2011) 470-491.

[54] A. Vogt, C. Wischke, A.T. Neffe, N. Ma, U. Alexiev, A. Lendlein, Nanocarriers for drug delivery into and through the skin — Do existing technologies match clinical challenges?, J Control Release, 242 (2016) 3-15.

[55] J. Lademann, H. Richter, A. Teichmann, N. Otberg, U. Blume-Peytavi, J. Luengo, B. Weiß, U.F. Schaefer, C.-M. Lehr, R. Wepf, W. Sterry, Nanoparticles – An efficient carrier for drug delivery into the hair follicles, Eur J Pharm Biopharm, 66 (2007) 159-164.

[56] J. Lademann, F. Knorr, H. Richter, U. Blume-Peytavi, A. Vogt, C. Antoniou, W. Sterry, A. Patzelt, Hair follicles--an efficient storage and penetration pathway for topically applied substances. Summary of recent results obtained at the Center of Experimental

and Applied Cutaneous Physiology, Charite -Universitatsmedizin Berlin, Germany, Skin Pharmacol Physiol, 21 (2008) 150-155.

[57] B. Young, J.S. Lowe, A. Stevens, J.W. Health, Chapter 9:Skin, in: B. Young (Ed.) Wheater's Functional Histology: A Text and Colour Atlas, Churchill Livingstone/Elsevier, Edinburg, 2006, pp. 167-187.

[58] S.V. Bettenay, A.M. Hargis, Histopathologic Responses of the Skin to Injury, Practical Veterinary Dermatopathology, Teton NewMedia2003, pp. 53-105.

[59] E. Fuchs, H. Green, The expression of keratin genes in epidermis and cultured epidermal cells, Cell, 15 (1978) 887-897.

[60] C. Fisher, M. Blumenberg, M. Tomic-Canic, Retinoid receptors and keratinocytes, Critical reviews in oral biology and medicine : an official publication of the American Association of Oral Biologists, 6 (1995) 284-301.

[61] D.S. Rosenthal, D.R. Roop, C.A. Huff, J.S. Weiss, C.N. Ellis, T. Hamilton, J.J. Voorhees, S.H. Yuspa, Changes in photo-aged human skin following topical application of all-trans retinoic acid, The Journal of investigative dermatology, 95 (1990) 510-515.

[62] R.L. Eckert, E.A. Rorke, Molecular biology of keratinocyte differentiation, Environ Health Persp, 80 (1989) 109-116.

[63] D.S. Rosenthal, C.E. Griffiths, S.H. Yuspa, D.R. Roop, J.J. Voorhees, Acute or chronic topical retinoic acid treatment of human skin in vivo alters the expression of epidermal transglutaminase, loricrin, involucrin, filaggrin, and keratins 6 and 13 but not keratins 1, 10, and 14, The Journal of investigative dermatology, 98 (1992) 343-350.

[64] F.X. Bernard, N. Pedretti, M. Rosdy, A. Deguercy, Comparison of gene expression profiles in human keratinocyte mono-layer cultures, reconstituted epidermis and normal human skin; transcriptional effects of retinoid treatments in reconstituted human epidermis, Experimental dermatology, 11 (2002) 59-74.

[65] B.M. Gilfix, R.L. Eckert, Coordinate control by vitamin A of keratin gene expression in human keratinocytes, The Journal of biological chemistry, 260 (1985) 14026-14029.

[66] B. Korge, R. Stadler, D. Mischke, Effect of retinoids on hyperproliferation-associated keratins K6 and K16 in cultured human keratinocytes: a quantitative analysis, The Journal of investigative dermatology, 95 (1990) 450-455.

[67] M. Virtanen, H. Torma, A. Vahlquist, Keratin 4 upregulation by retinoic acid in vivo: a sensitive marker for retinoid bioactivity in human epidermis, The Journal of investigative dermatology, 114 (2000) 487-493.

[68] M. Virtanen, A. Sirsjo, A. Vahlquist, H. Torma, Keratins 2 and 4/13 in reconstituted human skin are reciprocally regulated by retinoids binding to nuclear receptor RARalpha, Experimental dermatology, 19 (2010) 674-681.

[69] E. Fuchs, H. Green, Regulation of terminal differentiation of cultured human keratinocytes by vitamin A, Cell, 25 (1981) 617-625.

[70] D.L. Crowe, Retinoic acid mediates post-transcriptional regulation of keratin 19 mRNA levels, Journal of cell science, 106 (Pt 1) (1993) 183-188.

[71] V. Stellmach, A. Leask, E. Fuchs, Retinoid-mediated transcriptional regulation of keratin genes in human epidermal and squamous cell carcinoma cells, Proc Natl Acad Sci U S A, 88 (1991) 4582-4586.

[72] D.D. Lee, O. Stojadinovic, A. Krzyzanowska, C. Vouthounis, M. Blumenberg, M. Tomic-Canic, Retinoid-responsive transcriptional changes in epidermal keratinocytes, Journal of cellular physiology, 220 (2009) 427-439.

[73] R. Kopan, G. Traska, E. Fuchs, Retinoids as important regulators of terminal differentiation: examining keratin expression in individual epidermal cells at various stages of keratinization, The Journal of cell biology, 105 (1987) 427-440.

[74] H. Törmä, Regulation of keratin expression by retinoids, Dermatoendocrinol, 3 (2011) 136-140.

[75] B. Godin, E. Touitou, Transdermal skin delivery: Predictions for humans from in vivo, ex vivo and animal models, Adv Drug Deliver Rev, 59 (2007) 1152-1161.

[76] R.L. Bronaugh, R.F. Stewart, E.R. Congdon, Methods for in vitro percutaneous absorption studies II. Animal models for human skin, Toxicol Appl Pharm, 62 (1982) 481-488.

[77] M. Gołyński, M. Szczepanik, K. Lutnicki, Ł. Adamek, M. Gołyńska, P. Wilkołek, W. Sitkowski, Ł. Kurek, P. Dębiak, Biophysical parameters of rats' skin after the administration of methimazole, bvip, 58 (2014) 315-319.

[78] M.E. Roberts, K.R. Mueller, Comparisons of in vitro nitroglycerin (TNG) flux across yucatan pig, hairless mouse, and human skins, Pharmaceutical research, 7 (1990) 673-676.

[79] K. Sato, K. Sugibayashi, Y. Morimoto, Species differences in percutaneous absorption of nicorandil, Journal of pharmaceutical sciences, 80 (1991) 104-107.

[80] L. Semlin, M. Schäfer-Korting, C. Borelli, H.C. Korting, In vitro models for human skin disease, Drug Discov Today, 16 (2011) 132-139.

[81] J.L. MacGregor, H.I. Maibach, The Specificity of Retinoid-Induced Irritation and Its Role in Clinical Efficacy, Exog Dermatol, 1 (2002) 68-73.

[82] B.-H. Kim, Safety Evaluation and Anti-wrinkle Effects of Retinoids on Skin, Toxicol Res, 26 (2010) 61-66.

[83] E. Fuchs, Epidermal differentiation and keratin gene expression, Journal of cell science. Supplement, 17 (1993) 197-208.

[84] P. Pisetpackdeekul, P. Supmuang, P. Pan-In, W. Banlunara, B. Limcharoen, C. Kokpol, S. Wanichwecharungruang, Proretinal nanoparticles: stability, release, efficacy, and irritation, International journal of nanomedicine, 11 (2016) 3277-3286.

[85] OECD, OECD Guideline for Testing of Chemicals, OECD Publishing1981.

[86] ISO10993-10:2010, Biological Evaluation of Medical Devices Part 10: Tests for irritation and skin sensitization. In: ISO/TC 194 Biological evaluation of medical devices. , 3rd ed ed.2010.

[87] L.A. Machtinger, K. Kaidbey, J. Lim, K.H. Loven, T.E. Rist, D.C. Wilson, D.D. Parizadeh, J. Sefton, J.M. Holland, P.S. Walker, Histological effects of tazarotene 0.1% cream vs. vehicle on photodamaged skin: a 6-month, multicentre, double-blind, randomized, vehicle-controlled study in patients with photodamaged facial skin, The British journal of dermatology, 151 (2004) 1245-1252.

[88] C.C. Zouboulis, H. Seltmann, J.O. Sass, R. Ruhl, C. Plum, U. Hettmannsperger, U. Blume-Peytavi, H. Nau, C.E. Orfanos, Retinoid signaling by all-trans retinoic acid and all-trans retinoyl-beta-D-glucuronide is attenuated by simultaneous exposure of human keratinocytes to retinol, The Journal of investigative dermatology, 112 (1999) 157-164.

[89] M. Schroeder, C.C. Zouboulis, All-trans-retinoic acid and 13-cis-retinoic acid: pharmacokinetics and biological activity in different cell culture models of human

keratinocytes, Hormone and metabolic research = Hormon- und Stoffwechselforschung = Hormones et metabolisme, 39 (2007) 136-140.

[90] Y. Wang, J.C. Bell, D.S. Keeney, H.W. Strobel, Gene Regulation of CYP4F11 in Human Keratinocyte HaCaT Cells, Drug Metab Dispos, 38 (2010) 100-107.

[91] M. Stein, A. Bernd, A. Ramirez-Bosca, S. Kippenberger, H. Holzmann, Measurement of anti-inflammatory effects of glucocorticoids on human keratinocytes in vitro. Comparison of normal human keratinocytes with the keratinocyte cell line HaCaT, Arzneimittel-Forschung, 47 (1997) 1266-1270.

[92] N. Schurer, A. Kohne, V. Schliep, K. Barlag, G. Goerz, Lipid composition and synthesis of HaCaT cells, an immortalized human keratinocyte line, in comparison with normal human adult keratinocytes, Exp Dermatol, 2 (1993) 179-185.

[93] J. Varani, P. Perone, D.M. Spahlinger, L.M. Singer, K.L. Diegel, W.F. Bobrowski, R. Dunstan, Human Skin in Organ Culture and Human Skin Cells (Keratinocytes and Fibroblasts) in Monolayer Culture for Assessment of Chemically Induced Skin Damage, Toxicol Pathol, 35 (2007) 693-701.

[94] J.L. Armstrong, M. Ruiz, A.V. Boddy, C.P.F. Redfern, A.D.J. Pearson, G.J. Veal, Increasing the intracellular availability of all-trans retinoic acid in neuroblastoma cells, Br J Cancer, 92 (2005) 696-704.

[95] F. Knorr, A. Patzelt, M.E. Darvin, C.M. Lehr, U. Schafer, A.D. Gruber, A. Ostrowski, J. Lademann, Penetration of topically applied nanocarriers into the hair follicles of dog and rat dorsal skin and porcine ear skin, Veterinary dermatology, 27 (2016) 256-e260.

[96] B. Limcharoen, P. Toprangkobsin, W. Banlunara, S. Wanichwecharungruang, H. Richter, J. Lademann, A. Patzelt, Increasing the percutaneous absorption and follicular penetration of retinal by topical application of proretinal nanoparticles, Eur J Pharm Biopharm, 139 (2019) 93-100.

[97] R.M. Lavker, T.-T. Sun, H. Oshima, Y. Barrandon, M. Akiyama, C. Ferraris, G. Chevalier, B. Favier, C.A.B. Jahoda, D. Dhouailly, A.A. Panteleyev, A.M. Christiano, Hair Follicle Stem Cells, J Investig Dermatol Symp Proc, 8 (2003) 28-38.

[98] T. Christoph, S. Muller-Rover, H. Audring, D.J. Tobin, B. Hermes, G. Cotsarelis, R. Ruckert, R. Paus, The human hair follicle immune system: cellular composition and immune privilege, The British journal of dermatology, 142 (2000) 862-873.

[99] J.H. Saurat, L. Didierjean, E. Masgrau, P.A. Piletta, S. Jaconi, D. Chatellard-Gruaz, D. Gumowski, I. Masouye, D. Salomon, G. Siegenthaler, Topical retinaldehyde on human skin: biologic effects and tolerance, The Journal of investigative dermatology, 103 (1994) 770-774.

[100] M.J. Connor, N.J. Lowe, Induction of ornithine decarboxylase activity and DNA synthesis in hairless mouse epidermis by retinoids, Cancer research, 43 (1983) 5174-5177.

[101] G.J. Gendimenico, J.A. Mezick, Pharmacological effects of retinoids on skin cells, Skin pharmacology : the official journal of the Skin Pharmacology Society, 6 Suppl 1 (1993) 24-34.

[102] A. Astrom, A. Tavakkol, U. Pettersson, M. Cromie, J.T. Elder, J.J. Voorhees, Molecular cloning of two human cellular retinoic acid-binding proteins (CRABP). Retinoic acid-induced expression of CRABP-II but not CRABP-I in adult human skin in vivo and in skin fibroblasts in vitro, The Journal of biological chemistry, 266 (1991) 17662-17666.

[103] G.J. Fisher, J.J. Voorhees, Molecular mechanisms of retinoid actions in skin, FASEB journal : official publication of the Federation of American Societies for Experimental Biology, 10 (1996) 1002-1013.

[104] D.S. Rosenthal, C.E.M. Griffiths, S.H. Yuspa, D.R. Roop, J.J. Voorhees, Acute or Chronic Topical Retinoic Acid Treatment of Human Skin In Vivo Alters the Expression of Epidermal Transglutaminase, Loricrin, Involucrin, Filaggrin, and Keratins 6 and 13 but not Keratins 1, 10, and 14, The Journal of investigative dermatology, 98 (1992) 343-350.

[105] G.K. Patel, C.H. Wilson, K.G. Harding, A.Y. Finlay, P.E. Bowden, Numerous Keratinocyte Subtypes Involved in Wound Re-Epithelialization, The Journal of investigative dermatology, 126 (2006) 497-502.

[106] S. Luo, T. Yufit, P. Carson, D. Fiore, J. Falanga, X. Lin, L. Mamakos, V. Falanga, Differential keratin expression during epiboly in a wound model of bioengineered skin and in human chronic wounds, The international journal of lower extremity wounds, 10 (2011) 122-129.

[107] M.L. Usui, J.N. Mansbridge, W.G. Carter, M. Fujita, J.E. Olerud, Keratinocyte Migration, Proliferation, and Differentiation in Chronic Ulcers From Patients With Diabetes and Normal Wounds, J Histochem Cytochem, 56 (2008) 687-696.

[108] R.M. Gallucci, D.K. Sloan, J.M. Heck, A.R. Murray, S.J. O'Dell, Interleukin 6 indirectly induces keratinocyte migration, The Journal of investigative dermatology, 122 (2004) 764-772.

[109] J.-H. Saurat, Side effects of systemic retinoids and their clinical management, J. Am. Acad. Dermatol., 27 (1992) S23-S28.

[110] J.H. Saurat, L. Didierjean, E. Masgrau, P.A. Piletta, S. Jaconi, D. Chatellard-Gruaz, D. Gumowski, I. Masouyé, D. Salomon, G. Siegenthaler, Topical Retinaldehyde on Human Skin: Biologic Effects and Tolerance, J. Invest. Dermatol., 103 (1994) 770-774.

[111] L. Didierjean, C. Tran, O. Sorg, J.H. Saurat, Biological activities of topical retinaldehyde, J. Dermatol., 199 Suppl 1 (1999) 19-24.

[112] O. Sorg, C. Antille, G. Kaya, J.-H. Saurat, Retinoids in cosmeceuticals, Dermatol. Ther., 19 (2006) 289-296.

[113] J.-H. Saurat, O. Sorg, L. Didierjean, New Concepts for Delivery of Topical Retinoid Activity to Human Skin, in: H. Nau, W.S. Blaner (Eds.) Retinoids: The Biochemical and Molecular Basis of Vitamin A and Retinoid Action, Springer Berlin Heidelberg, Berlin, Heidelberg, 1999, pp. 521-538.

[114] M. Garcia-Fuentes, M.J. Alonso, Chitosan-based drug nanocarriers: where do we stand?, J. Control. Release, 161 (2012) 496-504.

[115] J.J. Wang, Z.W. Zeng, R.Z. Xiao, T. Xie, G.L. Zhou, X.R. Zhan, S.L. Wang, Recent advances of chitosan nanoparticles as drug carriers, Int. J. Nanomedicine, 6 (2011) 765-774.

[116] M. Prabaharan, J.F. Mano, Chitosan-based particles as controlled drug delivery systems, Drug Deliv., 12 (2005) 41-57.

[117] P.A. Lehman, J.T. Slattery, T.J. Franz, Percutaneous Absorption of Retinoids: Influence of Vehicle, Light Exposure, and Dose, J. Invest. Dermatol., 91 (1988) 56-61.

[118] V. Masini, F. Bonte, A. Meybeck, J. Wepierre, Cutaneous bioavailability in hairless rats of tretinoin in liposomes or gel, J. Pharm. Sci., 82 (1993) 17-21.

[119] N. Otberg, A. Teichmann, U. Rasuljev, R. Sinkgraven, W. Sterry, J. Lademann, Follicular penetration of topically applied caffeine via a shampoo formulation, Skin Pharmacol. Physiol., 20 (2007) 195-198.

[120] J. Lademann, F. Knorr, H. Richter, U. Blume-Peytavi, A. Vogt, C. Antoniou, W. Sterry, A. Patzelt, Hair follicles--an efficient storage and penetration pathway for topically applied substances. Summary of recent results obtained at the Center of Experimental and Applied Cutaneous Physiology, Charite -Universitatsmedizin Berlin, Germany, Skin Pharmacol. Physiol., 21 (2008) 150-155.

[121] M. Radtke, A. Patzelt, F. Knorr, J. Lademann, R.R. Netz, Ratchet effect for nanoparticle transport in hair follicles, Eur. J. Pharm. Biopharm., 116 (2017) 125-130.

[122] J.D. Bos, M.M. Meinardi, The 500 Dalton rule for the skin penetration of chemical compounds and drugs, Exp. Dermatol., 9 (2000) 165-169.

[123] B.W. Barry, Drug delivery routes in skin: a novel approach, Adv. Drug Deliv. Rev., 54 (2002) S31-S40.

[124] G.L. Flynn, S.H. Yalkowsky, T.J. Roseman, Mass transport Phenomena and Models: Theoretical Concepts, J. Pharm. Sci., 63 (1974) 479-510.

[125] P. Pisetpackdeekul, P. Supmuang, P. Pan-In, W. Banlunara, B. Limcharoen, C. Kokpol, S. Wanichwecharungruang, Proretinal nanoparticles: stability, release, efficacy, and irritation, Int. J. Nanomedicine, 11 (2016) 3277-3286.

[126] G.A. Simon, H.I. Maibach, The pig as an experimental animal model of percutaneous permeation in man: qualitative and quantitative observations--an overview, Skin pharmacology and applied skin physiology, 13 (2000) 229-234.

[127] A. Patzelt, H. Richter, R. Buettemeyer, H.J.R. Huber, U. Blume-Peytavi, W. Sterry, J. Lademann, Differential stripping demonstrates a significant reduction of the hair follicle reservoir in vitro compared to in vivo, Eur. J. Pharm. Biopharm., 70 (2008) 234-238.

[128] F. Knorr, A. Patzelt, H. Richter, S. Schanzer, W. Sterry, J. Lademann, Approach towards developing a novel procedure to selectively quantify topically applied substances in the hair follicles of the model tissue porcine ear skin, Exp. Dermatol., 22 (2013) 417-418.

[129] H. Weigmann, J. Lademann, H. Meffert, H. Schaefer, W. Sterry, Determination of the horny layer profile by tape stripping in combination with optical spectroscopy in the visible range as a prerequisite to quantify percutaneous absorption, Skin pharmacology and applied skin physiology, 12 (1999) 34-45.

[130] A. Patzelt, H. Richter, L. Dähne, P. Walden, K.-H. Wiesmüller, U. Wank, W. Sterry, J. Lademann, Influence of the Vehicle on the Penetration of Particles into Hair Follicles, Pharmaceutics, 3 (2011) 307-314.

[131] A. Patzelt, H. Richter, F. Knorr, U. Schafer, C.M. Lehr, L. Dahne, W. Sterry, J. Lademann, Selective follicular targeting by modification of the particle sizes, J. Control. Release, 150 (2011) 45-48.

[132] P. Batheja, L. Sheihet, J. Kohn, A.J. Singer, B. Michniak-Kohn, Topical drug delivery by a polymeric nanosphere gel: Formulation optimization and in vitro and in vivo skin distribution studies, J. Control. Release, 149 (2011) 159-167.

[133] A. Patzelt, F. Knorr, U. Blume-Peytavi, W. Sterry, J. Lademann, Hair follicles, their disorders and their opportunities, Drug Discov. Today Dis. Mech., 5 (2008) e173-e181.

[134] V. Jenning, A. Gysler, M. Schäfer-Korting, S.H. Gohla, Vitamin A loaded solid lipid nanoparticles for topical use: occlusive properties and drug targeting to the upper skin, Eur. J. Pharm. Biopharm., 49 (2000) 211-218.

[135] J. Liu, W. Hu, H. Chen, Q. Ni, H. Xu, X. Yang, Isotretinoin-loaded solid lipid nanoparticles with skin targeting for topical delivery, Int. J. Pharm., 328 (2007) 191-195.

[136] K. Miladi, S. Sfar, H. Fessi, A. Elaissari, Enhancement of alendronate encapsulation in chitosan nanoparticles, J. Drug Deliv. Sci. Technol., 30 (2015) 391-396.

[137] F. Jimenez-Acosta, L. Planas, N.S. Penneys, Lipase expression in human skin, J. Dermatol. Sci., 1 (1990) 195-200.

[138] W. Meyer, K. Neurand, The distribution of enzymes in the skin of the domestic pig, Laboratory animals, 10 (1976) 237-247.

[139] J. Lademann, N. Otberg, H. Richter, H.J. Weigmann, U. Lindemann, H. Schaefer, W. Sterry, Investigation of follicular penetration of topically applied substances, Skin pharmacology and applied skin physiology, 14 Suppl 1 (2001) 17-22.

[140] K. Moser, K. Kriwet, A. Naik, Y.N. Kalia, R.H. Guy, Passive skin penetration enhancement and its quantification in vitro, Eur. J. Pharm. Biopharm., 52 (2001) 103-112.

[141] B. Baroli, M.G. Ennas, F. Loffredo, M. Isola, R. Pinna, M. Arturo López-Quintela, Penetration of Metallic Nanoparticles in Human Full-Thickness Skin, J. Invest. Dermatol., 127 (2007) 1701-1712.

[142] R. Alvarez-Román, A. Naik, Y.N. Kalia, H. Fessi, R.H. Guy, Visualization of skin penetration using confocal laser scanning microscopy, Eur. J. Pharm. Biopharm., 58 (2004) 301-316.

[143] A. Teichmann, U. Jacobi, M. Ossadnik, H. Richter, S. Koch, W. Sterry, J. Lademann, Differential Stripping: Determination of the Amount of Topically Applied Substances Penetrated into the Hair Follicles, J. Invest. Dermatol., 125 (2005) 264-269.

[144] C.E. Griffiths, A.N. Russman, G. Majmudar, R.S. Singer, T.A. Hamilton, J.J. Voorhees, Restoration of collagen formation in photodamaged human skin by tretinoin (retinoic acid), The New England journal of medicine, 329 (1993) 530-535.

[145] R. Kong, Y. Cui, G.J. Fisher, X. Wang, Y. Chen, L.M. Schneider, G. Majmudar, A comparative study of the effects of retinol and retinoic acid on histological, molecular, and clinical properties of human skin, 15 (2016) 49-57.

[146] J.O. Sass, L. Didierjean, P. Carraux, C. Plum, H. Nau, J.H. Saurat, Metabolism of topical retinaldehyde and retinol by mouse skin in vivo: predominant formation of retinyl esters and identification of 14-hydroxy-4, 14-retro-retinol, Experimental dermatology, 5 (1996) 267-271.

[147] H.S. Kwon, J.H. Lee, G.M. Kim, J.M. Bae, Efficacy and safety of retinaldehyde 0.1% and 0.05% creams used to treat photoaged skin: A randomized double-blind controlled trial, Journal of cosmetic dermatology, 17 (2018) 471-476.

[148] T.P. Afra, T.M. Razmi, T. Narang, S. Dogra, A. Kumar, Topical Tazarotene Gel, 0.1%, as a Novel Treatment Approach for Atrophic Postacne Scars: A Randomized Active-Controlled Clinical Trial, JAMA facial plastic surgery, (2018).

[149] M.J. Loss, S. Leung, A. Chien, N. Kerrouche, A.H. Fischer, S. Kang, Adapalene 0.3% Gel Shows Efficacy for the Treatment of Atrophic Acne Scars, Dermatology and therapy, 8 (2018) 245-257.

[150] L.H. Kligman, C.H. Duo, A.M. Kligman, Topical retinoic acid enhances the repair of ultraviolet damaged dermal connective tissue, Connective tissue research, 12 (1984) 139-150.

[151] A.N. Geria, C.N. Lawson, R.M. Halder, Topical retinoids for pigmented skin, Journal of drugs in dermatology : JDD, 10 (2011) 483-489.

[152] B. Dreno, A. Katsambas, C. Pelfini, D. Plantier, E. Jancovici, V. Ribet, T. Nocera, P. Morinet, A. Khammari, Combined 0.1% Retinaldehyde/ 6% Glycolic Acid Cream in Prophylaxis and Treatment of Acne Scarring, Dermatology, 214 (2007) 260-267.

[153] H. Schaefer, A. Zesch, Penetration of vitamin A acid into human skin, Acta dermato-venereologica. Supplementum, 74 (1975) 50-55.

[154] C. Sinico, M. Manconi, M. Peppi, F. Lai, D. Valenti, A.M. Fadda, Liposomes as carriers for dermal delivery of tretinoin: in vitro evaluation of drug permeation and vesicle–skin interaction, Journal of Controlled Release, 103 (2005) 123-136.

[155] J.W. Wiechers, The barrier function of the skin in relation to percutaneous absorption of drugs, Pharm Weekbl Sci, 11 (1989) 185-198.

[156] T.R.R. Singh, A.D. Woolfson, Microneedle-based drug delivery systems: Microfabrication, drug delivery, and safety AU - Donnelly, Ryan F, Drug delivery, 17 (2010) 187-207.

[157] Y. Hiraishi, T. Nakagawa, Y.-S. Quan, F. Kamiyama, S. Hirobe, N. Okada, S. Nakagawa, Performance and characteristics evaluation of a sodium hyaluronate-based microneedle patch for a transcutaneous drug delivery system, International Journal of Pharmaceutics, 441 (2013) 570-579.

[158] K. Matsuo, Y. Yokota, Y. Zhai, Y.-S. Quan, F. Kamiyama, Y. Mukai, N. Okada, S. Nakagawa, A low-invasive and effective transcutaneous immunization system using a novel dissolving microneedle array for soluble and particulate antigens, Journal of Controlled Release, 161 (2012) 10-17.

[159] L. Guo, J. Chen, Y. Qiu, S. Zhang, B. Xu, Y. Gao, Enhanced transcutaneous immunization via dissolving microneedle array loaded with liposome encapsulated antigen and adjuvant, Int J Pharm, 447 (2013) 22-30.

[160] L.Y. Chu, S.-O. Choi, M.R. Prausnitz, Fabrication of Dissolving Polymer Microneedles for Controlled Drug Encapsulation and Delivery: Bubble and Pedestal Microneedle Designs, Journal of pharmaceutical sciences, 99 (2010) 4228-4238.

[161] W.M. Lau, K.W. Ng, K. Sakenyte, C.M. Heard, Distribution of esterase activity in porcine ear skin, and the effects of freezing and heat separation, Int J Pharm, 433 (2012) 10-15.

[162] M.S. Gerstel, V.A. Place, Drug delivery device. US Patent, No. 3,964,482, (1976).

[163] M. Moothanchery, R.Z. Seeni, C. Xu, M. Pramanik, In vivo studies of transdermal nanoparticle delivery with microneedles using photoacoustic microscopy, Biomedical optics express, 8 (2017) 5483-5492.

[164] X. Lan, J. She, D.A. Lin, Y. Xu, X. Li, W.F. Yang, V.W.Y. Lui, L. Jin, X. Xie, Y.X. Su, Microneedle-Mediated Delivery of Lipid-Coated Cisplatin Nanoparticles for Efficient and Safe Cancer Therapy, ACS applied materials & interfaces, 10 (2018) 33060-33069.

[165] L. Niu, L.Y. Chu, S.A. Burton, K.J. Hansen, J. Panyam, Intradermal delivery of vaccine nanoparticles using hollow microneedle array generates enhanced and balanced immune response, Journal of Controlled Release, 294 (2019) 268-278.

[166] Y. Hiraishi, S. Hirobe, H. Iioka, Y.-S. Quan, F. Kamiyama, H. Asada, N. Okada, S. Nakagawa, Development of a novel therapeutic approach using a retinoic acid-loaded microneedle patch for seborrheic keratosis treatment and safety study in humans, Journal of Controlled Release, 171 (2013) 93-103.

[167] S. Hirobe, R. Otsuka, H. Iioka, Y.-S. Quan, F. Kamiyama, H. Asada, N. Okada, S. Nakagawa, Clinical study of a retinoic acid-loaded microneedle patch for seborrheic keratosis or senile lentigo, Life Sciences, 168 (2017) 24-27.

[168] G. Yan, K.S. Warner, J. Zhang, S. Sharma, B.K. Gale, Evaluation needle length and density of microneedle arrays in the pretreatment of skin for transdermal drug delivery, International Journal of Pharmaceutics, 391 (2010) 7-12.

[169] G. Ma, C. Wu, Microneedle, bio-microneedle and bio-inspired microneedle: A review, Journal of Controlled Release, 251 (2017) 11-23.

[170] T. Rattanapak, J. Birchall, K. Young, M. Ishii, I. Meglinski, T. Rades, S. Hook, Transcutaneous immunization using microneedles and cubosomes: Mechanistic investigations using Optical Coherence Tomography and Two-Photon Microscopy, Journal of Controlled Release, 172 (2013) 894-903.

[171] J. Gupta, H.S. Gill, S.N. Andrews, M.R. Prausnitz, Kinetics of skin resealing after insertion of microneedles in human subjects, Journal of Controlled Release, 154 (2011) 148-155.

[172] P.P. Samant, M.R. Prausnitz, Mechanisms of sampling interstitial fluid from skin using a microneedle patch, Proceedings of the National Academy of Sciences, 115 (2018) 4583.

[173] J.H. Park, M.G. Allen, M.R. Prausnitz, Polymer microneedles for controlled-release drug delivery, Pharmaceutical research, 23 (2006) 1008-1019.

[174] A. Sdobnov, M.E. Darvin, J. Lademann, V. Tuchin, A comparative study of ex vivo skin optical clearing using two-photon microscopy, 10 (2017) 1115-1123.

[175] Y.-C. Kim, J.-H. Park, M.R. Prausnitz, Microneedles for drug and vaccine delivery, Advanced Drug Delivery Reviews, 64 (2012) 1547-1568.

[176] R.F. Donnelly, D.I.J. Morrow, F. Fay, C.J. Scott, S. Abdelghany, R.R.T. Singh, M.J. Garland, A. David Woolfson, Microneedle-mediated intradermal nanoparticle delivery: Potential for enhanced local administration of hydrophobic pre-formed photosensitisers, Photodiagnosis and Photodynamic Therapy, 7 (2010) 222-231.

[177] J. Lademann, H. Richter, A. Teichmann, N. Otberg, U. Blume-Peytavi, J. Luengo, B. Weiß, U.F. Schaefer, C.-M. Lehr, R. Wepf, W. Sterry, Nanoparticles – An efficient carrier for drug delivery into the hair follicles, European Journal of Pharmaceutics and Biopharmaceutics, 66 (2007) 159-164.

[178] R. Alvarez-Román, A. Naik, Y.N. Kalia, R.H. Guy, H. Fessi, Skin penetration and distribution of polymeric nanoparticles, Journal of Controlled Release, 99 (2004) 53-62.

[179] H. Schaefer, Penetration and percutaneous absorption of topical retinoids. A review, Skin pharmacology : the official journal of the Skin Pharmacology Society, 6 Suppl 1 (1993) 17-23.

[180] B. Mahe, A. Vogt, C. Liard, D. Duffy, V. Abadie, O. Bonduelle, A. Boissonnas, W. Sterry, B. Verrier, U. Blume-Peytavi, B. Combadiere, Nanoparticle-based targeting of vaccine compounds to skin antigen-presenting cells by hair follicles and their transport in mice, J. Invest. Dermatol., 129 (2009) 1156-1164.

[181] K. Pino-Lagos, Y. Guo, R.J. Noelle, Retinoic acid: A key player in immunity, BioFactors (Oxford, England), 36 (2010) 10.1002/biof.1117.

VITA

NAME	Benchaphorn Limcharoen
DATE OF BIRTH	12 May 1989
PLACE OF BIRTH	Chiang Mai. Thailand
INSTITUTIONS ATTENDED	2006: The Prince Royal's College, Chiang Mai, Thailand

2007-2012: Doctor of Veterinary Medicine (DVM), second-class honor, Chulalongkorn University

2013: PhD candidate at Department of Pathology, Faculty of Veterinary Science, Chulalongkorn University.

2017-2018: Research fellowship program, Center of Experimental and Applied Cutaneous Physiology (CCP), Department of Dermatology, Venerology and Allergology, Charité - Universitätsmedizin Berlin, Germany

HOME ADDRESS 80/93 P.Thana Tower1, Soi Ladprao 58/1, Ladprao rd., Wangthonglang, Wangthonglang, Bangkok, 10310

PUBLICATION Publications

- Limcharoen B.,Toprangkobsin P., Banlunara W., Wanichwecharungreaung S., Richter H., Lademann J., Patzelt A. 2019. Increasing the percutaneous absorption and follicular penetration of retinal by topical application of proretinal nanoparticles. Eur J Pharm Biopharm. 139:93-100

- Limcharoen B., Pisetpackdeekul P., Wanichwecharungruang S., Banlunara W. 2017. Pathological changes of Topical Proretinal Nanoparticles on Rat's Skin. Proceedings of the 16th Chulalongkorn University Veterinary Conference (CUVC 2017) : Research in Practice. Queen Sirikit National Convention Center Bangkok, Thailand March 22-24, 2017. Thai J Vet Med Suppl 47:317-318.

- Pisetpackdeekul P,Supmuang P, Pan-In P, Banlunara W, Limcharoen B., Kokpol C and Wanichwecharungruang S. 2016.Proretinal nanoparticles: stability, release, efficacy, and irritation. Int J Nanomedicine. 11: 3277-3286

- Banlunara W., Thunyakitpisal P., Limcharoen B.2017. Subcutaneous implantation of the light-activated pit and fissure resin-based sealant prototypes LAS-clear and LAS-opaque resulted in a mild transient tissue reaction. Thai J Vet Med. 47(3).

- Ninvilai P., Nonthabenjawan N., Limcharoen B., et al. 2018. The presence of duck Tembusu virus in Thailand since 2007: A retrospective study. Transboundary and Emerging Diseases. 65(5)1208-1216

Presentations

- Limcharoen B.,Banlunara W. and Chankow K. 2014. Ovarian tumors in a spayed female dog: a case report. VPAT Journal, Bangkok, May, 18-22, P41-42.

- Limcharoen B., Chankow K., Kongmakee P. and Banlunara W. 2014. Metabolic bone disease in a Veiled Chameleon (Chamaeleo calyptratus). Proceeding of 7th Asian Meeting on Zoo and Wildlife Medicine/Conservation "One Health in Asia Pacific", Hanoi, Vietnam, Oct.14-17 P18-19. (Oral presentation)

- Limcharoen B., Rungsipipat A. and Teankum K. 2015.T cell Rich B Ccll lymphoma in a cat. The14th Chulalongkorn University Veterinary Conference. Bangkok, Apr 20-22.

- Limcharoen B., Kaewamatawong T., Banlunara W., Lombardini E.,.2015.Immune-mediated encephalomyelitis in a Beagle. Proceeding of 40th World Small Animal Veterinary Association Congress, Bangkok, May 15-18.
- Limcharoen B., Banlunara W., Wanichwecharungruang S.,.2019.Hair follicle penetration of topically applied proretinal nanoparticles. The 19th International Symposium of World veterinary laboratory diagnosticians, Chiang Mai, June 19-22. Oral presentation

Patent

- Wanichweacharungrueng S., Rutwaree T., Asawanonda P., Pukfukdee P., Toprangkobsin P., Banlunara W., Limcharoen B., Thai Patent : Dissolvable microneedle with special feature that enables effective detachment of needles into skin. 2018

AWARD RECEIVED

April 25, 2019: The excellent research presentation in the topic of enhancing biological activities and increasing percutaneous absorption of retinal by topical proretinal nanoparticles from Chulalongkorn University Veterinary Conference 2019, Impact Arena, Bangkok, Thailand.